ADVANCED INTERFERENCE ALIGNMENT TECHNIQUES FOR CELLULAR COMMUNICATION NETWORKS

A thesis submitted to the University of Manchester
for the degree of Doctor of Philosophy
in the Faculty of Engineering and Physical Sciences

2016

By
Galymzhan Nauryzbayev
School of Electrical and Electronic Engineering

Contents

List of Tables

List of Figures

Abstract

Advanced Interference Alignment Techniques For Cellular Communication Networks

Galymzhan Nauryzbayev

A thesis submitted to the University of Manchester for the degree of Doctor of Philosophy, 2016

The rapid growth of data hungry wireless applications has boosted the demand for wireless communication systems with improved reliability, wider coverage, and higher throughput. The main challenges facing the design of such systems are the limited resources, such as bandwidth, restricted transmission power, etc., and the impairments of the wireless channels, including fading effects, interference, and noise. Multiple-input multiple-output (MIMO) communication has been shown to be one of the most promising emerging wireless technologies that can efficiently enhance link reliability, improve system coverage, and boost the data transmission rate. Consequently, MIMO is now extensively adopted by many mainstream wireless industry standards, including 3GPP WCDMA/HSDPA, LTE, EVDO, WiFi, and WiMAX. By deploying multiple antennas at both transmitter and receiver sides, MIMO techniques license a new dimension (spatial dimension) that can be applied in various ways for combating the impairments of wireless networks. Furthermore, this new dimension has introduced a new concept known as Interference Alignment that can efficiently deal with the interference present in the wireless communication networks. In particular, IA is highly attractive in terms of providing more degrees of freedom compared to techniques such as TDMA/FDMA. With this in mind, this thesis will focus on studying and developing advanced techniques and algorithms for reducing interference in cellular communication networks.

The contributions of the thesis are as follows. Initially, a review is provided

to reiterate some basic concepts of wireless communications and discuss the challenges faced by the techniques that deal with interference mitigation. Next, Chapter 3 presents a novel IA based cancellation scheme that is proposed for combating the interfering signals present in the compounded MIMO broadcast channels, where the users experience a multi-source transmission from several base stations. After defining the interference channel (IC) interference and X-channel interference, the partial transmit beamforming matrices of the closed-form downlink scheme alleviate the corresponding types of interference. Applying the proposed scheme allows one to treat the multi-cell network as a set of single-cell MIMO network, which leads to the simultaneous BER performance enhancement and data rate increase. Moreover, a generalization scheme is given to assign the appropriate antenna configuration for achieving maximum DoF. Furthermore, Chapter 4 demonstrates a comprehensive analysis on the number of DoF achievable by exploiting the transmit beamforming technique. Additionally, the proposed scheme is able to provide the maximum data rate under a certain antenna setting or compute a transmitter-receiver configuration in order to meet the required number of DoF. Chapter 5 considers a modified IA scheme for the compounded MIMO network when different classes of users communicate in the overlapped area. Due to various antenna settings of each receiver, the effect of spatial correlation on the achievable data rate is investigated. Moreover, an algorithm is derived for calculating the antenna configuration for different users classes. Then, the proposed scheme is extended for the case of Large-scale MIMO, which in turn provides sufficient insights into the impact of the deployment of a large number of antennas. Finally, Chapter 6 presents an alternative design of the IA scheme with no symbol extension for the cellular MIMO network. Subsequently, a modified eigenvalue-based scheme is proposed to enhance the overall system performance. Finally, the achievable data rate is calculated under different CSI acquisition scenarios. Chapter 7 concludes the thesis and provides a list of potential future work directions for further investigation.

Declaration

No portion of the work referred to in this thesis has been submitted in support of an application for another degree or qualification of this or any other university or other institute of learning.

Copyright

Acknowledgements

First and above all, I praise the Almighty for granting me this research degree opportunity as well as the capacity to proceed successfully. Also,

- My loving and caring family: parents and siblings, your endless love, support and encouragement have truly been important. To you, I owe the deepest and most sincere thanks.

- I would like to thank my supervisor, Dr. Emad Alsusa, for his professional guidance, unconditional support and help academically and otherwise throughout my doctoral journey. His unflagging encouragement and invaluable advice have been a great source of motivation. I have been extremely lucky to have a supervisor who cared so much about my work, and who made his best to provide all means of aid to my research.

- I am indebted to all my colleagues within the Microwave and Communication Systems group who made my journey interesting and supported me over the past years. In particular, I am obliged to Yongjian, Ammar, Ghassan, Khaled, Hassan, Makram and Priya.

- Last but not least, I gratefully acknowledge the funding received towards my PhD from Bolashak, International Scholarship of President of the Republic of Kazakhstan.

Preface

Mr. Galymzhan Nauryzbayev received the B.Sc. (Hons.) degree and M.Sc. (Hons.) degree in radio engineering, electronics and telecommunications from Almaty University of Power Engineering and Telecommunication (AUPET), Almaty, Kazakhstan, in June 2009 and June 2011, respectively. From 2009 to 2012 he worked as a network engineer in JSC "Kazakhtelecom", and then he started working as an assistant lecturer in AUPET from 2011 to 2014. Since September 2012, he has been pursuing his PhD degree in Electrical and Electronic Engineering with research focus on multi-user MIMO systems, signal processing and interference mitigation.

To my Family

List of Abbreviations

4G	Fourth Generation
AWGN	Additive White Gaussian Noise
BC	Broadcast Channel
BEP	Bit Error Probability
BER	Bit Error Rate
BF	Beamforming
BS	Base Station
CAGR	Compound Annual Growth Rate
CDF	Cumulative Distribution Function
CI	Channel Inversion
CoMP	Coordinated Multipoint
CSI	Channel State Information
CSIT	Channel State Information at the Transmitter
DL	Downlink
DoA	Direction of Arrival
DoD	Direction of Departure
DoF	Degree of Freedom
DPC	Dirty Paper Coding
FDD	Frequency Division Duplex
FFR	Fractional Frequency Reuse
GIBC	Gaussian Interference Broadcast Channel
HetNet	Heterogeneous Network
HomoNet	Homogeneous Network
i.i.d.	Independent and identically distributed
IA	Interference Alignment
IC	Interference Channel
ICI	Inter-Channel Interference

IUI	Inter-User Interference
LOS	Line-of-sight
LP	Linear Programming
LS	Large-Scale
LTE	Long Term Evolution
MAC	Media Access Control
MIMO	Multiple-Input Multiple-Output
MISO	Multiple-Input Single-Output
MMSE	Minimum Mean Square Error
MS	Mobile Station
MU	Multi-User
MUI	Multi-user Interference
NLOS	Non-line-of-sight
PDF	Probability Density Function
PEP	Pairwise Error Probability
PFR	Partial Frequency Reuse
PHY	Physical Layer
PIC	Parallel Interference Cancellation
QoS	Quality of Service
rref	Reduced Row-Echelon Form
RCI	Regularized Channel Inversion
RCRM	Rank Constrained Rank Minimization
RV	Random Variable
Rx	Receiver
SFR	Soft Frequency Reuse
SIC	Successive Interference Cancellation
SIMO	Single-Input Multiple-Output
SINR	Signal-to-Interference-plus-Noise Ratio
SIR	Signal-to-Interference Ratio
SISO	Single-Input Single-Output
SNR	Signal-to-Noise Ratio
SU	Single-User

SVD	Singular Value Decomposition
TDD	Time Division Duplex
THP	Tomlinson-Harashima Precoding
Tx	Transmitter
UL	Uplink
V-BLAST	Vertical-Bell Laboratories Layered Space-Time
WLI	Weighted Leakage Interference
XCI	X-channel Interference
ZF	Zero-Forcing
ZFBF	Zero-Forcing Beamforming

List of Mathematical Notations

$\otimes$	Kronecker product operator
∞	Infinity
$\Rightarrow$	Results in
$(\cdot)^+$	Always nonnegative
$(\cdot)^\dagger$	Complex conjugate
$(\cdot)^H$	Matrix Hermitian
$\|\| \cdot \|\|$	Norm of a vector
$(\cdot)^T$	Transpose
$\lfloor a \rfloor$	Largest integer not higher than a
$\mathbb{C}$	Field of complex numbers
$\mathcal{CN}(a, b)$	Univariate complex normal distribution with mean a and variance b
$\mathcal{CN}(\mathbf{a}, \mathbf{B})$	Multivariate complex normal distribution with mean vector $\mathbf{a}$ and covariance matrix $\mathbf{B}$
$\det(\cdot)$	Determinant of a square matrix
$\mathbb{E}(\cdot)$	Expectation operator of a random variable
lim	Limit
$\log_x(\cdot)$	Logarithmic function to base x
max	Maximize
$\max(a, b)$	Function that finds maximum between a and b
min	Minimize
$\min(a, b)$	Function that finds minimum between a and b
$\text{null}(\cdot)$	Null function
$\mathcal{O}$	Computational complexity
$\mathbb{R}_+$	Set of positive real numbers
$\text{rank}(\cdot)$	Rank of a matrix

$\text{sgn}(\cdot)$	Sign function
$\text{span}(\cdot)$	Span of a (sub)space
$\text{trace}(\cdot)$	Trace function
$\text{vec}(\cdot)$	Vectorization function
$\mathbf{I}$	Identity matrix
$\mathbf{0}$	Zero matrix

List of Variables

α	SNR exponent under channel estimation error scenario
β	SNR scaling factor under channel estimation error scenario
γ	Instantaneous SNR
Δ	Spacing between constellation points
ε	Arbitrary small number
η	Degrees of freedom
$\mu_{\max}$	The largest magnitude of a symbol constellation
ρ	Nominal SNR
σ^2	Noise variance
τ	Variance of channel estimation error
d_s	Number of data streams
E_s	Symbol energy
$f_{(\cdot)}$	Scaling factor
$\mathcal{I}$	Transmission rate
K	Number of users
$\mathcal{K}$	Number of users per cell in the overlapped area
L	Number of cells
$\mathcal{L}$	Number of cells interested in a certain message
N_0	Noise power spectrum density
N_r	Number of receive antennas
N_t	Number of transmit antennas
P	Transmit power
P_b	Average bit error probability
P_e	Average error probability
$q_{\max}$	Maximum diversity order

q_{opt}	Optimum diversity order
$\mathbf{e}$	Erroneous codeword
$\mathbf{n}$	Noise vector
$\mathbf{s}$	Data vector of symbols chosen from a desired constellation
$\mathbf{x}$	Transmitted signal vector
$\mathbf{y}$	Received signal
$\tilde{\mathbf{y}}$	Received signal after receive beamforming
$\mathbf{E}$	Error matrix
$\mathbf{H}$	Channel matrix
$\hat{\mathbf{H}}$	Estimated channel matrix
$\mathbf{K}$	Effective interference direction
$\mathbf{R}$	Covariance matrix
$\mathbf{U}$	Receive beamforming/suppression matrix
$\mathbf{U}^{[ICI]}$	Receive beamforming/suppression matrix responsible for the ICI
$\mathbf{U}^{[XCI]}$	Receive beamforming/ suppression matrix responsible for the XCI
$\mathbf{V}$	Transmit beamforming matrix
$\mathbf{V}^{[ICI]}$	Transmit beamforming matrix responsible for the ICI
$\mathbf{V}^{[XCI]}$	Transmit beamforming matrix responsible for the XCI

Chapter 1

Introduction

1.1 Modern Wireless Systems

The formation of radio started from 1861 when Maxwell, inspired by Faraday work on electricity, published a mathematical theory of electromagnetic waves. And eventually, in 1887 H. Hertz proved the existence of these waves by using stationary waves, [3]. Since then, wireless communications have attracted a significant number of researchers, and, consequently, radio systems have emerged in various areas.

The best evidence of the successful commercialisation of radio waves is the fact that communication networks connect globally more than 7.4 billion mobile devices with further plans to achieve more than 11.5 billion devices by the end of 2019, [1]. In [1], Cisco forecasts a mobile data traffic growth of 57 percent at a Compound Annual Growth Rate (CAGR) from 2014 to 2019, reaching 24.3 exabytes per month by 2019, a tenfold increase over 2014 (Fig. 1.1).

To respond to the fast-growing need for wireless data traffic, the wireless communication industry is already preparing for beyond fourth-generation (4G) wireless systems where there are many challenges. One of such challenges is how to satisfy the demand for much higher data rates at more stringent latencies. Another main challenge to be addressed is the impact of higher network densification and the corresponding increase in interference, [4]. These challenges and many more are currently under discussion in the research community, e.g., [5, 6]. The aim of this thesis is to focus on devising advanced interference management techniques to enable higher data rates in future wireless communication systems.

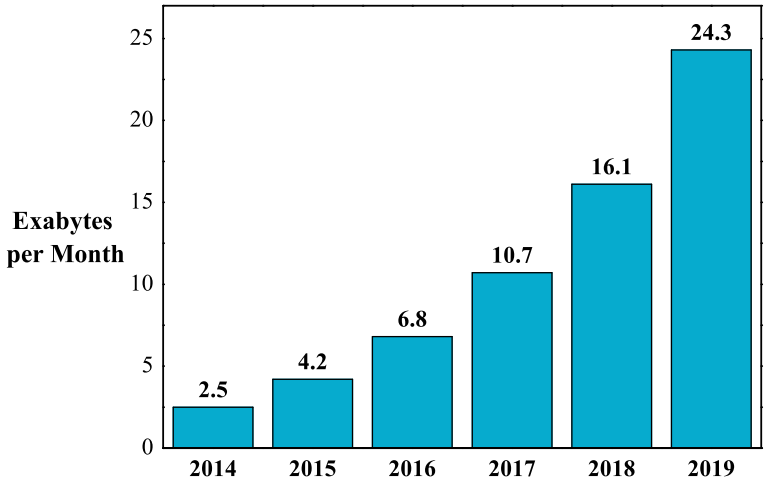

Figure 1.1. Global Mobile Data Traffic, 2014 to 2019, [1].

1.2 Motivation

Since future wireless systems require further cell densification to fulfil future demands, the volume of interference in the network will go up in proportion to the number of cells per area. As the cell size shrinks down more overlapping areas will appear in the network. In the case of a dense user distribution, a certain number of users can locate in the overlapping space built by the intersection of the base stations (BSs). Since the amount of power received from the interfering BSs is comparable to the power arriving from the serving BS, a mobile user in the overlapped area undergoes the worst network scenario where severe interference exists. Such users will experience low signal-to-interference ratio (SIR). Consequently, the user performance metrics such as bit error rate (BER) and sum rate degrade. This makes it important to analyse the performances of these users in a bid to find a way to improve their experience. Thus, as the interference becomes more intense, particularly for multiple-input multiple-output (MIMO) systems it becomes vital that novel efficient interference mitigation schemes should be developed to make possible for users under such scenarios to communicate successfully.

1.3 Key Contributions

The major contributions of this thesis are briefly listed below.

- A compounded MIMO broadcast channel (BC) scenario is proposed as a more appropriate design to model the dense cellular networks, where there are more users with high probability to be in the overlapped area. Accordingly, a closed-form interference alignment (IA) scheme is presented to deal with the interference. The proposed design converts the multi-cell network into a set of single-cell MIMO networks. Thus, BER of the user of interest matches the one achievable in the single-user MIMO (SU-MIMO) network. Moreover, the system performance, such as, sum rate, degrees of freedom (DoF) and computational complexity are investigated, and it is shown that the derived findings outperform the corresponding metrics of the benchmark techniques in the area.

- A comprehensive analysis of the DoF region is presented for the compounded MIMO BC network scenario. For a case study, an upper limit for the DoF metric is derived by solving a dual problem through linear programming. The proof of theoretical findings is demonstrated by comparing with the numerical results. Moreover, the minimum antenna configuration is calculated to achieve a certain number of DoF. Finally, a generalization of the proposed scheme is derived.

- Different classes of users are examined for the case of the compounded MIMO BC scenario. Due to a different antenna configuration at each receiver (Rx), an updated version of the proposed scheme with a lower complexity is designated. Moreover, the effect of spatial correlation is analysed to examine its impact on the network performances. Finally, the theoretical finding with appropriate supportive numerical results are presented for the case of Large-scale MIMO (LS-MIMO), when the transmitters (Txs) are deployed with a large number of antennas.

- An alternative closed-form IA-based interference mitigation scheme is presented for the case of the multi-cell downlink (DL) MIMO X-channel. Moreover, an eigenvalue-based method is utilized to achieve a higher data rate. The channel state information (CSI) mismatch is considered to evaluate its effect on the system performances.

1.4 Thesis Organization

The remainder of this thesis is organized as follows. Chapter 2 presents a literature review on the relevant background of MIMO systems. In addition, the issue of interference and the interference mitigation techniques utilized in different network layers are reviewed. Finally, modern techniques, generally known as IA algorithms, are introduced as a novel approach to deal with interference. Chapter 3 introduces a compounded MIMO BC scenario for the case of the densified multi-cell multi-user MIMO (MU-MIMO) network. A novel effective interference mitigation technique is proposed to enhance the achievable DoF and BER performances. Chapter 4 demonstrates the comprehensive analysis of the DoF region and respective upper limit of the DoF achievable in the compounded MIMO broadcast channel. The generalization of the proposed scheme is derived for identical and non-identical antenna configurations. Chapter 5 proposes different classes of users located in the area of interest in the compounded MIMO BC. Due to potential spatial correlation between the antennas, a modified low-complexity design of the interference mitigation technique is designated to consider various antenna configurations. Finally, the proposed scheme is expanded for the case of LS-MIMO. Chapter 6 examines the three-cell fully connected MIMO network. A novel closed-form IA scheme is developed and further enhanced by applying a search method which seeks the highest eigenvalue of the channel matrix. Additionally, an in-depth performance analysis is conducted in terms of the CSI mismatch, sum-rate and computational complexity. Chapter 7 concludes the thesis and outlines prospects for the future extension of the work.

1.5 List of Publications

Accepted papers

Journal Papers

- G. Nauryzbayev and E. Alsusa, "Enhanced Multiplexing Gain Using Interference Alignment Cancellation in Multi-cell MIMO Networks," *IEEE Transactions on Information Theory*, vol. 62, no. 1, pp. 357-369, January 2016.

- G. Nauryzbayev and E. Alsusa, "Interference Alignment Cancellation in Compounded MIMO Broadcast Channels with General Message Sets," *IEEE*

Transactions on Communications, vol. 63, no. 10, pp. 3702-3712, October 2015.

Conference Papers

- G. Nauryzbayev and E. Alsusa, "Identifying the Maximum DoF Region in the Three-cell Compounded MIMO Network," *IEEE Wireless Communications and Networking Conference (WCNC)*, Doha, Qatar, 2016.
- G. Nauryzbayev, E. Alsusa, and J. Tang, "An Alignment Based Interference Cancellation Scheme for Multi-cell MIMO Networks," *IEEE Vehicular Technology Conference (VTC2015-Spring)*, Glasgow, UK, 2015.

Submitted papers

Journal Papers

- G. Nauryzbayev and E. Alsusa, "Interference Alignment in Compounded MIMO Broadcast Channels with Antenna Correlation and Mixed User Classes," Submitted to *IEEE Transactions on Communications*.

To submit

Conference Papers

- G. Nauryzbayev and E. Alsusa, "The Compounded MIMO BC Channels: On the Effects of Both-End Correlation and Imperfect CSI."
- G. Nauryzbayev and E. Alsusa, "Efficient Interference Alignment and Cancellation in the Three-cell Compounded MIMO Network."

Under preparation

Journal Papers

- G. Nauryzbayev and E. Alsusa, "A Closed-Form Interference Alignment Cancellation for the MIMO X-channel," *IEEE Transactions on Wireless Communications*.

Chapter 2

Literature Review

In this chapter, we cover some basic concepts of wireless communications along with some advantages of MIMO signaling over single-input single-output (SISO) systems, wherein we review a diversity-multiplexing trade-off and describe various ways of CSI acquisition. Next, we discuss the forms of interference appearing in wireless networks and briefly go through some common interference management techniques used in the physical (PHY) and media access control (MAC) layers. Finally, we overview the-state-of-the-art in interference alignment techniques in wireless interference-limited networks.

2.1 MIMO System Model

Initially MIMO techniques were investigated for SU-MIMO network scenarios with multi-antenna nodes, [7], as shown in Fig. 2.1, where the transmitter (or base station, BS) and receiver (or mobile station, MS) are equipped with two antennas. The numbers of transmit and receive antennas are denoted as N_t and N_r, respectively; the received signal can be written as

$$\overbrace{\begin{bmatrix} y_1 \\ y_2 \\ \vdots \\ y_{N_r} \end{bmatrix}}^{\mathbf{y}} = \overbrace{\begin{bmatrix} h_{1,1} & h_{1,2} & \cdots & h_{1,N_t} \\ h_{2,1} & h_{2,2} & \cdots & h_{2,N_t} \\ \vdots & \vdots & \ddots & \vdots \\ h_{N_r,1} & h_{N_r,2} & \cdots & h_{N_r,N_t} \end{bmatrix}}^{\mathbf{H}} \overbrace{\begin{bmatrix} x_1 \\ x_2 \\ \vdots \\ x_{N_t} \end{bmatrix}}^{\mathbf{x}} + \overbrace{\begin{bmatrix} n_1 \\ n_2 \\ \vdots \\ n_{N_r} \end{bmatrix}}^{\mathbf{n}} \tag{2.1}$$

where $\mathbf{x} \in \mathbb{C}^{N_t \times 1}$ is the transmitted signal, $\mathbf{H} \in \mathbb{C}^{N_r \times N_t}$ indicates the channel matrix from transmitter to receiver, and $\mathbf{n} \in \mathbb{C}^{N_r \times 1}$ is the additive white Gaussian noise (AWGN) vector with variance σ^2 per entry at the receiver.

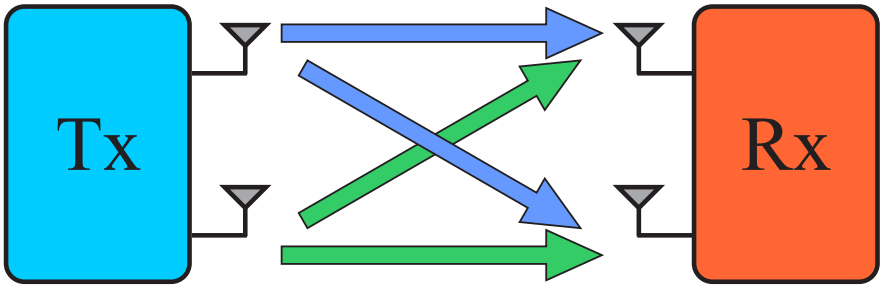

Figure 2.1. A single-cell SU-MIMO network with N_t transmit and N_r receive antennas.

The work in [8, 7, 9] forecasted remarkable spectral efficiencies for the multi-antenna systems when the channel undergoes rich scattering. Since *Long Term Evolution* (LTE) Release 8 exploits the SU-MIMO as a key technique and requires 75 Mb/s and 300 Mb/s for Uplink (UL) and Downlink throughput, respectively, [10], LTE Release 10 (LTE-Advanced) aims to obtain 500 Mb/s and 1 Gb/s for UL and DL, respectively. And one of the possible techniques to meet this target is multi-user MIMO which refers to the scenario when the multi-antenna BS simultaneously serves multiple users (Fig. 2.2).

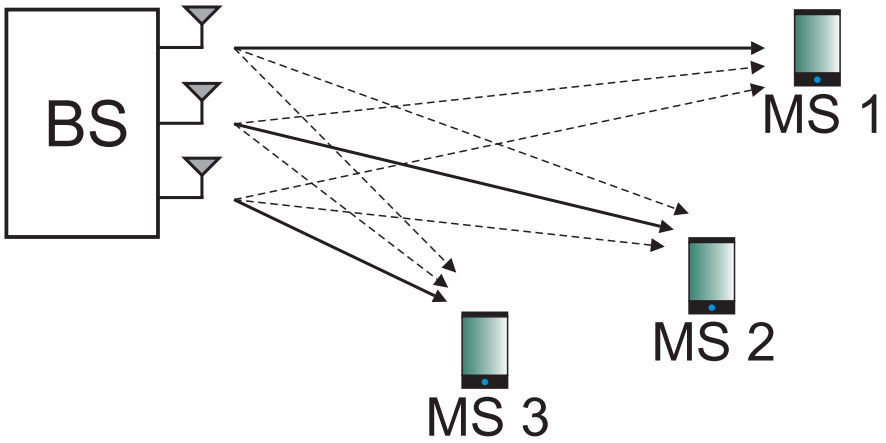

Figure 2.2. A single-cell MU-MIMO network with three mobile stations.

Compared to SISO systems, [11], the MIMO technology provides substantial benefits such as

- **Diversity gain**: replicas of the transmitted signal are received at the receiver. Consequently, the probability that all copies are in deep fade tends to zero. This provides a more reliable recovery of the transmitted signal, [12]. The diversity gain can be gleaned in both multiple-input single-output (MISO) and single-input multiple-output (SIMO) systems as well.

- **Power gain**: signal-to-noise ratio (SNR) at the receiver can be increased by coherently combining the received signals and/or by allocating more power to a transmit antenna with a better gain which enriches the reception quality. It is worth mentioning that a power gain can be gleaned in SIMO systems as well. In the case of the availability of CSI at the transmitter (CSIT), MISO systems are also able to deliver power gain.

- **Multiplexing gain or DoF**: the transmitter deployed with multiple antennas can simultaneously send parallel independent data streams to the receiver using the same radio frequency bands for all data streams. In contradistinction to the power and diversity gains which can be obtained for MISO and SIMO systems, the DoF is only achievable in MIMO systems.

- **Interference suppression**: under the case of usage of the same time and frequency resources, any data stream transmitted to a certain user causes interference to all unintended users in multi-user systems. The deployment with multiple antennas enables us to efficiently null out interference coming from the other transmitters. For the DL communication scenario, interference can be pre-cancelled by precoding techniques.

2.1.1 Diversity and Multiplexing Trade-off

The two key MIMO advantages mentioned above as the diversity and multiplexing gains oppose each other, i.e., an increase of one respectively causes a reduction in the second, and vice versa. The diversity-multiplexing trade-off is indeed the trade-off between the data rate and error probability of the system, [13].

Spatial diversity techniques are designed to exploit multiple antennas for further enhancement of the reliability of data transmission, [14]. In [15, 16], an upper bound for pairwise error probability (PEP) of space-time codes is derived as

$$P_{\mathbf{x}\to\mathbf{e}} \leq \alpha_c \left(\frac{E_s}{4N_0}\right)^{-N_r N_t}, \tag{2.2}$$

where $\mathbf{x}$ and $\mathbf{e}$ are the transmitted and erroneous codewords. E_s and N_0 denote the power levels of the signal and background noise, respectively, while α_c indicates a function of the channel and codeword and does not depend on the SNR. From (2.2), the maximum diversity order can be given as

$$q_{\max} = -\lim_{\mathrm{SNR}\to\infty} \frac{\log_2 P_e(\mathrm{SNR})}{\log_2(\mathrm{SNR})} = N_r N_t, \tag{2.3}$$

where P_e is the average error probability, and the channels between the transmit and receive antennas are assumed to fade independently.

Besides providing diversity to improve the transmission reliability, MIMO channels enables us to achieve a higher rate than SISO channels. To provide the spatial multiplexing gain, the transmission strategy is to split the data set into parallel simultaneous substreams, where each substream can be coded and modulated independently. In [7], it was shown that for high SNR the channel capacity with independent and identically distributed (i.i.d.) Rayleigh fading is given by

$$C(SNR) = r \log_2(\mathrm{SNR}) + O(1), \tag{2.4}$$

where $r = \min(N_r, N_t)$ stands for the rank of the channel matrix $\mathbf{H}$. This indicates that the channel capacity increases with SNR as $r \log_2(\mathrm{SNR})$, i.e., r times faster than the capacity of SISO channels. In other words, the MIMO channels can be regarded as r parallel channels, where r is equal to the number of DoF defined as the pre-log factor of the sum rate, [17, 18],

$$\eta = \lim_{\mathrm{SNR}\to\infty} \frac{\mathcal{I}(\mathrm{SNR})}{\log_2(\mathrm{SNR})} = r, \tag{2.5}$$

where $\mathcal{I}(SNR)$ and η are the achievable sum rate and DoF at a given SNR, respectively.

Finally, combining the above equations, the optimal diversity-multiplexing trade-off can be defined as, [13],

$$q_{opt}(i) = (N_r - i)(N_t - i), \ \forall i \in \{0, \ldots, r\}, \tag{2.6}$$

for $N \geq N_r + N_t - 1$, where N is the transmitted block length.

This result shows that one is able to obtain the data rate increase which

grows with SNR if the diversity order is reduced from the maximum achievable one. This trade-off implies that a higher spectral efficiency comes at the price of reduced diversity, and vice versa.

2.1.2 Channel State Information

Assuming perfect CSI is highly idealistic because in practice CSI is replaced by imperfect estimates of the channel which can degrade the network performance. The following model, [19], can be exploited to understand the impact of imperfect CSI on the system performance

$$\hat{\mathbf{H}} = \mathbf{H} + \mathbf{E}, \tag{2.7}$$

where $\hat{\mathbf{H}}$ indicates the mismatched channel, $\mathbf{H} \sim \mathcal{CN}(\mathbf{0}, \mathbf{I})$ is the real channel realization, and $\mathbf{E}$ is the error matrix assumed to be independent of $\mathbf{H}$. Then, $\mathbf{E}$ can be defined as $\text{vec}(\mathbf{E}) \sim \mathcal{CN}(\mathbf{0}, \tau\mathbf{I})$ with an error variance, τ, given by, [20],

$$\tau = \beta\rho^{-\alpha}, \ \alpha \geq 0, \beta > 0, \tag{2.8}$$

where ρ is a nominal SNR, and α and β are constants used to define various CSI scenarios. Thus, the error variance τ can depend on the SNR ($\alpha \neq 0$) or be independent of the SNR ($\alpha = 0$).

- **CSI Feedback**: when $\alpha = 0$. In this case, the channel realization is estimated by transmitting the pilot signals, and then the quantized channel estimate is fed back to BS via a dedicated feedback channel (common in frequency division duplex (FDD) systems). The level of the CSI mismatch is mainly determined by the quantization error. Moreover, the feedback delay can also effect the CSI quality, i.e., when the channel coherence time is less than the feedback delay, CSI derived at the BS can be outdated.

- **Mismatched Reciprocal Channels**: when $0 < \alpha < 1$. This scenario can be described by the substantial power imbalance between the transmitter and receiver sides, i.e., the power coming from the feedback channel is much smaller than the downlink channel power.

- **Reciprocal channels**: when $\alpha = 1$. In a wireless communication system using antenna arrays, CSIT can substantially improve the capacity of the

wireless link. In a time division duplex (TDD) system, CSIT can be obtained by exploiting the reciprocity of the wireless channel via sending pilot signals. Therefore, the downlink and uplink channels are reciprocal since they share the same frequency band. Then, the channel estimate is affected by error $\mathbf{E}$ which depends on the noise level at the BS and the pilot power, also known as a pilot contamination, [21, 22, 23]. Thus, the channel error estimation decreases when SNR increases.

Moreover, perfect CSI can be modeled as $\alpha \to \infty$.

Then, conditioned on $\hat{\mathbf{H}}$, [24], the real channel matrix can be expressed as follows

$$\mathbf{H} = \bar{\mathbf{H}} + \tilde{\mathbf{H}}, \tag{2.9}$$

where $\bar{\mathbf{H}} \sim \mathcal{CN}(0, \frac{1}{\tau+1}\mathbf{I})$ and $\tilde{\mathbf{H}} \sim \mathcal{CN}(0, \frac{\tau}{\tau+1}\mathbf{I})$, [25, 26, 27].

Justification of the channel modeling

Suppose $\mathbf{X}$ and $\mathbf{Y}$ are independent random matrices that are Rayleigh distributed as follows

$$\begin{aligned}
\mathbf{X} &\sim \mathcal{N}(0, \mathbf{I}), \\
\mathbf{Y} &\sim \mathcal{N}(0, a\mathbf{I}), \\
\mathbf{Z} &= \mathbf{X} + \mathbf{Y},
\end{aligned}$$

where a is a scalar.

Then, entries of the random matrix $\mathbf{Z}$ are drawn from distribution given as $\mathcal{N}(0, 1+a)$, [28], because

$$\begin{aligned}
\mathbf{Z} &\sim \mathcal{N}\left(\mu_Z, \sigma_Z^2\mathbf{I}\right) \\
&= \mathcal{N}\left(\mu_X + \mu_Y, (\sigma_X^2 + \sigma_Y^2)\mathbf{I}\right) \\
&= \mathcal{N}(0, (1+a)\mathbf{I}),
\end{aligned}$$

where the effective mean μ_Z equals zero ($\mu_X = \mu_Y = 0$) and the variance σ_Z^2 is given by the sum of these variances.

Conditioning the sum of matrices on $\mathbf{Z}$ by $\sqrt{1+a}$ results in, [24],

$$\frac{\mathbf{Z}}{\sqrt{1+a}} = \frac{\mathbf{X}}{\sqrt{1+a}} + \frac{\mathbf{Y}}{\sqrt{1+a}},$$

which in turn can be rewritten by using other terms as

$$\hat{\mathbf{Z}} = \hat{\mathbf{X}} + \hat{\mathbf{Y}},$$

where new matrices can be defined as follows

$$\begin{aligned}
\hat{\mathbf{Z}} &\sim \mathcal{N}\left(0, \frac{1+a}{1+a}\mathbf{I}\right) = \mathcal{N}\left(0, \mathbf{I}\right), \\
\hat{\mathbf{X}} &\sim \mathcal{N}\left(0, \frac{1}{1+a}\mathbf{I}\right), \\
\hat{\mathbf{Y}} &\sim \mathcal{N}\left(0, \frac{a}{1+a}\mathbf{I}\right).
\end{aligned}$$

Consequently, the channel and its estimate are not biassed. However, regarding the matrix independence, the conditioned matrices can not be treated as independent ones if they are conditioned on the other matrix. This is based on the concepts of probability theory such as a conditional probability and conditional expectation: conditioning means that we restrict ourselves to a certain condition that consequently leads to the fact that the two conditioned RVs become dependent random variables.

2.2 Capacity Increasing Techniques

The evolution of mobile terminals and the popularity of wireless networks have exacerbated the demand for increased capacity. Thus, the network capacity of wireless systems has to be enhanced to meet the Quality of Service (QoS) requirements of mobile applications. With this, telecommunication operators and vendors have also forecast the further exponential growth of the network data load, [1]. Consequently, the current situation in wireless systems requires new techniques to support the observed demands for next-generation wireless networks.

Since a link capacity in wireless networks is not constant and depends on many factors such as the transmission power over the link and interference caused by transmission over the other links, the cell capacity may not support the exponentially increasing number of users. Therefore, cell splitting and sectoring are common techniques employed for increasing the capacity of cellular communication systems. In other words, a cellular network can be classified as Homogeneous

Networks (HomoNet) with only macrocell deployed and Heterogeneous Networks (HetNet) with both macrocell and small cells, [29].

The cell-splitting technique subdivides a congested cell into smaller cells, called microcells. Each microcell is equipped with a BS that is reassigned a frequency band. Due to a smaller size of the microcell, an antenna has a reduced height and a reduced transmission power so that the receiving power at the new and old cell boundaries are equal to each other. After a cell is split into microcells, changes in the frequency plan are required to retain the frequency reuse constraint. On the other hand, this also increases the number of handoffs between cells for moving users. The large amount of signaling for handoffs reduces the spectral efficiency. Picocells and femtocells further reduce the size of a microcell, [30, 31]. They provide better coverage in some locations and enable higher data rates at a significantly lower cost than a macrocell/microcell BS. The cellular BSs are interconnected via an existing access network.

The cell-sectoring technique replaces a single omnidirectional antenna at the BS by several directional antennas, typically three sectors of 120° each, [29]. These directional antennas can be made of patched antenna arrays. Unlike omnidirectional antennas, the directional antennas interfere only with the neighbouring cells in their directions. When a cell is sectorized into N sectors, interference power is reduced by roughly a factor of N under heavy loading. Cell sectoring also suffers from a considerable loss in trunking inefficiency, which can be a major concern for operation.

A more complex method to increase the system capacity is to use smart antenna techniques, [29, 32, 33]. Antenna arrays are used to generate beam patterns for each of the desired users while rejecting all interfering signals. Due to the excellent interference rejection capability, each BS can cover a wider area. The smart antenna technique achieves a significant improvement in system capacity. Smart antennas can be either a switched-beam or an adaptive array system. The switched-beam system continually chooses one pattern from many predefined patterns to steer towards the desired user. This method is incapable of enhancing the desired signal when an interfering signal is close to it, since the beam patterns are predefined. This problem can be solved by using an adaptive array, which creates a beam pattern for each user adaptively by enhancing the desired signal and suppressing all interfering signals. Adaptive antenna array techniques are much more complex for implementation.

2.3 Interference Management in Cellular Communication Networks

When several source nodes communicate in wireless networks at the same time, a certain phenomenon, interference, appears due to the nature of wireless transmission. In the downlink of LTE system, mobile users commonly suffer from different types of interference. In the case of SU-MIMO, the received signal includes a linear combination of multiple streams, which causes inter-stream interference which can be cancelled at the receiver side without requiring any additional information. On the other hand, for the MU-MIMO scenario, where a BS communicates with many users simultaneously using the same time-frequency resources, the received signal at each mobile user suffers from interference caused by the signals intended for the other receivers served by the same BS, and the corresponding interference is called inter-user interference (IUI). The cell-edge user endures inter-cell interference, i.e., interference caused by the signals sent from the adjacent cells to their mobile users using the same frequency band. To mitigate the above types of interference, receivers need to apply different interference cancellation schemes. Inter-user interference cancellation may require knowledge of the precoding matrices of the other MSs that one wishes to cancel, e.g., IUI can also be mitigated because of the extreme narrow beam by exploiting large number of antennas at the transmitter side, [34]. Even with extremely low intra-cell interference, inter-cell interference (ICI) is a great challenge that severely limits the network performance, especially for the cell-edge users. Moreover, the inter-cell interference cancellation requires channel estimates between the interfering BSs and users. Since the degrees of freedom, e.g., time, frequency bandwidth and number of orthogonal codes, are limited, interference becomes an inevitable issue. Therefore, it is essential to capture all the forms of interference present in different network layers. In the following sections, we consider only the PHY and MAC layers.

2.3.1 PHY Layer

Interference mitigation in the physical layer implies that techniques are employed to reduce the impact of interference during the transmission or/and after the reception of the signal. A number of different techniques to address the issue of MU-MIMO downlink transmission and reception were proposed in [3, 12].

Detection Techniques

When transmit antennas in MIMO systems transmit different symbols simultaneously, the signals are summed on each receive antenna and the receiver subsequently has to separate them in order to detect the desired message. If each transmit antenna is considered as user, the system can be thought of as a multiple access system and multi-user detection techniques can be employed by the MIMO system. This section reviews several basic linear and nonlinear multi-user detection techniques.

Zero-Forcing Detection

The received signal vector has a form

$$\mathbf{y} = \mathbf{H}\mathbf{x} + \mathbf{n} = \sum_{i=1}^{N_t} \mathbf{h}_i x_i + \mathbf{n}, \tag{2.10}$$

where $\mathbf{h}_i$ indicates the i^{th} column of $\mathbf{H}$, channel between the transmitter and receiver sides. x_i is the symbol of the data vector $\mathbf{x}$ transmitted from the i^{th} antenna. Regarding the data stream l $(1 \leq l \leq N_t)$, the received signal can be rewritten as

$$\mathbf{y} = \mathbf{h}_l x_l + \underbrace{\sum_{i \neq l} \mathbf{h}_i x_i}_{\text{interference}} + \mathbf{n},$$

where the l^{th} data stream is subject to the interference given by the second term. A simple approach to decode the desired data is to project the received signal onto the subspace orthogonal to the one spanned by the vectors $\mathbf{h}_{i\{i \neq l\}}$, thus nullifying the inter-stream interference. Such projection operation is called Zero-Forcing (ZF) given by the Moore-Penrose pseudo-inverse, [35],

$$\mathbf{G}_{ZF} = \begin{cases} \left(\mathbf{H}^H \mathbf{H}\right)^{-1} \mathbf{H}^H, \text{ if rank}\left(\mathbf{H}\right) = N_t, \\ \mathbf{H}^H \left(\mathbf{H}\mathbf{H}^H\right)^{-1}, \text{ if rank}\left(\mathbf{H}\right) = N_r. \end{cases} \tag{2.11}$$

The ZF detection filter at the receiver side is actually the left inverse of the channel matrix $\mathbf{H}$ from (2.11). The estimation of the transmitted data vector $\hat{\mathbf{x}}_{ZF}$ is

$$\hat{\mathbf{x}}_{ZF} = \mathbf{x} + \mathbf{G}_{ZF}\mathbf{n}. \tag{2.12}$$

Accordingly, an error covariance matrix $\mathbf{R}_{ZF}$ of the ZF detection can be obtained as

$$\mathbf{R}_{ZF} = \mathbb{E}\left\{\left(\hat{\mathbf{x}}_{ZF} - \mathbf{x}\right)\left(\hat{\mathbf{x}}_{ZF} - \mathbf{x}\right)^{H}\right\} = \sigma_n^2 \mathbf{G}_{ZF}\mathbf{G}_{ZF}^{H}. \tag{2.13}$$

From (2.12), for the case of ill-conditioned channels, the noise power can be significantly enlarged by $\mathbf{G}_{ZF}$, and consequently the BER performance of the ZF detector will be greatly reduced. This is known as noise enhancement in wireless communications.

Minimum Mean Square Error Detection

The minimum mean square error (MMSE) technique is an optimal detector that tries to balance between interference cancellation and reduction of noise enhancement. To reduce the noise amplification caused by the ZF detector, the MMSE criterion takes into account the noise term and is based on the following

$$\mathbf{G}_{MMSE} = \arg\min_{\mathbf{G}} \mathbb{E}\left\{\|\mathbf{G}\mathbf{y} - \mathbf{x}\|\right\}. \tag{2.14}$$

The $\mathbf{G}_{MMSE}$ can be easily derived as

$$\mathbf{G}_{MMSE} = \left(\mathbf{H}^{H}\mathbf{H} + \rho^{-1}\mathbf{I}\right)^{-1}\mathbf{H}^{H}, \tag{2.15}$$

with respect to the orthogonality principle $\mathbb{E}\left\{\|\mathbf{G}\mathbf{y} - \mathbf{x}\|\mathbf{y}^{H}\right\} = \mathbf{0}$, and ρ stands for the SNR.

Spatial interference can be mitigated since the non-diagonal terms of $\mathbf{G}_{MMSE}\mathbf{H}$ are smaller than the diagonal terms and can be neglected in a suboptimal receiver. As a result, some residual spatial interference remains, but as an approximation it can be disregarded. Therefore, a better performance can be obtained by performing the MMSE detection since the multi-user interference (MUI) mitigation is balanced with noise enhancement.

Successive Interference Cancellation

In the above, we considered two linear detection schemes that utilize separate filters to detect the data streams. However, when the data messages are decoded successively, the outcomes of previous detectors can be exploited to facilitate the detection of the next data streams by utilizing appropriate algorithms including successive interference cancellation (SIC), [36, 37], parallel interference cancellation (PIC) [38, 39], and multi-stage detection [40, 41]. However, for the sake of

brevity, only successive interference cancellation is considered.

The Vertical-Bell Laboratories Layered Space-Time (V-BLAST) detection scheme is a good example that employs ZF-SIC with optimal ordering, [42]. The key idea of SIC detection is layer peeling, that is, the first symbol is decoded first, and then the decoded symbol is cancelled in the next layer peeling. Assuming that the detector decodes the first symbol correctly, the result can be used to mitigate the interference from the received vector regarding the symbols due to be decoded. By layer peeling, the interference caused by the already detected symbols is cancelled. The conventional structure of the SIC detection was given in [3, 42], and multiple channel inversion operations are required, which increases the computational complexity. For the case of ZF-SIC, the importance of the SIC usage is to reduce the effect of noise enhancement since the interference is already nulled due to the ZF technique. The ordering is based on the norm of the nulling vector, when at each stage of cancellation, the nulling vector is chosen that has the smallest norm to detect the corresponding data stream. The nulling vector $\mathbf{g}_1$ (the first row of the detection matrix $\mathbf{G}$) filters the received vector $\mathbf{y}$ as

$$\hat{x}_1 = \text{sgn}\left(\mathbf{g}_1^T \mathbf{y}\right),$$

where $\text{sgn}(\cdot)$ indicates a function that extracts the sign of a number.

Assuming $\hat{x}_1 = x_1$, by substituting x_1 from the received signal, the modified received signal can be rewritten as

$$\mathbf{y}_1 = \mathbf{y} - (\mathbf{H})_1 x_1,$$

where $(\mathbf{H})_1$ indicates the first column of the channel matrix $\mathbf{H}$. After detecting the first stream, the first channel column of $\mathbf{H}$ can be eliminated because it becomes useless. This operation needs to be repeated by N_t times until all the transmitted symbols are detected. The post-detection SNR gradually increases for each next symbol.

Precoding Techniques

All transmitter-based techniques that facilitate the detection at the receiver side are known as precoding methods, [43]. In downlink cellular networks, it was shown that significant throughput gains can be achieved if the base station is deployed with multiple antennas, [18]. Although using multiple antennas at the BS

results in higher multiplexing gains, the multi-user scenario can be highly affected by interference, i.e., each transmitted signal intended for a specific receiver causes multi-user interference to other receivers in the network. The advantages of MU-MIMO systems can be obtained by utilizing precoding techniques, for instance, in MU-MIMO systems precoding is essential to mitigate or minimize MUI. The current challenges and problems for MU-MIMO precoding can be listed as

- The BER and sum-rate performances
  Unlike the receivers in SU-MIMO systems, the users in MU-MIMO receive the signal affected by the noise and the inter-antenna and multi-user types of interference. However, the traditional ZF and MMSE-based precoding techniques can be still utilized in the MU-MIMO systems, they decrease the sum rate and BER performances, [43].

- Computational complexity
  With precoding schemes realized at the transmitter side, the required computational power at each mobile station can be significantly reduced, and, consequently, the user architecture can be simplified, [12]. To achieve the maximum diversity order, MU-MIMO BC needs to be decomposed into multiple individual parallel SU-MIMO channels because of the MUI. And traditional techniques used for the channel parallelization come at the price of the considerable computational complexity. Therefore, it is regarded as a challenge to design an appropriate precoding technique that simultaneously provides the acceptable overall performance and low computational complexity.

- Scalability for a large number of antennas
  In [44], the authors demonstrated that Large-scale MIMO systems can dramatically improve the achievable rate and channel reliability and can be very promising for the next generation of wireless communication systems. However, the proposed schemes in the literature are not always applicable and scalable to the case of Large-scale MIMO.

There are two main reasons that the precoding techniques are so important in wireless MIMO systems. One is that the precoding scheme is usually realized at the transmitter side before a signal transmission, and accordingly prevents the performance loss provoked by the interference and fading. Thus, the performance

of the MIMO system can be enhanced. On the other hand, it is well-known that a power supply at the transmitter side is usually not an issue and, subsequently, the base station has a tremendous computational capacity. Therefore, if the detection process moves to the transmitter side, the complexity of the user device can be reduced and an immense amount of power can be saved which is very important to consider in terms of the mobility of a mobile station.

There are various precoding schemes, each of which has been designed to meet a certain criterion, [11]. Based on how the transmitted signals are related to the input data streams, the precoding techniques are categorized as linear and nonlinear. Linear precoding can be outlined by its simplicity since the received signal is represented by a weighted version of the original data signal transformed at the transmitter. The nonlinear precoding can be characterized by nonlinear processing and achieves better performance compared to the linear precoding algorithms. However, nonlinear precoding techniques such as a dirty paper coding (DPC), [45, 46], and Tomlinson-Harashima precoding (THP), [47, 48], can be characterized with high complexity compared to the linear schemes.

Linear Precoding

To give a brief explanation of this precoding technique, we consider the simplest transmission scheme for multi-antenna downlink which is a linear channel inversion (CI), [49, 50], by which interference can be pre-cancelled at the BS to enable each mobile station to receive its intended interference-free signal. Note that the number of single-antenna receivers N has to be equal to or less than the number of available transmit antennas M, i.e., $N \leq M$. The BS aims to transmit a data vector $\mathbf{s} \in \mathbb{C}^{N\times 1}$ which symbols are designed to different N receivers. Assuming the CSI available at the transmitter, the data signal $\mathbf{x}$ in (2.1) transmitted from the base station can be expressed as

$$\mathbf{x}_{CI} = f_{CI}\mathbf{\Phi}_{CI}\mathbf{s}, \tag{2.16}$$

where the precoding matrix is $\mathbf{\Phi}_{CI} = \mathbf{H}^H \left(\mathbf{H}\mathbf{H}^H\right)^{-1}$, and the scaling factor f_{CI} can be defined as, [49],

$$f_{CI} = \frac{1}{\sqrt{\text{trace}\left[(\mathbf{H}\mathbf{H}^H)^{-1}\right]}}, \tag{2.17}$$

where $\mathbb{E}\left\{\mathbf{s}\mathbf{s}^H\right\} = \mathbf{I}$. After substitution, the received signal (2.1) can be presented

as follows

$$\begin{aligned}\mathbf{y}_{CI} &= \sqrt{P}\mathbf{H}\mathbf{x} + \mathbf{n} \\ &= \sqrt{P} f_{CI} \mathbf{H}\boldsymbol{\Phi}_{CI}\mathbf{s} + \mathbf{n} \\ &= \sqrt{P} f_{CI} \underbrace{\mathbf{H}\mathbf{H}^H \left(\mathbf{H}\mathbf{H}^H\right)^{-1}}_{\text{interference cancellation}} \mathbf{I}\mathbf{s} + \mathbf{n} \\ &= \sqrt{P} f_{CI}\mathbf{s} + \mathbf{n}, \end{aligned} \tag{2.18}$$

where P is the transmit power. As shown, all the intra-cell interference is cancelled and each mobile station receives a scaled version of the transmitted signal which can be easily recovered. And, consequently, the output SNR of each mobile station is equal to

$$\rho_{CI} = \frac{P f_{CI}^2}{\sigma^2}. \tag{2.19}$$

Due to the fact that some signals can experience a deep fade, the channel matrix might be ill-conditioned. Thus, taking the inverse of the $\mathbf{H}\mathbf{H}^H$ can be challenging. In this case, an addition of the appropriate identity matrix before inverting can significantly improve the CI performance. The modified CI technique is named as the Regularized Channel Inversion (RCI), [49, 51]. Therefore, the signal transmitted from the BS can be written as

$$\mathbf{x}_{RCI} = f_{RCI}\boldsymbol{\Phi}_{RCI}\mathbf{s}, \tag{2.20}$$

where the RCI precoder is defined as follows

$$\boldsymbol{\Phi}_{RCI} = \mathbf{H}^H \left(\mathbf{H}\mathbf{H}^H + \varepsilon\mathbf{I}\right)^{-1}, \tag{2.21}$$

where ε indicates the regularization parameter given as $\varepsilon = N\rho^{-1}$ where ρ is the nominal SNR, [51]. The scaling factor can be then expressed in the same manner as for CI precoding as

$$f_{RCI} = \frac{1}{\sqrt{\text{trace}\left[\left(\mathbf{H}\mathbf{H}^H + \varepsilon\mathbf{I}\right)^{-1}\mathbf{H}\mathbf{H}^H\left(\mathbf{H}\mathbf{H}^H + \varepsilon\mathbf{I}\right)^{-1}\right]}}, \tag{2.22}$$

where this factor satisfies the unity power constraint at the BS. If the CI precoding cancels all the interference, the RCI precoding scheme allows to have some interference in the received signal.

Nonlinear Precoding

Though RCI provides a linearly increasing transmission rate with respect to the number of antennas it is still far from achieving the theoretical capacity of a MIMO channel. A step towards achieving this goal has been proposed in [52, 53, 54]. Theoretical work of Costa in [45] showed that the capacity of fading channel with interference is equal to that of an interference-free AWGN channel under the assumption that the transmitter has knowledge of the interference. In practical downlinks, the knowledge of CSI and all symbols to be transmitted allows the expected interference to be measured. Therefore the potential for achieving AWGN channel capacity exists. The aforementioned conclusion stimulated research towards this direction and subsequently introduced "dirty paper" precoding techniques, [54].

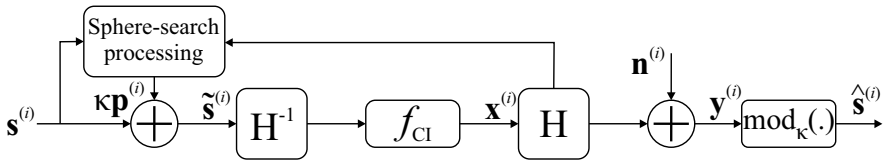

Figure 2.3. A block diagram of DPC in MIMO systems.

In more practical MIMO systems, the dirty paper coding, [54], can be applied as shown in Fig. 2.3. A perturbation quantity is added to the signal to be transmitted such as

$$\tilde{\mathbf{s}}^{(i)} = \mathbf{s}^{(i)} + \kappa\mathbf{p}^{(i)}. \tag{2.23}$$

Then the CI-processed received signal can be written as

$$\begin{aligned}\mathbf{y}^{(i)} &= f_{CI}\mathbf{H}\mathbf{H}^{H}\left(\mathbf{H}\mathbf{H}^{H}\right)^{-1}\tilde{\mathbf{s}}^{(i)} + \mathbf{n}^{(i)} \\ &= f_{CI}\left(\mathbf{s}^{(i)} + \kappa\mathbf{p}^{(i)}\right) + \mathbf{n}^{(i)}\end{aligned} \tag{2.24}$$

The initial symbols can be retrieved by dividing by f_{CI} and applying the modulo operation

$$\hat{\mathbf{s}}^{(i)} = \mathrm{mod}_{\kappa}\left(\frac{1}{f_{CI}}\left(f_{CI}\tilde{\mathbf{s}}^{(i)} + \mathbf{n}^{(i)}\right)\right)$$

$$= \mathrm{mod}_{\kappa}\left(\mathbf{s}^{(i)} + \kappa\mathbf{p}^{(i)} + \frac{\mathbf{n}^{(i)}}{f_{CI}}\right)$$
$$= \mathbf{s}^{(i)} + \mathrm{mod}_{\kappa}\left(\frac{\mathbf{n}^{(i)}}{f_{CI}}\right). \tag{2.25}$$

The base of the modulo operation κ, which is used in the precoding in (2.23) is calculated as

$$\kappa = 2\left(\mu_{\max} + \frac{\Delta}{2}\right), \tag{2.26}$$

where $\mu_{\max}$ and Δ indicate the largest magnitude of the symbol constellation and the spacing between the constellation points, respectively. Due to the noise term in (2.25), it is obvious that the scaling factor should be increased.

2.3.2 MAC Layer

If interference in the physical layer is not fully removed, then how to design MAC layer will be an issue.

The interference between multiple sessions is the prevailing challenge for the multi-source networks comprising of multiple Tx-Rx pairs. Currently, in wireless networks, interference is mainly treated in two main ways. First, interference in some systems can be avoided by orthogonalization, i.e., at any given point in frequency domain (or time), only one transmitter is active. On the other hand, interference can be ignored by treating it as additional noise, i.e., some communication strategies can deal with increased noise level. These strategies can be adopted to the collision avoidance and detection MAC protocols and cell planning in cellular systems. However, from the fundamental perspective, these two treatments are not sufficient to obtain optimal performance. In [55, 56], it was shown that decoding interference first and then decoding the intended message can enhance the achievable rate region compared to orthogonalization and treating interference as additional noise when the cross-channel gains are sufficiently large.

The most conventional technique dealing with the ICI is to manage the frequency usage over different network channels. The network elements utilize frequency reuse planning algorithms to restrain or assign certain resources (frequency and time) and power levels among users in different cells. These techniques aim to enhance the signal-to-interference-plus-noise ratio (SINR) and allow the network to support the maximum number of users; at the same time, they

must meet the power constraint in each cell by ensuring that the transmission power allocated to the BS does not exceed the maximum acceptable. The most common concept of interference avoidance schemes lies in a classification of users according to their average SINR to a number of users classes (cell regions). Then, these schemes apply different reuse factors to frequency bands utilized by different cell regions.

Interference avoidance techniques can be classified as static and dynamic. Static methods include conventional hard frequency planning schemes, fractional frequency reuse (FFR), [57, 58, 59], partial frequency reuse (PFR), [60, 61], and soft frequency reuse (SFR), [62, 63]. Static allocation schemes can be characterized by a radio planning process during which the resources allocated to each cell and cell region are calculated and evaluated and only their long-term readjustments can be performed during the network operation. This implies that a certain set of the allocated subcarriers and power levels is static. It is relatively easy to implement these schemes as they do not require frequent signalling flow among involved BSs. However, once this allocation algorithm is employed, it is difficult to modify the major frequency distributions, [64]. Accordingly, these techniques do not meet dynamic demand changes per sector as it adapts to the cell loads only by changing power used over different subcarriers. This consequently leads to significant performance degradation in terms of cell and user throughput, [65]. Hence, it is found to be critical to design the interference coordination schemes that can adapt to different network interference conditions, user traffic load, and user distribution in order to maximize the total network throughput. Cell coordination means that the interference reduction is performed in real time by using adaptive algorithms to efficiently control the resource usage among cells without apriori resource partitioning. However this solution represents a flexible framework with no required apriori frequency planning, it may need extra signalling between the involved BSs to perform the required coordination; this can be considered as an issue related to both overhead and delay. Coordination-based schemes can be categorized, based on the level of coordination, into four main categorizes: centralized, [66, 67, 68], semi-distributed, [61, 69], coordinated-distributed, [63, 70], and autonomous-distributed, [71, 72].

2.4 Interference Alignment

In multi-source networks, one of the main challenges is the interference arising from the simultaneous transmission of other sessions. As a result, it becomes extremely important for the overall network performance to efficiently manage interference from other sessions.

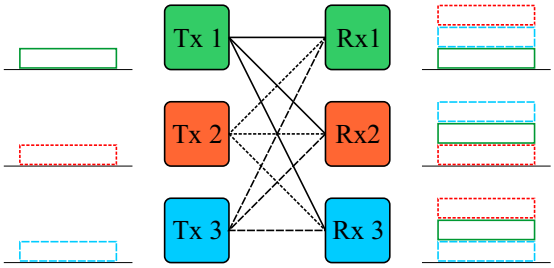

(a) Non-orthogonal transmission and decoding by treating interference as noise

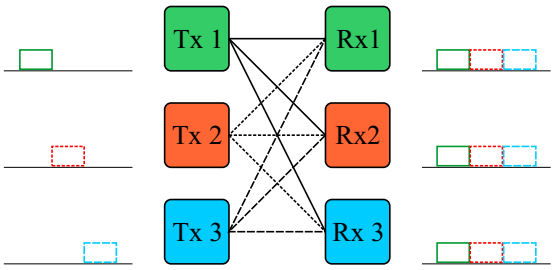

(b) Orthogonal transmission

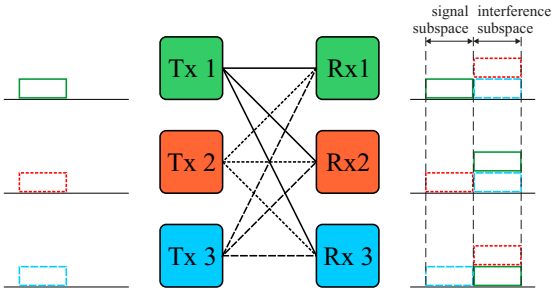

(c) Interference Alignment

Figure 2.4. Transmission modes in the three-cell interference network with single antenna per node, [2].

The traditional approaches, i.e., orthogonalization, characterizing it as noise, and interference decoding, turn out to be significantly suboptimal for general multi-source networks. Now the importance of IA in wireless interference networks can be more pronounced with the help of DoF. Interference alignment was proposed in [2] to achieve the optimal degrees of freedom of $\frac{K}{2}$ for the K-user

Gaussian interference channel (IC) with time-varying channel coefficients and minimizes the overall interference space by aligning the interfering signals from the undesired transmitters at each receiver. Considering that orthogonalization only provides one degree of freedom, IA can significantly improve the degrees of freedom region of the K-user IC, especially for large K.

By exploiting a diversity of tools from linear algebra, algebraic geometry as well as coding and traditional Shannon theory, the concept of interference alignment was successfully adapted to various network environments such as MIMO interference channels, [17, 73, 74], X-networks, [75, 76], cellular downlink and uplink, [77, 78, 79], lattice alignment, [80, 81, 82, 83], asymptotic alignment, [2, 84], asymmetric complex signal alignment, [85, 86], opportunistic alignment, [87, 88], ergodic alignment, [89, 90, 91], two-way communication networks, [92, 93, 94], blind alignment, [95, 96, 97], and retrospective alignment schemes, [98, 99], multicast and compound networks, [100, 101], and index coding networks, [102, 103], to name a few.

IA is a broad area of research and it mainly falls within two separate fields. The first one includes information theoretic studies like the achievable DoF, [2, 17, 85], and the second one includes signal processing aspects like assessing the feasibility conditions, [104, 105], or designing different algorithms meant for particular scenarios or/and based on different optimization criteria. Designing IA algorithms can be split into distinct directions. For example, while some IA schemes have been designed based on symbol extension across time or frequency, [2, 85, 106], some other IA techniques have been proposed by relying on the signal space alignment using multiple antennas, [107, 108, 109, 110, 111], to cancel the interference. These IA schemes, which have been set upon the spatial dimensions, are mostly iterative but dissolve the need of symbol extension across time or frequency, and therefore they are more practical and appealing. Of such schemes, minimum weighted leakage interference (Min-WLI), [107], alternating minimization (Alt-Min), [112], Max-SINR, [107], weighted MMSE, [108], and rank constrained rank minimization (RCRM), [110], are the most representative IA algorithms. Consequently, in this thesis, we place our focus on both information theoretic and signal processing aspects of IA by addressing the achievable sum rates and DoF under imperfect CSI, feasibility conditions of IA in partially coordinated networks and also designing new non-iterative IA techniques based on the concept of signal space alignment using multiple antennas.

2.4.1 IA scheme for MIMO Interference Networks

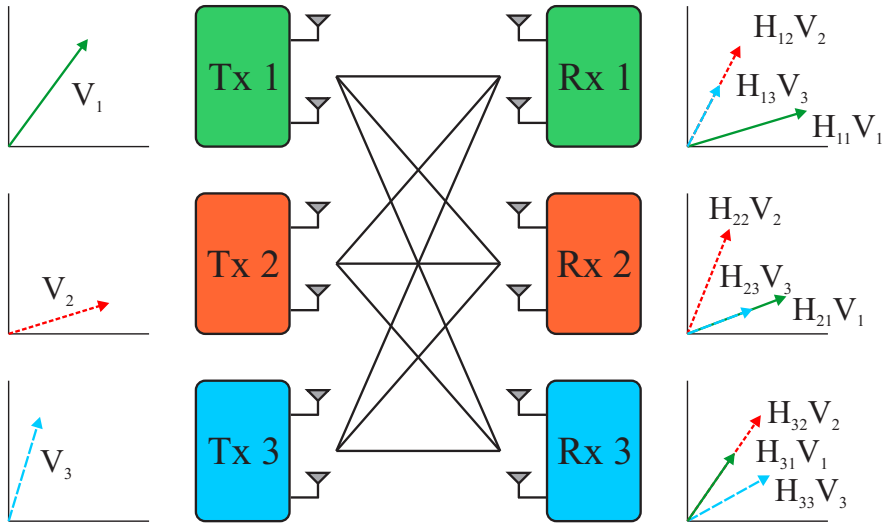

Figure 2.5. The three-cell SU-MIMO network with two antennas per node.

In this section, a simple example is provided to show how IA can be proceeded for the three-cell MIMO network with a single MIMO user per cell where each node is deployed with M antennas and each receiver desires to obtain $\frac{M}{2}$ DoF (for the sake of simplicity, M is assumed to be an even number). Then, the received signal at the user of interest can be written as

$$\mathbf{y}_j = \sum_{i=1}^{L=3} \mathbf{H}_{j,i}\mathbf{x}_i + \mathbf{n}_j, \ \forall i \in \{1,2,3\}, \tag{2.27}$$

where $\mathbf{H}_{j,i} \in \mathbb{C}^{M\times M}$ is the channel matrix between transmitter i and receiver j, and $\mathbf{x}_i \in \mathbb{C}^{M\times 1}$ stands for the transmitted signal from transmitter i. $\mathbf{n}_i \in \mathbb{C}^{M\times 1}$ is the zero-mean AWGN vector. The channel is assumed to be time-invariant and does not change during transmission. Each transmitter i sends $\frac{M}{2}$ independent data streams $\mathbf{s}_i \in \mathbb{C}^{\frac{M}{2}\times 1}$ as follows

$$\begin{aligned}\mathbf{x}_i &= \mathbf{V}_i\mathbf{s}_i \\ &= \sum_{k=1}^{M/2} \mathbf{v}_i^{[k]} s_i^{[k]}, \ \forall i \in \{1,2,3\},\end{aligned} \tag{2.28}$$

where $\mathbf{V}_i$ is the transmit BF matrix exploited at transmitter i and $\mathbf{v}_i^{[k]}$ denotes the k^{th} column vector of $\mathbf{V}_i$ carrying the symbol $s_i^{[k]}$. With this, the received

signal can be rewritten as

$$\mathbf{y}_j = \sum_{i=1}^{L=3} \mathbf{H}_{j,i}\mathbf{V}_i\mathbf{c}_i + \mathbf{n}_j, \ \forall i \in \{1,2,3\}. \tag{2.29}$$

Each receiver attempts to recover the desired message from the received signal while other two extra data sets interfere with the user of interest. To align the interfering signals at the receiver side, the transmit beamforming (BF) matrices $\mathbf{V}_1$, $\mathbf{V}_2$ and $\mathbf{V}_3$ need to satisfy the following conditions

$$\text{Alignment at Rx 1}: \quad \text{span}\left(\mathbf{H}_{1,2}\mathbf{V}_2\right) = \text{span}\left(\mathbf{H}_{1,3}\mathbf{V}_3\right), \tag{2.30}$$

$$\text{Alignment at Rx 2}: \quad \text{span}\left(\mathbf{H}_{2,1}\mathbf{V}_1\right) = \text{span}\left(\mathbf{H}_{2,3}\mathbf{V}_3\right), \tag{2.31}$$

$$\text{Alignment at Rx 3}: \quad \text{span}\left(\mathbf{H}_{3,1}\mathbf{V}_1\right) = \text{span}\left(\mathbf{H}_{3,2}\mathbf{V}_2\right), \tag{2.32}$$

where $\text{span}\left(\cdot\right)$ indicates the space spanned by the column vectors of a matrix, [2, 113].

Outline, [114]. Let $\mathbb{A}$ denote a matrix space over $\mathbb{F}$. Given matrices $\mathbf{A}_1$, $\mathbf{A}_2, \ldots, \mathbf{A}_m \in \mathbb{A}$, a matrix $\mathbf{A} \in \mathbb{A}$ is a linear combination of $(\mathbf{A}_1, \mathbf{A}_2, \ldots, \mathbf{A}_m)$ if there exist scalars $a_1, \ldots, a_m \in \mathbb{F}$ such that

$$\mathbf{A} = a_1\mathbf{A}_1 + a_2\mathbf{A}_2 + \cdots + a_m\mathbf{A}_m.$$

Definition. The linear span (or simply span) of $(\mathbf{A}_1, \mathbf{A}_2, \ldots, \mathbf{A}_m)$ is defined as

$$\text{span}(\mathbf{A}_1, \mathbf{A}_2, \ldots, \mathbf{A}_m) := \left\{a_1\mathbf{A}_1 + \cdots + a_m\mathbf{A}_m | a_1, \ldots, a_m \in \mathbb{F}\right\}.$$

It is worth to mention that assuming perfect aligning allows one to write the interfering signals in (2.30)–(2.32) as

$$\begin{aligned}
\mathbf{H}_{1,2}\mathbf{V}_2 &= \mathbf{H}_{1,3}\mathbf{V}_3, \\
\mathbf{H}_{2,1}\mathbf{V}_1 &= \mathbf{H}_{2,3}\mathbf{V}_3, \\
\mathbf{H}_{3,1}\mathbf{V}_1 &= \mathbf{H}_{3,2}\mathbf{V}_2,
\end{aligned}$$

where equality of the spanned spaces implies that the arguments of the function equal each other. With this in mind, it is feasible to express the beamforming

matrices as follows

$$\begin{aligned}\mathbf{V}_2 &= \mathbf{H}_{1,2}^{-1}\mathbf{H}_{1,3}\mathbf{V}_3,\\ \mathbf{V}_3 &= \mathbf{H}_{2,3}^{-1}\mathbf{H}_{2,1}\mathbf{V}_1,\\ \mathbf{V}_1 &= \mathbf{H}_{3,1}^{-1}\mathbf{H}_{3,2}\mathbf{V}_2,\end{aligned}$$

After substituting the beamforming matrices, we obtain

$$\text{span}\left(\mathbf{V}_1\right) = \text{span}\left(\mathbf{H}_{2,1}^{-1}\mathbf{H}_{2,3}\mathbf{H}_{1,3}^{-1}\mathbf{H}_{1,2}\mathbf{H}_{3,2}^{-1}\mathbf{H}_{3,1}\mathbf{V}_1\right).$$

Consequently, the interfering signals occupy only a subspace with $M/2$ dimensions and IA at receiver 1 is satisfied. Since the elements of $\mathbf{H}_{j,i}$ are drawn from i.i.d. distribution, the rank of the matrix equals M with probability 1. Then, equations (2.30)–(2.32) can be rewritten as

$$\begin{aligned}\text{span}\left(\mathbf{V}_1\right) &= \text{span}\left(\mathbf{T}\mathbf{V}_1\right),\\ \mathbf{V}_2 &= \mathbf{F}\mathbf{V}_1,\\ \mathbf{V}_3 &= \mathbf{J}\mathbf{V}_1,\end{aligned}$$

where

$$\begin{aligned}\mathbf{T} &= \mathbf{H}_{2,1}^{-1}\mathbf{H}_{2,3}\mathbf{H}_{1,3}^{-1}\mathbf{H}_{1,2}\mathbf{H}_{3,2}^{-1}\mathbf{H}_{3,1},\\ \mathbf{F} &= \mathbf{H}_{3,2}^{-1}\mathbf{H}_{3,1},\\ \mathbf{J} &= \mathbf{H}_{2,3}^{-1}\mathbf{H}_{2,1}.\end{aligned}$$

This can be solved as follows

$$\mathbf{V}_1 = \left[\mathbf{t}_1\ \mathbf{t}_2\ \cdots\ \mathbf{t}_{M/2}\right], \tag{2.33}$$

$$\mathbf{V}_2 = \mathbf{F}\left[\mathbf{t}_1\ \mathbf{t}_2\ \cdots\ \mathbf{t}_{M/2}\right], \tag{2.34}$$

$$\mathbf{V}_3 = \mathbf{J}\left[\mathbf{t}_1\ \mathbf{t}_2\ \cdots\ \mathbf{t}_{M/2}\right], \tag{2.35}$$

where $\mathbf{t}_k$ is the k^{th} eigenvector of $\mathbf{T}$.

To extract the desired message from the received signal, it is important to ensure that the desired signal and interference subspaces are linearly independent

This condition can be satisfied if the following is true

$$\begin{aligned}\text{rank}\left([\mathbf{H}_{1,1}\mathbf{V}_1 \quad \mathbf{H}_{1,3}\mathbf{V}_3]\right) &= M,\\ \text{rank}\left([\mathbf{H}_{2,2}\mathbf{V}_2 \quad \mathbf{H}_{2,1}\mathbf{V}_1]\right) &= M,\\ \text{rank}\left([\mathbf{H}_{3,3}\mathbf{V}_3 \quad \mathbf{H}_{3,1}\mathbf{V}_1]\right) &= M.\end{aligned}$$

In [2], it was shown that this condition can be surely satisfied. Therefore, a total DoF of $\frac{3M}{2}$ is achievable in the considered network model. Fig. 2.5 illustrates a network scenario when each node is deployed with $M = 2$ antennas and each transmitter sends one data stream. The users can extract their desired messages from the received signal by using ZF detector. If the feasibility conditions of IA are fulfilled, the transmit beamforming matrices and receive suppression matrices meet the following conditions

$$\mathbf{U}_j^H \mathbf{H}_{j,i} \mathbf{V}_i = \mathbf{0}, \ \forall i \neq j, \ j, i \in \{1, 2, 3\}, \tag{2.36}$$

$$\text{rank}\left(\mathbf{U}_j^H \mathbf{H}_{j,j} \mathbf{V}_j\right) = \frac{M}{2}, \ \forall j \in \{1, 2, 3\}, \tag{2.37}$$

where $\mathbf{U}_j$ is the receive suppression matrix at receiver j.

It is clear that a global CSI is required to be available at each node, i.e., $\mathbf{T}$ is needed to calculate (2.33)–(2.35) and also to find the ZF suppression matrix at each receiver.

Chapter 3

IA Cancellation in Compounded MIMO Broadcast Channels

In a multi-cell multi-user wireless network, each BS serves multiple users randomly distributed around the network. Considering a dense user distribution, it is feasible to assume that a certain number of users can be located in the overlapping area built by the intersection of the base stations. Therefore, any user in the cell-edge area is disadvantaged as the amount of power it receives from the serving BS is comparable to the power received from the non-serving BSs. Moreover, these users are heavily affected by the X-channel interference (XCI) due to the (served by the same BSs) users that are co-located in the overlapped area. Thus the SIR for these users tends to be relatively low. Consequently, the user performances such as BER and sum rate degrade.

3.1 Introduction

Interference alignment is a perspective idea that has recently facilitated the capacity analysis of interference affected networks. The concept of IA was proposed in [2] as an effective multi-user capacity achieving approach in the high SNR region. The core idea of IA lies in aligning all the interfering signals into a certain subspace at each receiving node so that an interference-free orthogonal subspace can be exclusively allocated for data transmission. In a relatively short time, a variety of IA algorithms have been proposed for MIMO IC networks, [17, 104, 105, 115, 116, 117, 118, 119, 120], X-channel networks, [75, 76, 121, 122, 123, 124], and cellular networks, [77, 78, 79, 125], to name a

few.

As was mentioned before, the authors in [2] achieved additional degrees of freedom in a SISO IC model by applying the idea of IA. It was shown that IA can achieve an optimal DoF of $\frac{K}{2}$ in a K-user time varying IC. In [17], the authors considered the case of K-user SIMO $1 \times N_r$ interference channel, where each transmitter is deployed with only one antenna. For this scenario, each user is able to achieve $\frac{N_r}{N_r+1}$ DoF, when $N_r < K$. The reciprocity property of the wireless network was established in [76, 126, 127] for the MISO IC scenario. Furthermore, for the case of K-user $N_r \times N_t$ MIMO network, the achievable total number of DoF is equal to

$$\text{DoF} = \begin{cases} K\min(N_r, N_t), \text{ if } K \leq R, \\ \frac{RK}{R+1}\min(N_r, N_t), \text{ if } K > R, \end{cases}$$

where $R = \frac{\max(N_r,N_t)}{\min(N_r,N_t)}$. Since IA solutions work best at high SNR, the proposed algorithm in [126] achieves some benefits at the low to intermediate SNR values and approaches total IA at high SNR. In [112], the authors proposed an alternative minimization approach that does not explicitly assume the channel reciprocity as in [126].

Work on the X-channel that was initiated in [121] discovered a surprisingly high DoF relative to the results in [117]. The remarkable DoF results of [75, 121] motivated the work in [123] where an IA scheme was presented for the two-user X-channel, which does not rely on dirty paper coding, successive decoding or iterative solutions. For the case of a two-user X-channel, where all nodes are equipped with three antennas, each user achieves two DoF. In [76], the authors determined the DoF of $N \times M$ X-networks consisting of M single-antenna transmitters and N single-antenna receivers. It was shown that a total of $\frac{MN}{M+N-1}$ DoF can be achieved in this setting under time-varying channels. Moreover, the authors in [124] proposed a one-sided IA decomposition scheme for $M \times N$ user MIMO X-networks that can achieve $A\left(\frac{MN}{M+N-1}\right)$ DoF with A antennas at each node.

The authors in [78] proposed an IA scheme and subsequently characterized the DoF region for cellular networks. This was based on aligning interference into a multi-dimensional subspace for a synchronous alignment at multiple non-intended BSs. In multi-cell MIMO Gaussian interfering broadcast channels (GIBC), each BS serves multiple users within a corresponding cell. In [128], the ZF scheme for the MIMO-GIBC was extended to the case of multiple receiver antennas.

The authors provided a precise expression for the achievable DoF region in the case of two mutually interfering MIMO BCs using a linear transceiver. On the other hand, the authors in [77] developed an IA technique for a downlink cellular system which requires feedback only within each cell. The scheme provided a substantial gain, especially, when interference from a dominant interferer is significantly stronger than the remaining interference. On the other hand, for a two-cell MIMO-GIBC, the authors in [79] proposed a novel IA technique for jointly designing the transmitter and receiver BF vectors using a closed-form expression and without the need for iterative computation.

3.2 Main Contributions

In this Chapter, we propose a closed-form downlink interference alignment beamforming scheme for a multi-cell MU-MIMO. We consider the scenario when multiple users per cell are located in the overlapped area with each user experiencing interference from $(L-1)$ BSs, where L is the number of cells. Furthermore, we devise a transmission scheme in which each BS sends signals to multiple users in different cells simultaneously; hence, each user in the network receives data from more than one BS. As such, this scenario is described as a compounded broadcast scenario in which, the user of interest can classify the observed channels as inter-channel interference and inter-stream, i.e. X-channel, interference links. To be more specific, inter-channel interference represents interference coming from a nonserving BS that does not transmit any useful data to this user while inter-stream interference indicates a portion of the signal from the serving BS that designated to another user and subsequently treated as interference at the user of interest. Compared with [79], where the authors proposed a two-step algorithm to mitigate only IC interference within the two-cell scenario, our two-step IA scheme is designed to eliminate both the IC and X-channel interference for any number of interfering cells. By utilizing the proposed technique, the multi-cell MU-MIMO can be transformed into a set of single-cell SU-MIMO channels. This makes the BER performance for each user similar to the BER performance of the SU-MIMO network scenario irrespective of the number of cells. In terms of sum rates, the proposed scheme is able to achieve up to $(L-1)$ DoF for every user and for any number of users located in the overlapped area. We also derive the relationship between the essential network elements such as the transmit/receive antennas,

cells, users and data streams at each BS. Therefore, the proposed scheme allows us to implement interference alignment using less antenna resources. Finally, we quantify the impact of CSI quality on the system performances.

We compare the proposed algorithm with the Zero-Forcing beamforming (ZFBF) technique, [50]. Since a key idea of ZFBF is block diagonalization, [129], this technique is feasible to be implemented in a wireless network with IC channels. As a result, all users obtain the desired signal transmitted from a certain BS. But, under our scenario when the user of interest also observes the presence of the X-channels, ZFBF can not be regarded as an appropriate technique to combat all types of interference presented in the system model. Moreover, our technique implements the grouping method that allows us to calculate the effective direction of inter-channel interference for a group of users.

3.3 System Model

The system model considered here presents a cellular MIMO network comprising of L cells with each cell serving multiple users. For simplicity, it is assumed that all cells have an equal coverage area and serve the same number of users per cell, K, randomly distributed as shown in Fig. 3.1. The user of interest is defined as user $[j,k]$, [113, 130], where j and k are the cell and user indexes, respectively, i.e., the k^{th} user within cell j which it nominally belongs to. Therefore, each user decodes the received signal by multiplying it with a receiver beamforming matrix; the received signal can be then written as follows

$$\tilde{\mathbf{y}}_j^{[k]} = \underbrace{\mathbf{U}_j^{[k]\,H}\mathbf{H}_{j,j}^{[k]}\mathbf{V}_j\mathbf{s}_j}_{\text{desired signal}} + \underbrace{\mathbf{U}_j^{[k]\,H}\sum_{i=1,i\neq j}^{L}\mathbf{H}_{j,i}^{[k]}\mathbf{V}_i\mathbf{s}_i + \tilde{\mathbf{n}}_j^{[k]}}_{\text{interference}},\ \forall j \in L,\ \forall k \in K, \tag{3.1}$$

where $\mathbf{U}_j^{[k]} \in \mathbb{C}^{N_r \times d_s}$ stands for a receive BF matrix at user $[j,k]$, and $\tilde{\mathbf{n}}_j^{[k]} = \mathbf{U}_j^{[k]\,H}\mathbf{n}_j^{[k]} \in \mathbb{C}^{d_s \times 1}$ is the effective zero-mean AWGN vector at the output of the beamformer, with $\mathbb{E}\{\tilde{\mathbf{n}}_j^{[k]}\tilde{\mathbf{n}}_j^{[k]H}\} = \sigma_{\tilde{n}}^2\mathbf{I}$. $\mathbf{H}_{j,i}^{[k]} \in \mathbb{C}^{N_r \times N_t}$ indicates the channel between the user of interest and BS i, where each entry of $\mathbf{H}_{j,i}^{[k]}$ is modeled by i.i.d. random variables (RVs) according to $\mathcal{CN}(0,1)$, [19, 79]. Moreover, each channel is assumed to be quasi-stationary and frequency flat fading. $\mathbf{V}_i \in \mathbb{C}^{N_t \times d_s}$ is a transmit BF matrix, with $\text{trace}\{\mathbf{V}_i\mathbf{V}_i^H\} = 1$, where d_s is the number of data streams transmitted from each BS. It is also assumed that $\mathbf{s}_i$ is the vector

containing the symbols drawn from i.i.d. Gaussian input signaling and chosen from a desired constellation, with $\mathbb{E}\{\mathbf{s}_i\mathbf{s}_i^H\} = \mathbf{I}$. All these conditions sufficiently satisfy the average power constraint at BS i.

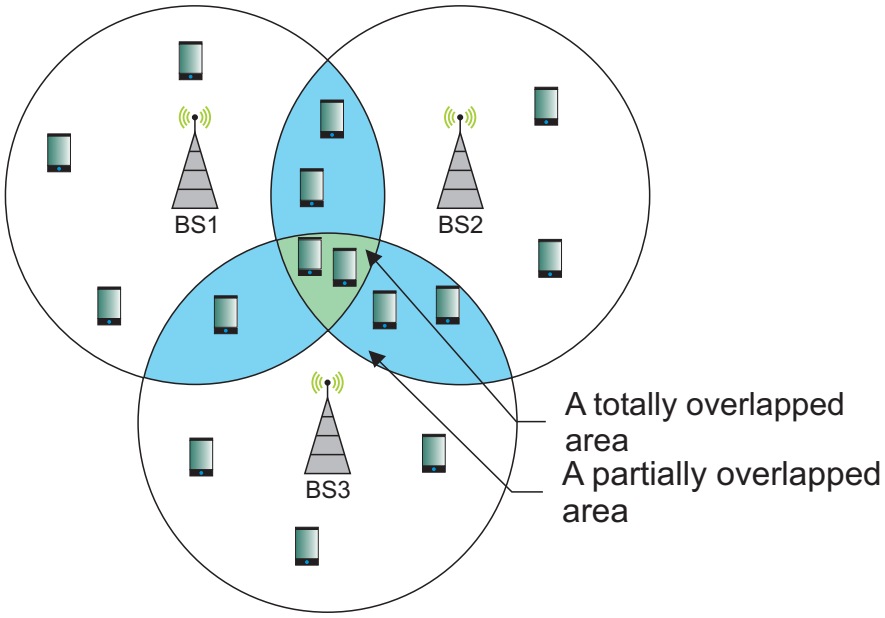

Figure 3.1. The three-cell MU-MIMO network with totally and partially overlapped areas.

To successfully decode the desired signal, it needs to be linearly independent of the interference, which can be obtained by allocating the desired signal into the orthogonal interference-free subspace along $\mathbf{U}_j^{[k]}$. Therefore, with respect to the considered network, the user of interest should meet the following conditions

$$\mathbf{U}_j^{[k]\,H}\mathbf{H}_{j,i}^{[k]}\mathbf{V}_i = \mathbf{0},\ i \neq j,\ \forall i, j \in L,\ \forall k \in K, \tag{3.2}$$

$$\text{rank}\left(\mathbf{U}_j^{[k]\,H}\mathbf{H}_{j,j}^{[k]}\mathbf{V}_j\right) = d_j^{[k]},\ \forall j \in L,\ \forall k \in K, \tag{3.3}$$

where $d_j^{[k]}$ is the maximum number of resolvable data streams at the receiver side.

Regarding the network coverage, the whole intersecting region can be classified as non-overlapped and overlapped areas, [131, 132], where the latter denotes the space where several BSs cover the same region. Hence, the number of BSs forming the overlapped area varies from 2 to L. According to the number of overlapping BSs, we can define totally and partially overlapped areas (Table 3.1).

Fig. 3.1 presents a multi-cell MU-MIMO network where each cell maintains multiple users. Moreover, under a dense network scenario, it can be assumed

Table 3.1. The cell area classification

The number of intersecting BSs, l	Area name	Notation
$l = 1$	Non-overlapped area	Area 1
$2 < l < L$	Partially overlapped area	Area 2
$l = L$	Totally overlapped area	Area 3

that each BS serves $\mathcal{K} \leq K$ users located in Area 3, and that $\mathcal{K}$ is the same for all L cells. Therefore, any user located in the overlapped area experiences the worst scenario when high interference degrades the network performance. This fact makes it important to analyse the network performances of these users.

Since a multi-cell MIMO network is based on the concept of a point-to-point MIMO model, we consider extreme network scenarios such as MIMO IC and X channels that are distinguishable from each other by a different message set. For example, the MIMO IC depicts a scenario when each BS i serves only the corresponding user i, while the MIMO X-channel can be described with a message set when each BS has an individual data designated to each user in the network.

Since receivers are commonly deployed with multiple antennas, it can be assumed that the user of interest in the totally overlapped area may be interested in data arriving from several base stations. Therefore, the considered network scenario can be classified as a compounded MIMO Broadcast Channel scenario when each cell consists of users experiencing a multi-source transmission from $\mathcal{L}$ BSs such that $1 < \mathcal{L} < L$.

To justify the concept of multi-source transmission, it needs to bear in mind that an immense volume of research has been done for the MIMO IC scenario, [17, 104, 105, 116, 117, 118], and for the MIMO X-network, [75, 76, 121, 122, 123], however network models characterized by a gap in message set ups between these two network scenarios have not been analysed yet and subsequently present a promising area for carrying future research. Thus, a certain user desires to receive data from several sources. Another proof of applicability of the multi-source transmission is the coordinated multipoint (CoMP) technology such as joint processing schemes for transmitting in the downlink when data is transmitted to the user of interest simultaneously from a number of different BSs, [133, 134, 135, 136, 137].

Hence, each user of interest can classify the observed network as a set of $(L - \mathcal{L})$ ICs and $\mathcal{L}$ X-channels, and then the corresponding types of interference

can be determined as the ICI and XCI, respectively. To consider all the types of interference, the system model has to consists at least of three cells. For simplicity, but without loss of generality, we can assume that the receivers, belonging to a certain cell, desire to decode the same data, however, the proposed scheme is also applicable for a scenario when receivers within one cell wish to obtain distinct messages from the respective base station. Accordingly, the signal designed to be transmitted from BS i can be expressed as

$$\mathbf{s}_i = \left[c^{[i,1]}\ c^{[i+1,2]}\ \cdots\ c^{[i+\mathcal{L}-1,\mathcal{L}]}\right]^T,\ \forall i \in L,\ 1 < \mathcal{L} < L, \tag{3.4}$$

where $c^{[j,l]}$ is the l^{th} entry of the signal sent from BS i to the receivers of cell j, and then the number of data streams at BS is equal to the number of cells interested in the particular message set ($d_s = \mathcal{L}$). The signal structure given in (3.4) implies that the first data stream transmitted from BS i is designated to the users belonging to cell i, while the second stream is dedicated to the users in cell $(i+1)$, and so on. The index numeration $(i+\mathcal{L}-1)$ changes circularly, e.g., for $\mathcal{L} = 2$ ($L = 3$) and $i = 3$, $(i+\mathcal{L}-1) = 4 \rightarrow 1$.

With respect to (3.4), the received signal in (3.1) can be rewritten as follows

$$\tilde{\mathbf{y}}_j^{[k]} = \underbrace{\mathbf{U}_j^{[k]\,H} \sum_{i=j-\mathcal{L}+1}^{j} \mathbf{H}_{j,i}^{[k]} \mathbf{V}_i \mathbf{s}_i}_{\text{desired+XCI signals}} + \underbrace{\mathbf{U}_j^{[k]\,H} \sum_{l=j+1, l\neq i}^{L} \mathbf{H}_{j,l}^{[k]} \mathbf{V}_l \mathbf{s}_l}_{\text{ICI}} + \tilde{\mathbf{n}}_j^{[k]},\ \forall j \in L,\ \forall k \in \mathcal{K}, \tag{3.5}$$

where the first term comprises of both the desired and XCI signals, while the second term stands for the ICI component. Consequently, it is feasible to split the transmit BF matrix into two parts as follows

$$\mathbf{V}_i = \mathbf{V}_i^{[ICI]} \times \mathbf{V}_i^{[XCI]},\ \forall i \in L, \tag{3.6}$$

where $\mathbf{V}_i \in \mathbb{C}^{N_t \times d_s}$, $\mathbf{V}_i^{[ICI]} \in \mathbb{C}^{N_t \times D}$ and $\mathbf{V}_i^{[XCI]} \in \mathbb{C}^{D \times d_s}$ are the complete transmit BF matrix and partial transmit beamformers responsible for the ICI and XCI, respectively. The cancellation schemes of the ICI and XCI terms are presented in Sections 3.4.1 and 3.4.2. D as the number of columns in matrix

$\mathbf{V}_i^{[ICI]}$, as well as the number of rows in matrix $\mathbf{V}_i^{[XCI]}$, depends on the number of data streams designated for each user. The value of D is generalised in Section 3.4.4.

We define the DoF region achievable by the user of interest as a pre-log factor of the sum rate, [17, 18], utilized to assess the performance of the multi-antenna system in the high SNR region defined as

$$\eta = \lim_{\mathrm{SNR}\to\infty} \frac{\mathcal{I}_j^{[k]}(\mathrm{SNR})}{\log_2(\mathrm{SNR})} = \mathcal{L},\ \forall j \in L,\ \forall k \in \mathcal{K}, \tag{3.7}$$

where $\mathcal{I}_j^{[k]}(\mathrm{SNR})$ is the data rate of the user of interest achievable at a given SNR, and $\mathcal{L}$ is the number of useful data sources which is equal to the interference-free data streams resolvable at user $[j,k]$. Thus, the sum rate can be defined as $\mathcal{I}_\Sigma(\mathrm{SNR}) = \sum_{j=1}^{L}\sum_{k=1}^{\mathcal{K}} \mathcal{I}_j^{[k]}(\mathrm{SNR})$. Therefore, from the network perspective, the total achievable DoF can be written as

$$\eta_{tot} = \lim_{\mathrm{SNR}\to\infty} \frac{\mathcal{I}_\Sigma(\mathrm{SNR})}{\log_2(\mathrm{SNR})} = L\mathcal{K}\mathcal{L},\ 1 < \mathcal{L} < L. \tag{3.8}$$

In the following section, we propose the closed-form transmit beamforming design for the three-cell compounded MIMO BC network scenario with $\mathcal{K} = 2$ users per cell. We then generalize this for the case of $L \geq 3$ and $\mathcal{K} \geq 1$.

3.4 Transmit Beamforming Design

Fig. 3.2 presents a MIMO network with $L = 3$ cells, where each cell serves an equal number of users ($\mathcal{K} = 2$) residing in Area 3. Therefore, generally speaking, each mobile station experiences the interference from two non-relative BSs ($\mathcal{L} = 2$). However, with respect to the signal structure given in (3.4), BSs transmit data signals to the receivers in the following manner. BS 1 sends the data vector $\mathbf{s}_1 = \left[c^{[1,1]}\ \ c^{[2,2]}\right]^T$ required to be decoded at the users in cells 1 and 2 and causing interference to cell 3. The data $\mathbf{s}_2 = \left[c^{[2,1]}\ \ c^{[3,2]}\right]^T$ transmitted from BS 2 needs to be delivered to the users belonging to cells 2 and 3, and, accordingly, $\mathbf{s}_2$ can be regarded as interference at the users in cell 1. Analogously, BS 3 with the signal $\mathbf{s}_3 = \left[c^{[3,1]}\ \ c^{[1,2]}\right]^T$ interferes with the mobile stations in cell 2, and, consequently, plans to deliver the message to the users in cells 1 and 3. Thus, all the channel

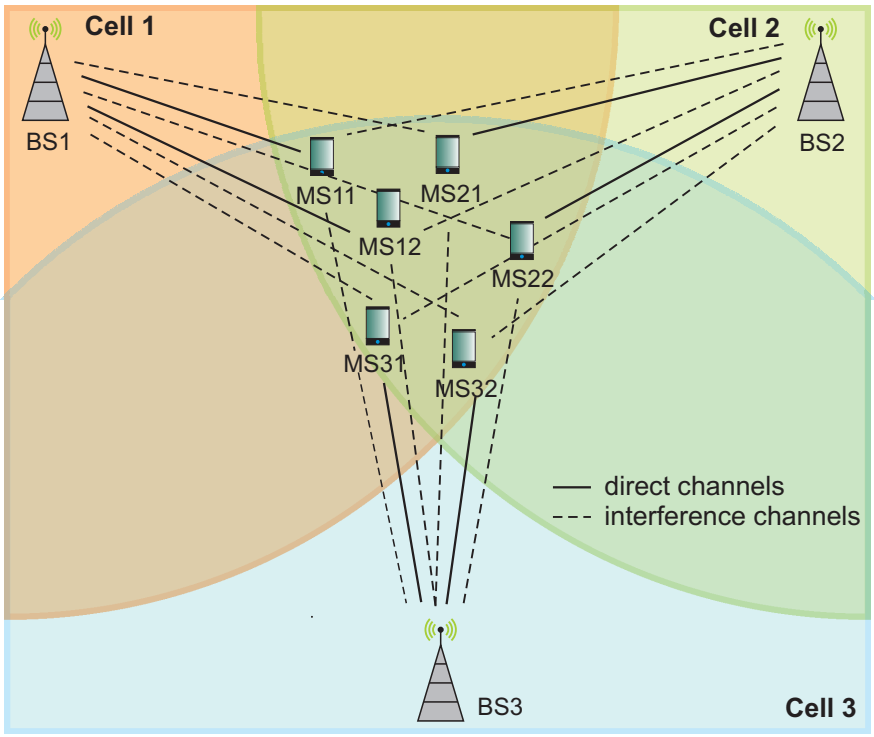

Figure 3.2. The MIMO network with three cells where each BS serves two users.

Table 3.2. Types of interference observed by the network users

Type 1 = ICI, Type 2 = XCI	BS 1	BS 2	BS 3
$\text{user}_{1,k}$	Type 2	Type 1	Type 2
$\text{user}_{2,k}$	Type 2	Type 2	Type 1
$\text{user}_{3,k}$	Type 1	Type 2	Type 2

links causing interference can be regarded as the IC channels (dashed lines in Fig. 3.3). Therefore, other channels, shown as solid lines in Fig. 3.3, convey the useful message signals to the corresponding groups of users.

Regarding the receiver side, the mobile stations of cell 1 take an interest only in $\left[c^{[1,1]} \;\; c^{[1,2]}\right]^T$, while receivers operating in cells 2 and 3 wish to receive the $\left[c^{[2,1]} \;\; c^{[2,2]}\right]^T$ and $\left[c^{[3,1]} \;\; c^{[3,2]}\right]^T$ signals, accordingly. However, with respect to (3.4) apart from the IC interference, each MS also observes the non-corresponding symbols transmitted from the desired BSs. In other words, each group of mobile stations in a particular cell desires to decode only a determined part of the message set arriving from the desired directions, and the rest of the delivered data is regarded as interference related to the X-channels (Table 3.2).

With this in mind, for the case given in Fig. 3.3, the received signal at the

user of interest can be rewritten as

$$\tilde{\mathbf{y}}_j^{[k]} = \underbrace{\mathbf{U}_j^{[k]\,H} \sum_{i=1,\, i\neq j+1}^{L=3} \mathbf{H}_{j,i}^{[k]} \mathbf{V}_i \mathbf{s}_i}_{\text{desired + XCI signals}} + \underbrace{\mathbf{U}_j^{[k]\,H} \mathbf{H}_{j,j+1}^{[k]} \mathbf{V}_{j+1} \mathbf{s}_{j+1}}_{\text{ICI}} + \tilde{\mathbf{n}}_j^{[k]},\ \forall j \in L,\ \forall k \in \mathcal{K}. \quad (3.9)$$

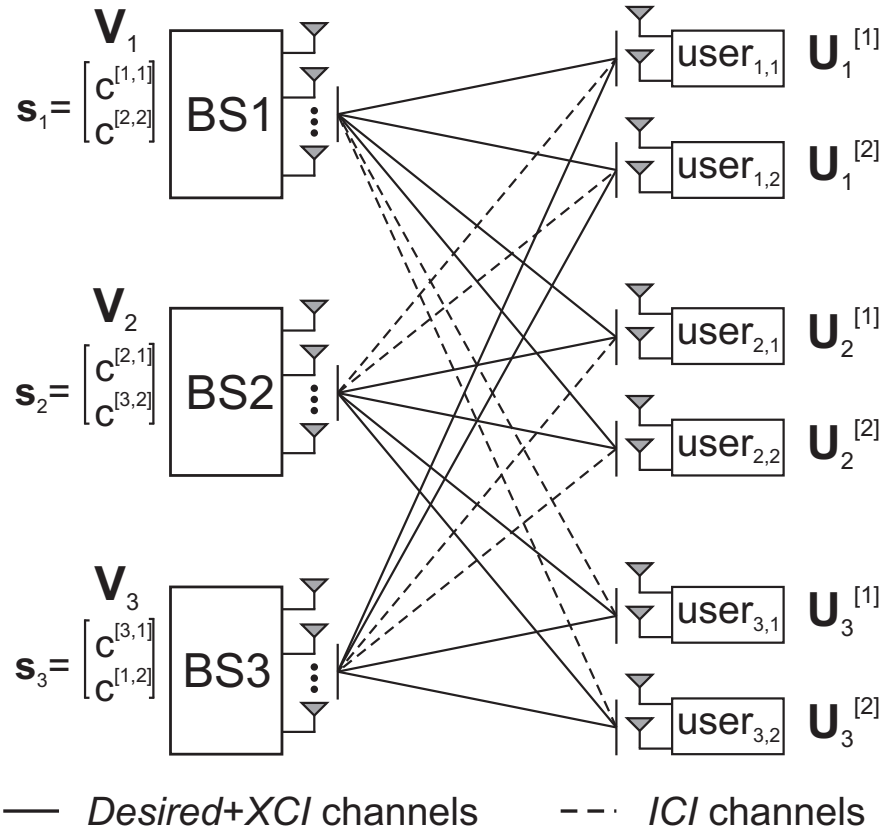

Figure 3.3. The three-cell MU-MIMO network with $\mathcal{K} = 2$ users in the totally overlapped area per cell.

3.4.1 The ICI Mitigation Scheme

The system model presented in Fig. 3.3 consists of three BSs with two receivers per cell residing in the totally overlapped area, and each MS desires to achieve two DoF. In order to explain the proposed IA-based interference mitigation scheme, it needs to consider the mobile stations belonging to cell 1. Due to the assumption

on the broadcast nature of transmission, the receivers in cell 1 are grouped to determine the mutual space spanned by the IC interference coming from BS 2, which can be written as

$$\mathbf{K}_2 = \text{span}\left(\mathbf{H}_{1,2}^{[1]H}\mathbf{U}_1^{[1]}\right) = \text{span}\left(\mathbf{H}_{1,2}^{[2]H}\mathbf{U}_1^{[2]}\right), \tag{3.10}$$

where span$(\cdot)$ indicates the subspace occupied by the matrix. $\mathbf{K}_2$ denotes the space spanning the IC interference caused by BS 2. Superscripts in (3.10) refer to a certain user within cell 1. Each spanned term in (3.10) can be written as

$$\mathbf{K}_2 - \mathbf{H}_{1,2}^{[1]H}\mathbf{U}_1^{[1]} = \mathbf{0}$$
$$\text{and}$$
$$\mathbf{K}_2 - \mathbf{H}_{1,2}^{[2]H}\mathbf{U}_1^{[2]} = \mathbf{0}.$$

Thus, it is possible to determine the intersecting subspace satisfying (3.10) by solving the following matrix equation

$$\begin{bmatrix} \mathbf{I}_{N_t} & -\mathbf{H}_{1,2}^{[1]H} & \mathbf{0} \\ \mathbf{I}_{N_t} & \mathbf{0} & -\mathbf{H}_{1,2}^{[2]H} \end{bmatrix} \begin{bmatrix} \mathbf{K}_2 \\ \mathbf{U}_1^{[1]} \\ \mathbf{U}_1^{[2]} \end{bmatrix} = \mathbf{C}_1\mathbf{D}_1 = \mathbf{0}, \tag{3.11}$$

where $\mathbf{K}_2$ stands for the effective interference direction from BS 2 to users of cell 1. Since the dimension of $\mathbf{C}_1$ is $(2N_t \times (N_t + 2N_r))$, its null space can be derived if only $2N_r > N_t$, which is not always feasible to equip receivers with a large number of antennas. When base stations and users are equipped with a large number of antennas, it becomes difficult to find the solutions. Therefore, to reduce the complexity and requirement on the number of receive antennas, we decompound (3.11) into two matrix equations as

$$\begin{bmatrix} \mathbf{I}_{N_t} & -\mathbf{H}_{1,2}^{[1]H} \end{bmatrix} \begin{bmatrix} \tilde{\mathbf{K}}_2^{[1]} \\ \tilde{\mathbf{U}}_1^{[1]} \end{bmatrix} = \tilde{\mathbf{C}}_1^{[1]}\tilde{\mathbf{D}}_1^{[1]} = \mathbf{0}, \tag{3.12}$$

$$\begin{bmatrix} \mathbf{I}_{N_t} & -\mathbf{H}_{1,2}^{[2]H} \end{bmatrix} \begin{bmatrix} \tilde{\mathbf{K}}_2^{[2]} \\ \tilde{\mathbf{U}}_1^{[2]} \end{bmatrix} = \tilde{\mathbf{C}}_1^{[2]}\tilde{\mathbf{D}}_1^{[2]} = \mathbf{0}, \tag{3.13}$$

where $\tilde{\mathbf{K}}_2^{[1]}$ and $\tilde{\mathbf{K}}_2^{[2]}$ indicate the directions of the interference arriving from BS 2 to MSs 1 and 2 residing in cell 1 (MS11 and MS12 in Fig. 3.2). Hence, it is

feasible to compute the nullspaces $\tilde{\mathbf{D}}_1^{[1]}$ and $\tilde{\mathbf{D}}_1^{[2]}$ of the $\tilde{\mathbf{C}}_1^{[1]}$ and $\tilde{\mathbf{C}}_1^{[2]}$ matrices, respectively. These nullspaces are always attainable because the dimensions of $\tilde{\mathbf{C}}_1^{[1]}$ and $\tilde{\mathbf{C}}_1^{[2]}$ are identical and equal to $N_t \times (N_t + N_r)$. Thus, the receive BF or suppression matrices always exist. The effective interference directions $\tilde{\mathbf{K}}_2^{[1]}$ and $\tilde{\mathbf{K}}_2^{[2]}$ will be utilized to design the transmit BF matrix $\mathbf{V}_2^{[ICI]}$ responsible for the ICI mitigation. After applying the interference suppression matrices, MS11 and MS12 are grouped together such that the IC interference from BS 2 is allocated in the $\tilde{\mathbf{K}}_2^{[1]}$ and $\tilde{\mathbf{K}}_2^{[2]}$ subspaces. To determine the receive BF matrix $\mathbf{U}_1^{[k]}$ from $\tilde{\mathbf{D}}_1^{[k]}$, we find the intersection of the subspaces spanned by $\tilde{\mathbf{K}}_2^{[k]}$ that is equal to the subspace spanned by $\mathbf{K}_2$, [113].

Similar to the mobile stations belonging to cell 1, we define the subspaces spanning the IC interference appearing in cells 2 and 3 as follows

$$\mathbf{K}_3 = \text{span}\left(\mathbf{H}_{2,3}^{[1]\,H}\mathbf{U}_2^{[1]}\right) = \text{span}\left(\mathbf{H}_{2,3}^{[2]\,H}\mathbf{U}_2^{[2]}\right), \tag{3.14}$$

$$\mathbf{K}_1 = \text{span}\left(\mathbf{H}_{3,1}^{[1]\,H}\mathbf{U}_3^{[1]}\right) = \text{span}\left(\mathbf{H}_{3,1}^{[2]\,H}\mathbf{U}_3^{[2]}\right). \tag{3.15}$$

Analogously, $\mathbf{K}_1$ and $\mathbf{K}_3$ are decomposed by applying (3.12)–(3.13). As a result, we obtain the corresponding sets of subspaces denoted as $\tilde{\mathbf{K}}_1^{[k]}$ and $\tilde{\mathbf{K}}_3^{[k]}$ ($\forall k \in \mathcal{K}$), and then derive the suppression matrices $\mathbf{U}_2^{[k]}$ and $\mathbf{U}_3^{[k]}$. Since, under the considered network model, each receiver observes only one ICI channel related to $\mathbf{K}_i$, the first component accountable for the ICI can be determined as

$$\mathbf{V}_i^{[ICI]} = \text{null}\left(\left[\mathbf{K}_i \ \left\{\left(\mathbf{U}_{i-1}^{[k]H}\mathbf{H}_{i-1,i}^{[k]}\right)^H\right\}\right]^H\right), \ \forall i \in L, \forall k \in \mathcal{K}, \tag{3.16}$$

where the index $(i-1)$ changes circularly, e.g., for $i = 1 \rightarrow (i-1) = 3$.

Hence, after applying the first part of the transmit beamforming matrices, the system model (see Fig. 3.3) can be regarded as an ICI-free network (without dashed lines).

3.4.2 The XCI Mitigation Scheme

After applying the ICI mitigation scheme, each user has two channel observations with one desired symbol per channel. Therefore, the received signal at any user

k in cell 1 can be expressed as

$$\begin{aligned}\tilde{\mathbf{y}}_1^{[k]} &= \mathbf{U}_1^{[k]\,H}\mathbf{H}_{1,1}^{[k]}\mathbf{V}_1^{[ICI]}\mathbf{V}_1^{[XCI]}\mathbf{s}_1 + \underbrace{\mathbf{U}_1^{[k]\,H}\mathbf{H}_{1,2}^{[k]}\mathbf{V}_2^{[ICI]}\mathbf{V}_2^{[XCI]}\mathbf{s}_2}_{\text{ICI}=0} \\ &\quad + \mathbf{U}_1^{[k]\,H}\mathbf{H}_{1,3}^{[k]}\mathbf{V}_3^{[ICI]}\mathbf{V}_3^{[XCI]}\mathbf{s}_3 + \tilde{\mathbf{n}}_1^{[k]} \\ &= \sum_{i=1,\, i\neq 2}^{L=3} \mathbf{U}_1^{[k]}\mathbf{H}_{1,i}^{[k]}\mathbf{V}_i^{[ICI]}\mathbf{V}_i^{[XCI]}\mathbf{s}_i + \tilde{\mathbf{n}}_1^{[k]},\ \forall k \in \mathcal{K}. \end{aligned} \tag{3.17}$$

Accordingly, this expression can be used for any user $[j,k]$ as follows

$$\tilde{\mathbf{y}}_j^{[k]} = \sum_{i=1,\, i\neq j+1}^{L=3} \mathbf{U}_j^{[k]H}\mathbf{H}_{j,i}^{[k]}\mathbf{V}_i^{[ICI]}\mathbf{V}_i^{[XCI]}\mathbf{s}_i + \tilde{\mathbf{n}}_j^{[k]},\ \forall j \in L, \forall k \in \mathcal{K}, \tag{3.18}$$

where, from the viewpoint of the data intended to the user of interest, $\mathbf{H}_{j,j}^{[k]}$ indicates the channel carrying the first stream from BS j to user $[j,k]$, while the channel $\mathbf{H}_{j,i}^{[k]}$ $(j \neq i)$ stands for the collateral one conveying the second stream from BS i desired by user $[j,k]$. The absence of the channel matrix $\mathbf{H}_{j,i}^{[k]}$ $(i = j+1)$ denotes the successive ICI cancellation.

For the current scenario, each cell maintains two mobile stations ($\mathcal{K} = 2$). Since the numbers of receive antennas and data streams at the BS are equal to each other ($d_s = N_r$), two dimensions are given to extract two desired symbols from four received symbols. This means that the second part of the transmit BF matrix has to deal with the other two symbols considered as the unwanted messages.

Since it is assumed that all mobile stations belonging to one cell tend to decode the same messages, each single channel matrix $\mathbf{H}_{j,i}^{[k]}$ between BS i and the user of interest can be combined as

$$\mathbf{H}_{j,i} = \begin{bmatrix} \mathbf{H}_{j,i}^{[1]} \\ \mathbf{H}_{j,i}^{[2]} \end{bmatrix},\ \forall i, j \in L, \tag{3.19}$$

where $\mathbf{H}_{j,i} \in \mathbb{C}^{\mathcal{K}N_r \times N_t}$ is the generic channel matrix, superscripts refer to the user's index within cell j, and $\mathcal{K} = 2$ users per cell in the totally overlapped area.

Since the transmitted signal vector $\mathbf{s}_i$ has a size of $d_s \times 1$, $\mathbf{V}_i^{[XCI]}$ has to consist of d_s columns. Therefore, the design of the second part of the transmit BF matrix

can be expressed as

$$\mathbf{V}_i^{[XCI]} = \left[\begin{array}{cc} \mathbf{p}_1^{[i]} & \mathbf{p}_2^{[i]} \end{array} \right], \ \forall i \in L, \tag{3.20}$$

where column vectors $\mathbf{p}_1^{[i]}$ and $\mathbf{p}_2^{[i]}$ aim to nullify interference under the X-channel scenario. These columns can be obtained by substituting (3.19) as follows

$$\mathbf{p}_1^{[i]} = \text{null}\left(\mathbf{H}_{j,i}\mathbf{V}_i^{[ICI]}\right) = \text{null}\left(\mathbf{J}_1^{[i]}\right), \ \forall i \in L, \tag{3.21}$$

$$\mathbf{p}_2^{[i]} = \text{null}\left(\mathbf{H}_{i,i}\mathbf{V}_i^{[ICI]}\right) = \text{null}\left(\mathbf{J}_2^{[i]}\right), \ \forall i \in L, \tag{3.22}$$

where $\mathbf{J}_1^{[i]} = \mathbf{H}_{j,i}\mathbf{V}_i^{[ICI]}$ and $\mathbf{J}_2^{[i]} = \mathbf{H}_{i,i}\mathbf{V}_i^{[ICI]}$ are the effective channels obtained by multiplication of the generic channel matrices (3.19) with the partial BF matrix responsible for the ICI mitigation (3.16). The former effective channel matrix stands for the collateral link between BS i and the mobile stations in cell j ($j \neq i$), while the latter denotes the direct effective channel from BS i to the users in cell i. To provide a well-designed transmit BF matrix responsible for the XCI, $\mathbf{V}_i^{[XCI]}$, we need to find at least one vector per each effective channel matrix satisfying (3.21)–(3.22). Thus, the dimension of $\mathbf{J}_l^{[i]}$ ($\forall i \in L, \forall l \in d_s$) is $2N_r \times (N_t - 2N_r)$. The way to solve (3.21)–(3.22) is to satisfy the condition arising from the dimension of $\mathbf{J}_l^{[i]}$ presented by $(N_t - 2N_r) > 2N_r$. With $N_r = 2$, a minimum number of columns of the effective channel matrix after applying the ICI mitigation algorithm equals five. The procedure given by (3.20)–(3.22) should be repeated for the rest of cells $i \in L$ ($L = 3$).

With this in mind, the received signal at the user of interest (3.18) can be rewritten in more details as follows

$$\begin{aligned}
\tilde{\mathbf{y}}_j^{[k]} &= \mathbf{U}_j^{[k]H} \sum_{i=1,\, i\neq j+1}^{L=3} \mathbf{H}_{j,i}^{[k]}\mathbf{V}_i^{[ICI]}\mathbf{V}_i^{[XCI]}\mathbf{s}_i + \tilde{\mathbf{n}}_j^{[k]} \\
&= \left[\begin{array}{cc} \tilde{h}_{j,j}^1 & 0 \\ \tilde{h}_{j,j}^2 & 0 \end{array} \right] \left[\begin{array}{c} c^{[j,1]} \\ c^{[j+1,2]} \end{array} \right] + \left[\begin{array}{cc} 0 & \tilde{h}_{j,i}^1 \\ 0 & \tilde{h}_{j,i}^2 \end{array} \right] \left[\begin{array}{c} c^{[i,1]} \\ c^{[j,2]} \end{array} \right] + \tilde{\mathbf{n}}_j^{[k]} \\
&= \left[\begin{array}{c} \tilde{h}_{j,j}^1 \\ \tilde{h}_{j,j}^2 \end{array} \right] c^{[j,1]} + \left[\begin{array}{c} \tilde{h}_{j,i}^1 \\ \tilde{h}_{j,i}^2 \end{array} \right] c^{[j,2]} + \tilde{\mathbf{n}}_j^{[k]} \\
&= \left[\begin{array}{cc} \tilde{h}_{j,j}^1 & \tilde{h}_{j,i}^1 \\ \tilde{h}_{j,j}^2 & \tilde{h}_{j,i}^2 \end{array} \right] \left[\begin{array}{c} c^{[j,1]} \\ c^{[j,2]} \end{array} \right] + \tilde{\mathbf{n}}_j^{[k]} \\
&= \tilde{\mathbf{H}}_j^{[k]}\mathbf{c}_j + \tilde{\mathbf{n}}_j^{[k]}, \ \forall j \in L, \forall k \in \mathcal{K},
\end{aligned} \tag{3.23}$$

where $\tilde{\mathbf{n}}_j^{[k]} = \mathbf{U}_j^{[k]H}\mathbf{n}_j^{[k]}$ stands for the effective noise AWGN vector. $\bar{\mathbf{H}}_j^{[k]}$ and $\mathbf{c}_j$ indicate the overall effective channel matrix and the vector of the desired symbols after applying the proposed algorithm, respectively. Each entry of $\bar{\mathbf{H}}$ is a random variable according to $\mathcal{CN}(0,\xi^2)$, with $\mathbb{E}\{\mathbf{U}_j^{[k]H}\mathbf{H}_{j,l}\mathbf{V}_l\mathbf{V}_l^H\mathbf{H}_{j,l}^H\mathbf{U}_j^{[k]}\} = \xi^2\mathbf{I}$ (BS l sends data to user of interest, $l \in L$).

From (3.23), it is seen that each mobile station detects the network as a 2×2 SU-MIMO with two data streams. Assuming perfect CSI, the achievable data rate of the user of interest can be computed by

$$\mathcal{I}_j^{[k]} = \log_2\left[\det\left(\mathbf{I} + \frac{\mathrm{SNR}}{N_r}\bar{\mathbf{H}}_j^{[k]}\bar{\mathbf{H}}_j^{[k]\,H}\right)\right],\ \forall j \in L, \forall k \in \mathcal{K}, \tag{3.24}$$

where $\bar{\mathbf{H}}_j^{[k]}$ denotes the effective channel matrix obtained in (3.23).

To validate the proposed technique, we calculate the achievable data rate of the user of interest at 30 dB which equals $\mathcal{I}_j^{[k]} = 19.78$ bits/s/Hz (Fig. 3.7). Therefore, each receiver achieves theoretical $\mathcal{L}$ DoF (for the considered network scenario $\mathcal{L} = 2$) such that $\frac{\mathcal{I}_j^{[k]}(30\ dB)}{\log_2(30\ dB)} = 1.9848 \approx 2$.

3.4.3 Imperfect CSI

In this Chapter, it is assumed so far perfect CSI, however, perfect CSI is highly idealistic because in practice CSI is presented by imperfect estimates of channel states which can degrade the network performance. To analyse the effect of the CSI mismatch, the model described in Chapter 2 is applied to the considered system model.

Therefore, under CSI mismatch the transmit and receive beamforming matrices are calculated according to the imperfect CSI and denoted by $\hat{(\cdot)}$. Thus, the received signal (3.17) at user $[1,k]$ can be rewritten as

$$\begin{aligned}\tilde{\mathbf{y}}_1^{[k]} = &\underbrace{\hat{\mathbf{U}}_1^{[k]\,H}\left(\frac{1}{\tau+1}\hat{\mathbf{H}}_{1,1}^{[k]} + \tilde{\mathbf{H}}_{1,1}^{[k]}\right)\hat{\mathbf{V}}_1^{[ICI]}\hat{\mathbf{V}}_1^{[XCI]}\mathbf{s}_1}_{\text{desired + XCI signals}}\\ &+\underbrace{\hat{\mathbf{U}}_1^{[k]\,H}\left(\frac{1}{\tau+1}\hat{\mathbf{H}}_{1,3}^{[k]} + \tilde{\mathbf{H}}_{1,3}^{[k]}\right)\hat{\mathbf{V}}_3^{[ICI]}\hat{\mathbf{V}}_3^{[XCI]}\mathbf{s}_3}_{\text{desired + XCI signals}}\\ &+\underbrace{\hat{\mathbf{U}}_1^{[k]\,H}\left(\frac{1}{\tau+1}\hat{\mathbf{H}}_{1,2}^{[k]} + \tilde{\mathbf{H}}_{1,2}^{[k]}\right)\hat{\mathbf{V}}_2^{[ICI]}\hat{\mathbf{V}}_2^{[XCI]}\mathbf{s}_2}_{\text{ICI}} + \tilde{\mathbf{n}}_1^{[k]}\end{aligned}$$

$$= \underbrace{\frac{1}{\tau+1}\hat{\mathbf{U}}_1^{[k]\,H}\hat{\mathbf{H}}_{1,1}^{[k]}\hat{\mathbf{V}}_1^{[ICI]}\hat{\mathbf{V}}_1^{[XCI]}\mathbf{s}_1}_{\text{desired signal, } \boldsymbol{\Upsilon}_1} + \underbrace{\frac{1}{\tau+1}\hat{\mathbf{U}}_1^{[k]\,H}\hat{\mathbf{H}}_{1,3}^{[k]}\hat{\mathbf{V}}_3^{[ICI]}\hat{\mathbf{V}}_3^{[XCI]}\mathbf{s}_3}_{\text{desired signals, } \boldsymbol{\Upsilon}_2}$$
$$+ \underbrace{\frac{1}{\tau+1}\hat{\mathbf{U}}_1^{[k]\,H}\hat{\mathbf{H}}_{1,2}^{[k]}\hat{\mathbf{V}}_2^{[ICI]}\hat{\mathbf{V}}_2^{[XCI]}\mathbf{s}_2}_{\text{ICI=0}} + \underbrace{\hat{\mathbf{U}}_1^{[k]\,H}\tilde{\mathbf{H}}_{1,2}^{[k]}\hat{\mathbf{V}}_2^{[ICI]}\hat{\mathbf{V}}_2^{[XCI]}\mathbf{s}_2}_{\text{ICI based on CSI mismatch, } \boldsymbol{\Psi}_1}$$
$$+ \underbrace{\hat{\mathbf{U}}_1^{[k]\,H}\tilde{\mathbf{H}}_{1,1}^{[k]}\hat{\mathbf{V}}_1^{[ICI]}\hat{\mathbf{V}}_1^{[XCI]}\mathbf{s}_1}_{\text{XCI based on CSI mismatch, } \boldsymbol{\Psi}_2} + \underbrace{\hat{\mathbf{U}}_1^{[k]\,H}\tilde{\mathbf{H}}_{1,3}^{[k]}\hat{\mathbf{V}}_3^{[ICI]}\hat{\mathbf{V}}_3^{[XCI]}\mathbf{s}_3}_{\text{XCI based on CSI mismatch, } \boldsymbol{\Psi}_3} + \tilde{\mathbf{n}}_1^{[k]}, \quad (3.25)$$
$$\forall k \in \mathcal{K}.$$

Thus, SINR of the user of interest in cell 1, $J_1^{[k]}$, can be defined as

$$J_1^{[k]} = \text{trace}\left\{\frac{|\boldsymbol{\Upsilon}_1|^2 + |\boldsymbol{\Upsilon}_2|^2}{|\boldsymbol{\Psi}_1|^2 + |\boldsymbol{\Psi}_2|^2 + |\boldsymbol{\Psi}_3|^2 + \tilde{\sigma}_n^2\mathbf{I}}\right\}, \ \forall k \in \mathcal{K}, \quad (3.26)$$

where $\sigma_{\tilde{n}}^2$ is variance of the effective noise vector $\tilde{\mathbf{n}}_1^{[k]}$.

Consequently, in the presence of CSI mismatch the achievable sum rate of the user of interest in cell 1, $\mathcal{I}_1^{[k]}$, can be expressed as

$$\mathcal{I}_1^{[k]} = \log_2\left(1 + J_1^{[k]}\right), \forall k \in \mathcal{K}. \quad (3.27)$$

Analogously, the sum rate of any user k in any cell j can be calculated by utilizing (3.25)–(3.27).

3.4.4 Generalization of the proposed scheme

It is worth noting that the case study with $L = 3$ and $\mathcal{K} = 2$ was based on the assumption $d_s = \mathcal{L} = 2$ with only one interfering channel link in each cell ($L - \mathcal{L} = 1$). Nonetheless, the proposed technique can be utilized for any case that can be defined as $L \geq 3, \mathcal{K} \geq 1$ and $2 \leq d_s \leq (L-1)$. For the sake of simplicity of explanation, it is assumed that each BS broadcasts the same message to each group of mobile stations in the same cell. The system model with the implemented compound MIMO BC defines the inequality conditions on the number of data streams (d_s) at the base station. For instance, the case of $d_s = 2$ comes from the minimal requirements to maintain the presence of the MIMO X-channel from the viewpoint of the receiver; the minimal X-channel scenario can be described by a 2×2 MIMO network configuration when two transmitters send individual

messages to each receiver. By the same token, for the case of $d_s = 1$, the network setting reduces to the conventional MIMO IC channel scenario. Then, we set the maximum number of data streams per user to keep at least one IC channel as $d_s = (L-1)$. Otherwise, for the case of $d_s = L$, the system model can be regarded as the complete MIMO X-channel where no base station causes the ICI to any receiver, and hence the grouping method is not applicable. And this case can be solved by applying only the XCI mitigation scheme. Finally, for the case of $2 < d_s < (L-1)$, it was demonstrated that each mobile station experiences more than one IC, and the interference can be mitigated by applying the idea of allocating the interfering signals in the subspace that is orthonormal to the combination of the desired signal and the XCI component.

Now we can calculate the minimum numbers of transmit and receive antennas required for an efficient design of the proposed scheme for any network case $L \geq 3,\ \mathcal{K} \geq 1$. Since the transmit BF matrix is decoupled into two parts as in (3.6), these requirements must satisfy the conditions for the existence of both $\mathbf{V}_i^{[ICI]} \in \mathbb{C}^{N_t \times D}$ and $\mathbf{V}_i^{[XCI]} \in \mathbb{C}^{D \times d_s}$ where D denotes a value that presents a connection amongst the above matrices.

Consider the $\mathbf{V}_i^{[XCI]}$ matrix. Since we have $d_s = \mathcal{L}$ data streams, equation (3.20) can be rewritten as

$$\mathbf{V}_i^{[XCI]} = \left[\mathbf{p}_1^{[i]}\ \mathbf{p}_2^{[i]}\ \cdots\ \mathbf{p}_{d_s}^{[i]}\right].$$

Based on (3.21)–(3.22) and the assumption $d_s = N_r$, we have to compute the $\mathbf{p}_l^{[i]}$ column vectors N_r times. Since it is assumed that all the receivers within a certain cell desire to decode the same message whose components arrive from different directions according to (3.4), we can combine all $\mathcal{K}$ channel links between BS i and the users of cell j in a generic channel matrix as

$$\mathbf{H}_{j,i} = \begin{bmatrix} \mathbf{H}_{j,i}^{[1]} \\ \vdots \\ \mathbf{H}_{j,i}^{[k]} \\ \vdots \\ \mathbf{H}_{j,i}^{[\mathcal{K}]} \end{bmatrix},\ \forall i, j \in L,\ \forall k \in \mathcal{K}. \tag{3.28}$$

Consequently, the dimension of the $\mathbf{J}_l^{[k]}$ matrix in (3.20)–(3.22) equals $\mathcal{K}N_r \times D$. Since we require a nullspace of dimension 1 at least, the first condition on D can

$$\begin{bmatrix} \mathbf{I}_{N_t} & -\mathbf{H}_1^{[1,2]H} & \mathbf{0} & \cdots & \mathbf{0} \\ \mathbf{I}_{N_t} & \mathbf{0} & -\mathbf{H}_1^{[2,2]H} & \cdots & \mathbf{0} \\ \vdots & \vdots & \mathbf{0} & \ddots & \vdots \\ \mathbf{I}_{N_t} & \mathbf{0} & \mathbf{0} & \cdots & -\mathbf{H}_1^{[K,2]H} \end{bmatrix} \begin{bmatrix} \mathbf{G}_1 \\ \mathbf{U}^{[1,2]} \\ \mathbf{U}^{[2,2]} \\ \vdots \\ \mathbf{U}^{[K,2]} \end{bmatrix} = \mathbf{F}_1\mathbf{X}_1 = \mathbf{0} \quad (3.30)$$

$$\begin{bmatrix} \mathbf{I}_{N_t} & -\mathbf{H}_{j,i}^{[1]H} & \mathbf{0} & \cdots & \mathbf{0} \\ \mathbf{I}_{N_t} & \mathbf{0} & -\mathbf{H}_{j,i}^{[2]H} & \cdots & \mathbf{0} \\ \vdots & \vdots & \mathbf{0} & \ddots & \vdots \\ \mathbf{I}_{N_t} & \mathbf{0} & \mathbf{0} & \cdots & -\mathbf{H}_{j,i}^{[\mathcal{K}]H} \end{bmatrix} \begin{bmatrix} \mathbf{K}_i \\ \mathbf{U}_j^{[1]} \\ \mathbf{U}_j^{[2]} \\ \vdots \\ \mathbf{U}_j^{[\mathcal{K}]} \end{bmatrix} = \mathbf{C}_i\mathbf{D}_i = \mathbf{0} \quad (3.31)$$

be defined as follows

$$D = \mathcal{K}N_r + 1. \quad (3.29)$$

Next, we consider the $\mathbf{V}_i^{[ICI]}$ matrix responsible for the ICI mitigation. In [113], the authors proposed the grouping method to deal with the interfering signals by utilizing (3.30), where $\mathbf{G}_1$ accounts for the direction of the aligned effective interference channels from BS 1, $\mathbf{U}^{[K,2]}$ denotes the suppression matrix at each user within cell 2, and K is the number of users per cell, [113]. According to the given system model and proposed signal structure (3.4), the matrix equation (3.30) can be adapted to the network scenario with any L and $\mathcal{K}$ as shown in (3.31), where $\mathbf{K}_i$ accounts for the direction of the aligned effective interference channels from BS i ($i = j-1$). $\mathbf{U}_i^{[k]}$ and $\mathcal{K}$ indicate the receive BF matrix at user $[j,k]$ and the number of users per cell in the totally overlapped area, respectively.

Similar to (3.12)–(3.13), we decompose (3.31) into $\mathcal{K}$ matrix equations, and the k^{th} matrix equation can be written as

$$\begin{bmatrix} \mathbf{I}_{N_t} & -\mathbf{H}_{j,i}^{[k]H} \end{bmatrix} \begin{bmatrix} \tilde{\mathbf{K}}_i^{[k]} \\ \mathbf{U}_j^{[k]} \end{bmatrix} = \tilde{\mathbf{C}}_i^{[k]}\tilde{\mathbf{D}}_i^{[k]} = \mathbf{0},\ \forall i,j \in L,\ \forall k \in \mathcal{K}, \quad (3.32)$$

where $\tilde{\mathbf{K}}_i^{[k]}$ indicates the direction of the interference channels from BS i to the user of interest after applying the interference suppression matrices at the receiver side. First, we find the nullspace $\tilde{\mathbf{D}}_i^{[k]}$ of $\tilde{\mathbf{C}}_i^{[k]}$, and accordingly, the dimension of $\tilde{\mathbf{C}}_i^{[k]}$ equals $N_t \times (N_t + N_r)$. This implies that it is always feasible to calculate the

$$\mathbf{V}_i^{[ICI]} = \text{null}\left(\left[\underbrace{\mathbf{K}_i}_{\text{effective interference direction}} \underbrace{\left(\mathbf{U}_{j(j\neq\{i-1,i,\ldots,i+d_s-1\})}^{[k(k\in\mathcal{K})]H}\mathbf{H}_{j(j\neq\{i-1,i,\ldots,i+d_s-1\}),i}^{[k(k\in\mathcal{K})]}\right)^H}_{\text{effective ICI channels}}\right]^H\right) \quad (3.33)$$

nullspace $\tilde{\mathbf{D}}_i^{[k]}$.

Once we have derived all the terms indicating the effective directions of the ICI component and receive BF matrices in (3.31)–(3.32), one is able to calculate the transmit BF matrices $\mathbf{V}_i^{[ICI]}$ as in (3.33), where $\mathbf{U}_{j(j\neq\{i-1,i,\ldots,i+d_s-1\})}^{[k(k\in\mathcal{K})]}$ is the receive BF matrix at user $[j,k]$ that considers BS i as a source of the ICI, excluding the cell used to find solutions for (3.32). Consequently, the $\mathbf{H}_{j(j\neq\{i-1,i,\ldots,i+d_s-1\}),i}^{[k(k\in\mathcal{K})]}$ matrices refer to the links between the base stations and receivers defined above. To find the matrix $\mathbf{V}_i^{[ICI]}$, the matrix inside the null function should be regarded. This matrix combines $\mathcal{K}N_r$ columns of the effective directions given by the $\mathbf{K}_i$ matrix and $(L-d_s-1)\mathcal{K}N_r$ columns vectors indicating the other ICI channels existing under a certain network configuration. As a result, the matrix inside the null function contains $(L-d_s)\mathcal{K}N_r$ vectors. Thus, the dimension of this matrix is $N_t \times (L-d_s)\mathcal{K}N_r$. Furthermore, any successful derivation of the nullspace of the matrix implies that the number of column vectors is equal to the positive difference between the number of rows and the number of columns. Since the nullspace of dimension D needs to be found, we substitute (3.29) in this difference as

$$D = N_t - (L-d_s)\mathcal{K}N_r,$$

and then obtain the minimum number of transmit antennas as

$$N_t = (L-d_s+1)\mathcal{K}N_r + 1. \quad (3.34)$$

After applying $\mathbf{V}_i^{[ICI]}$, the network configuration can be regarded as the reduced one with specific features of the MIMO X-channel scenario when, from the user's viewpoint, each channel is seen as a link carrying not only a useful data, but also interference. That results in the presence of XCI component of

interference, and the design of the second part of the transmit BF matrix is dedicated to mitigate exactly this type of interference. If the proposed algorithm is successively implemented, the whole multi-cell multi-user MIMO network can be treated as a set of L independent $N_r \times N_r$ SU-MIMO networks.

In fact, the proposed scheme reduces the number of total antenna resources required for interference alignment. For instance, in the three-cell case with $\mathcal{K} = 1$ user per cell in the totally overlapped area, the required total number of antennas for the proposed technique equals $N_t + N_r = 5 + 2 = 7$, while the minimum total number of antennas derived from the IA feasibility in [104] is $N_t + N_r = (L + 1)d_s = 8$. One may think that the antenna resources reduction is achieved by extra signaling overhead, however, this reduction is obtainable in the system where each mobile station experiences a multi-source transmission strategy from several adjacent BSs having independent messages generated at each base station. Moreover, each BS demands only local CSI and hence there will be no CSI overhead between the base stations.

3.4.5 Computational Complexity

The complexity of the proposed technique mainly depends on the number of arithmetic operations required for the matrix multiplication and singular value decomposition (SVD). For a given $m \times n$ matrix, the complexity of SVD is given by $\mathcal{O}\left(\min\left\{mn^2, m^2n\right\}\right)$, [138]. Regarding the matrix multiplication, the multiplication of two $m \times n$ and $n \times p$ matrices requires mnp arithmetic operations. Since the transmit BF matrix is split into two parts, the complexities for each part are calculated separately and then summed up to find the overall complexity.

First, we consider the part responsible for the ICI cancellation which involves two SVD and one matrix multiplication. Since the dimension of the $\tilde{\mathbf{C}}_1^{[1]}$ matrix in (3.12) is $N_t \times (N_t + N_r)$, the corresponding number of arithmetic operations equals $\mathcal{O}\left(\min\left\{N_t^3 + 2N_t^2N_r + N_tN_r^2, N_t^3 + N_t^2N_r\right\}\right)$, where the minimum is $(N_t^3 + N_t^2N_r)$. The next step is the matrix multiplication in (3.16) that demands $N_tN_r^2$ operations. The final stage required to calculate $\mathbf{V}_i^{[ICI]}$ is SVD. Since the dimension of the matrix of interest is $N_r \times N_t$, the respective complexity is $\mathcal{O}\left(N_tN_r^2\right)$. Therefore, the overall complexity of $\mathbf{V}_i^{[ICI]}$ is equal to $\mathcal{O}\left(N_t^3 + N_t^2N_r + 2N_tN_r^2\right)$, which can be bounded by $\mathcal{O}\left(N_t^3 + 3N_t^2N_r\right)$.

Next, we consider the second part of the transmit BF matrix, which comprises two SVD and two matrix multiplications for each column vector of $\mathbf{V}_i^{[XCI]}$. $N_r \times$

$(N_t - N_r)$ indicates the dimension of the matrix for the first SVD, and the corresponding complexity is given by $\mathcal{O}\left(\min\left\{N_r^3 - 2N_tN_r^2 + N_t^2N_r, N_tN_r^2 - N_r^3\right\}\right)$, where the minimum is $(N_tN_r^2 - N_r^3)$. Two matrix multiplications in (3.21) require $\mathcal{O}\left(N_tN_r^2\right)$ and $\mathcal{O}\left(N_t^2N_r - N_tN_r^2\right)$, respectively. The second SVD utilizes the $N_r \times (N_t - N_r)$ matrix and needs $N_tN_r^2 - N_r^3$ operations. Consequently, with respect to the number of column vectors in $\mathbf{V}_i^{[XCI]}$, the respective complexity equals $\mathcal{O}\left(3N_t^2N_r^3 - N_r^4\right)$.

Finally, we need to calculate the number of operations needed for the multiplication of two $\mathbf{V}_i^{[ICI]}$ and $\mathbf{V}_i^{[XCI]}$ matrices. The dimensions of the corresponding matrices are $N_t \times (N_t - N_r)$ and $(N_t - N_r) \times N_t$. Then, its complexity is equal to $\mathcal{O}\left(N_t^2N_r - N_tN_r^2\right)$. Hence, by combining all the operations above, the overall computational complexity of the proposed scheme can be written as $\mathcal{O}\left(N_t^2\left(N_t + 3N_r^2 + 4N_r\right) - N_r^2\left(N_r^2 + N_t\right)\right)$ for each base station.

3.5 Simulation Results

This section presents our results using Monte Carlo simulations to investigate the network performances such as BER and achievable data rate assuming both perfect and imperfect CSI scenarios. The simulations assume QPSK modulation and frequency flat fading which is designed according to (2.9). To make a fair comparison, the total transmit power at the BS is constrained to unity irrespective of the number of transmit antennas. The following notation $(N_t, N_r, \mathcal{K}, L, d_s)$ is used to describe the network configuration, where N_t and N_r are the numbers of transmit and receive antennas, $\mathcal{K}$ is the number of mobile stations located in the totally overlapped area, L is the number of cells, and d_s is the number of data streams at each base station.

In the first simulation, we want to estimate the BER performances achievable by each mobile station ($\mathcal{K} = 2$) located in the totally overlapped area of the three-cell MIMO network. The lines presented in Fig. 3.4 are the BER graphs averaged over each cell. As shown in Fig. 3.4, the BER performances of all the receivers match the BER performance of the single-cell SU-MIMO, where a checking point is 24 dB with the BER value of 0.001. Therefore, the proposed scheme is able to mitigate all the interference in the network, and consequently, the system model simply reduces to the SU-MIMO scenario.

In the next simulation, we consider several network scenarios comprising of

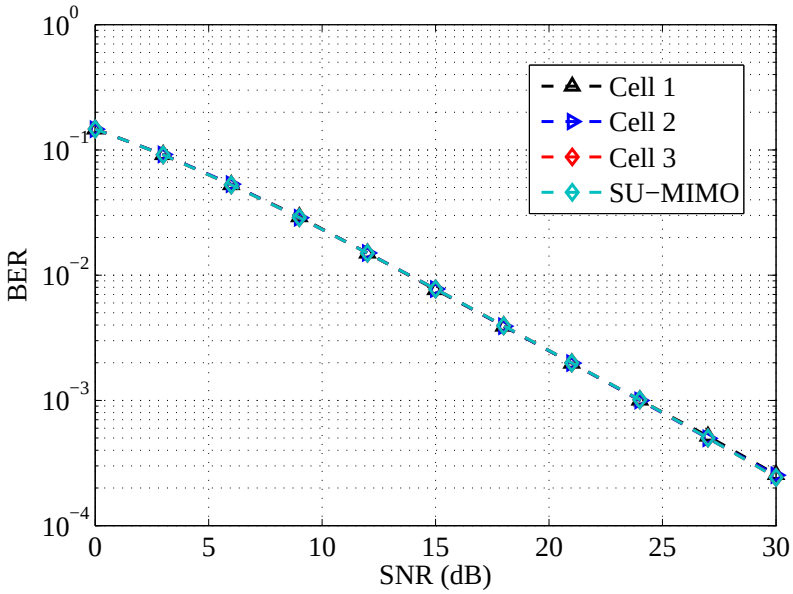

Figure 3.4. The BER performance across each cell for the considered system model with $L = 3$ cells and $\mathcal{K} = 2$ users per cell in the totally overlapped area.

three, four, five and six cells (it is assumed that each cell serves only one mobile station). 10 dB and 20 dB are chosen as the observation points to evaluate the achievable BER at each scenario. Thus, the BER values for all the scenarios are equal to 0.0232 and 0.0025, respectively. In addition, the derived results match the BER values obtainable in the single-cell SU-MIMO model. Therefore, as shown in Fig. 3.5, the proposed scheme allows each system configuration to attain the same BER performance irrespective of the number of cells/users.

Next, we consider the system configuration as $(9, 2, 2, 3, 2)$ consisting of three cells with two mobile stations achieving two data streams each with nine transmit and two receive antennas per node, respectively. Therefore, we aim to compare the BER performances achievable by the proposed scheme and ZFBF, [50]. Since the proposed technique simplifies the observed network to a 2×2 MIMO model, a 2×2 MIMO system is considered to calculate the BER by utilizing ZFBF. As shown in Fig. 3.6, the proposed scheme outperforms ZFBF by 3 dB due to the impact of the scaling factor needed in the precoding matrix design of ZFBF to ensure a unity gain at the output of the precoder.

We then want to compare the data rates per user obtainable by the proposed scheme and ZFBF. For this reason, the $(5, 2, 1, 3, 2)$ and $(6, 2, 1, 3, 2)$ system scenarios are considered for the proposed algorithm and ZFBF, respectively (please

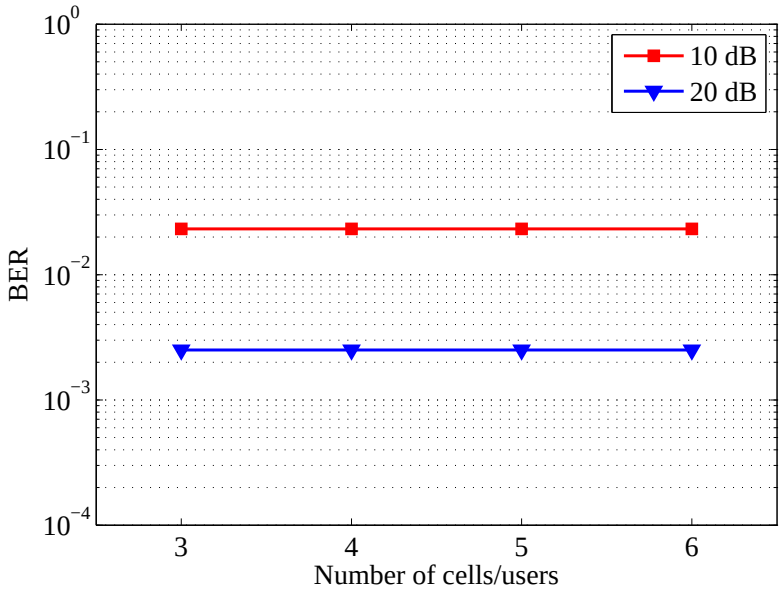

Figure 3.5. The BER values at 10 and 20 dB for different network scenarios when each BS serves one user per cell.

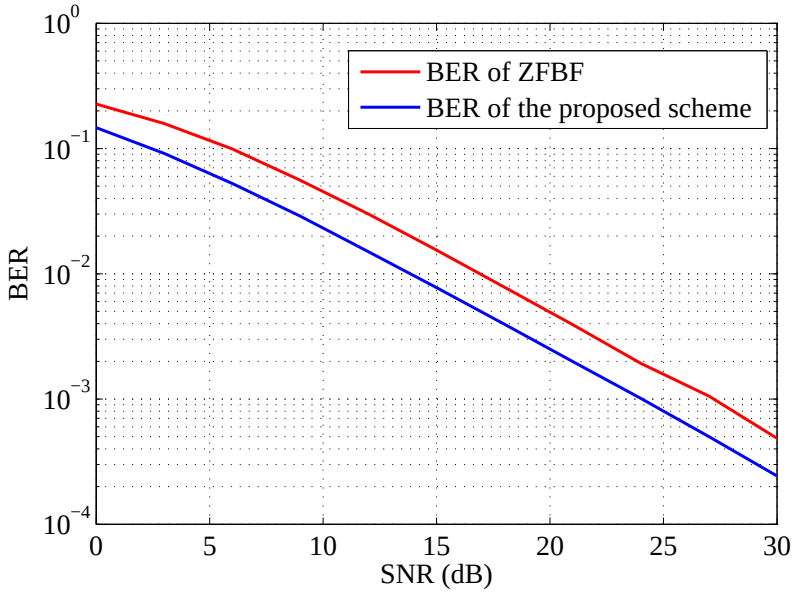

Figure 3.6. The BER performances derived by utilizing the proposed scheme and ZFBF.

note that the proposed scheme utilizes less antennas than ZFBF does). Thus, it is shown in Fig. 3.7 that the proposed is persistently superior; at SNR = 30 dB, the ZFBF technique obtains 19.3 bits/s/Hz, while the proposed scheme achieves 19.78 bits/s/Hz.

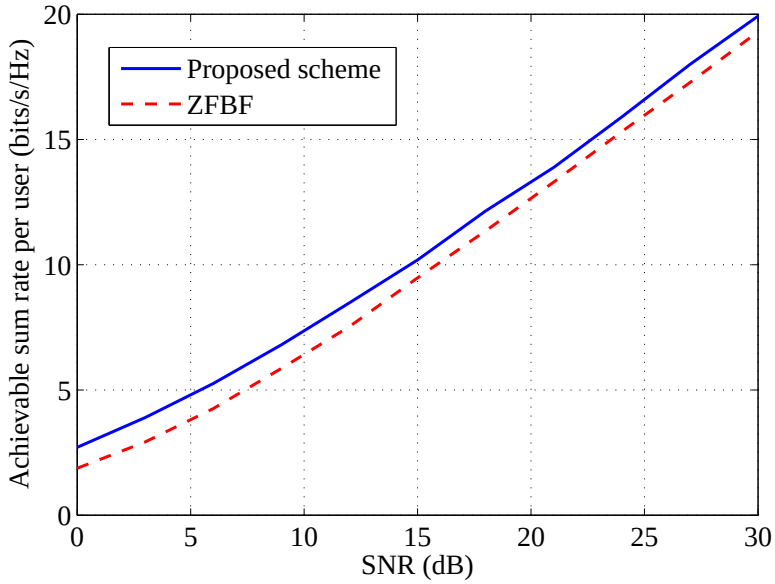

Figure 3.7. Maximum data rate per user achievable by the proposed scheme and ZFBF.

In the next simulation, the achievable data rate is evaluated by utilizing (3.7) and (3.24), with respect to the different system configurations. For the system settings such as $(9, 2, 2, 3, 2)$, $(13, 2, 2, 4, 2)$, $(13, 2, 3, 3, 2)$ and $(19, 2, 3, 4, 2)$, the proposed scheme can achieve 118.67, 158.01, 177.76 and 237.02 bits/s/Hz, respectively. The observation point is 30 dB.

Furthermore, we want to investigate the effect of different CSI scenarios on the BER and transmission rates attainable by utilizing the proposed scheme. As before, 30 dB is regarded as the reference point to compare the derived results. The channel acquisition method as in (2.7) is applied for different scenarios. The first scenario is known as perfect CSI and can be modeled as $\alpha \to \infty$ and $\rho > 1$, while the CSI mismatch can be defined by different values of α and β in (2.7). The second case, known as the reciprocal channel, represents the network scenario, where the impact of CSI errors on the system is inversely proportional to SNR (when $\alpha = 1$, $\tau = \beta\rho^{-1}$, equation (2.7)). Finally, the channel

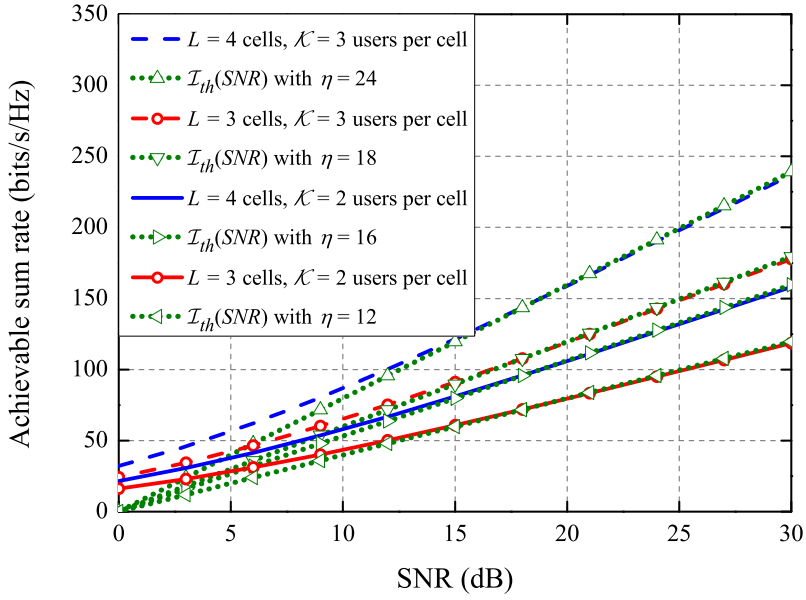

Figure 3.8. The sum rates achievable for various network configurations.

acquisition, where the CSI mismatch is independent of the SNR, can be determined by $\alpha = 0$ and is known as the CSI feedback. To describe various ways of the CSI acquisition, we consider different values for pairs of (α, β) as follows $(1.5, 15)$, $(1, 10)$, $(0.75, 10)$, $(0, 0.05)$, $(0, 0.001)$.

For the considered different CSI scenarios, we first aim to analyse the BER metric. It can be seen from Fig. 3.9, the cases with $\alpha = 0$ perform better than the ones with the SNR-dependent CSI mismatch at low SNR (up to 16 dB); however, in the high SNR region, the scenario with $\alpha = 0$ experiences a significant degrade as SNR increases. For instance, the BER performances for the $(0, 0.001)$ and perfect CSI scenarios match each other up to 9 dB. Therefore, it can be noticed that for the cases of $\alpha = 0$, the value of β has a large impact and degrades the BER performance. Regarding the SNR-dependent CSI mismatch, it can be seen that imperfect CSI makes it infeasible to decode the transmitted data at low SNR, however, further increase of SNR enhances the decodability of the transmitted data. Consequently, the larger α is, the sooner the BER performance improves. Therefore, regarding the message decodability, it can be stated that the proposed technique is applicable for all the scenarios with SNR-independent small CSI impairments (small β) at low SNR and the reciprocal channels at high

SNR.

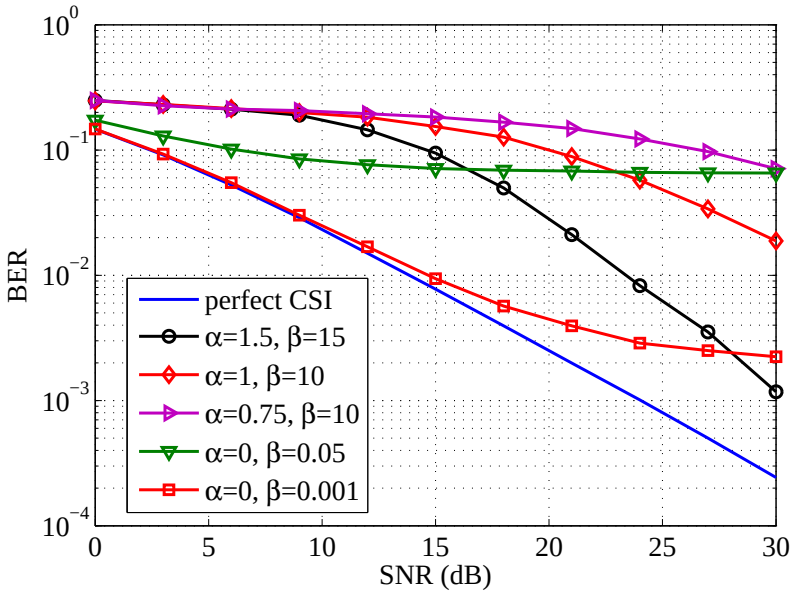

Figure 3.9. The BER performances achievable under various CSI conditions.

Fig. 3.10 presents an insight into how the CSI mismatch affects the achievable data rates per user. The case of $\alpha = 0$ allows us to analyse the impact of β, and thus it can be seen that β has a significant impact on the performance when $\alpha = 0$. Accordingly, this case with $\alpha = 0$ can be treated as the worst scenario because increasing SNR does not provide any increase in the achievable data rate. For the specific case with $\beta = 0.001$, it is feasible to apply the proposed scheme at low SNR regime (up to 15 dB); however, with $\beta = 0.05$, the DoF loss is significant within the whole SNR range. For the case of $\alpha \neq 0$, we notice that the proposed scheme provides poor performances in the low SNR region; however, the SNR dependence leads to the increase in the achievable data rate when SNR increases. Therefore, the larger α is, the sharper the curve slope becomes.

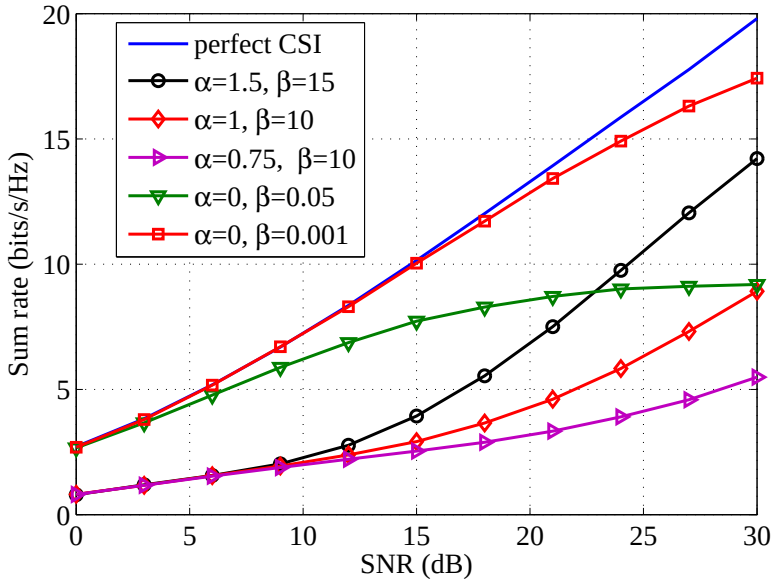

Figure 3.10. The achievable data rate per user under various CSI conditions.

3.6 Chapter Summary

This Chapter proposed an IA scheme for a downlink network transmission with multiple cells and multiple MIMO users under a Gaussian interfering BC scenario. We jointly designed the transmitter and receiver BF matrices utilizing a closed-form expression for $L \geq 3$ cells and $\mathcal{K} \geq 1$ users per cell in the totally overlapped area. As a result, the proposed scheme ensures that interference is cancelled, and hence makes it possible to achieve the maximum $(L-1)$ DoF for each mobile station. Furthermore, it is demonstrated that the cellular multi-user MIMO scenario can be regarded as a set of the single-cell SU MIMO channels. We also derived an expression standing for the relationship between the numbers of cells (L), antennas (N_t and N_r), receivers $(\mathcal{K})$ and data streams (d_s) which is given by $N_t = (L-d_s+1)\mathcal{K}N_r+1$. Moreover, the proposed scheme demands less antenna resources than the one presented in [104]. The simulation results verified the powerful performance of the algorithm under different network settings where it was shown that the achievable BER performance is equal to the BER performance of the single-cell SU-MIMO network irrespective of the number of cells. Furthermore, in terms of the BER performance and achievable sum rate, the proposed scheme outperforms the ZFBF technique. Finally, we estimated the effect of the CSI mismatch on the system performances.

Chapter 4

Enhanced Multiplexing Gain Using Interference Alignment Cancellation in Multi-cell Compounded MIMO BC Networks

This Chapter focuses on establishing a closed-form downlink IA beamforming scheme for a multi-cell MIMO network. In contrast to [123], we propose a scheme that allows us to apply the MIMO X-channel scenario for the compounded $L-$cell MIMO BC network and to enhance the achievable sum rate per user located in the cell-edge area. It is assumed that each user operates under a multi-source transmission set-up when several BSs send individual data to the user of interest. Then the transmit BF matrices are jointly designed according to the types of interference presented at the receiver side. Compared with Chapter 3, the system model will be defined from a concept of a point-to-point MIMO model. For the sake of keeping an explanation uncomplicated, it is assumed that each BS will serve only one user per cell and the antenna configurations of network nodes are not restricted to be identical. Consequently, the latter assumption allows one to generalize the achievable DoF region. Therefore, by utilizing the proposed technique, the DoF region is estimated for the case study with $L = 3$ cells and provides an upper limit for the DoF metric by solving the dual problem for the linear program $\max_{\mathcal{D}_{out}^{M-X}}$. Moreover, we validate the analytical DoF

derivation with the numerical results (simulation). Finally, the proposed scheme is generalized for the case of $L \geq 3$ and further the required minimum antenna configuration is calculated to maintain the proposed scheme. The work in this Chapter also provides an insight into the impact of different message set ups on the achievable DoF and required number of antenna resource. It is shown that, for a fixed number of antennas, certain set ups can be exploited to achieve more DoF than the conventional ones used in [104, 121, 123]. Furthermore, the results provide a means to identify the maximum achievable DoF for the considered set ups and the required conditions for achieving this maximum.

4.1 System Model

Since a cellular MIMO network can be developed from the concept of a point-to-point MIMO model, the MIMO IC and X-channels are considered which distinguish from each other by a different message set. For example, IC represents the scenario when transmitter i serves only the corresponding receiver i while the X-channel scenario is characterised by a message set when each source node i has different messages to a number of receivers. In Fig. 4.1, a $L-$user point-to-point MIMO network is presented, where each transmitter-receiver pair is deployed with N_t and N_r antennas, respectively.

4.1.1 The MIMO IC Model

In the MIMO IC scenario, [17, 104, 105, 116, 117, 118], the received signal $\mathbf{y}_j$ at $Rx\ j$ can be written as

$$\mathbf{y}_j = \underbrace{\mathbf{H}_{j,j}\mathbf{x}_j}_{\text{desired signal}} + \underbrace{\sum_{i=1, i\neq j}^{L} \mathbf{H}_{j,i}\mathbf{x}_i + \mathbf{n}_j}_{\text{interference}},\ \forall j \in L. \tag{4.1}$$

If the signal $\mathbf{x}_i \in \mathbb{C}^{N_t \times 1}$ transmitted from $Tx\ i$ is expressed by

$$\mathbf{x}_i = \mathbf{V}_i \mathbf{s}_i,\ \forall i \in L, \tag{4.2}$$

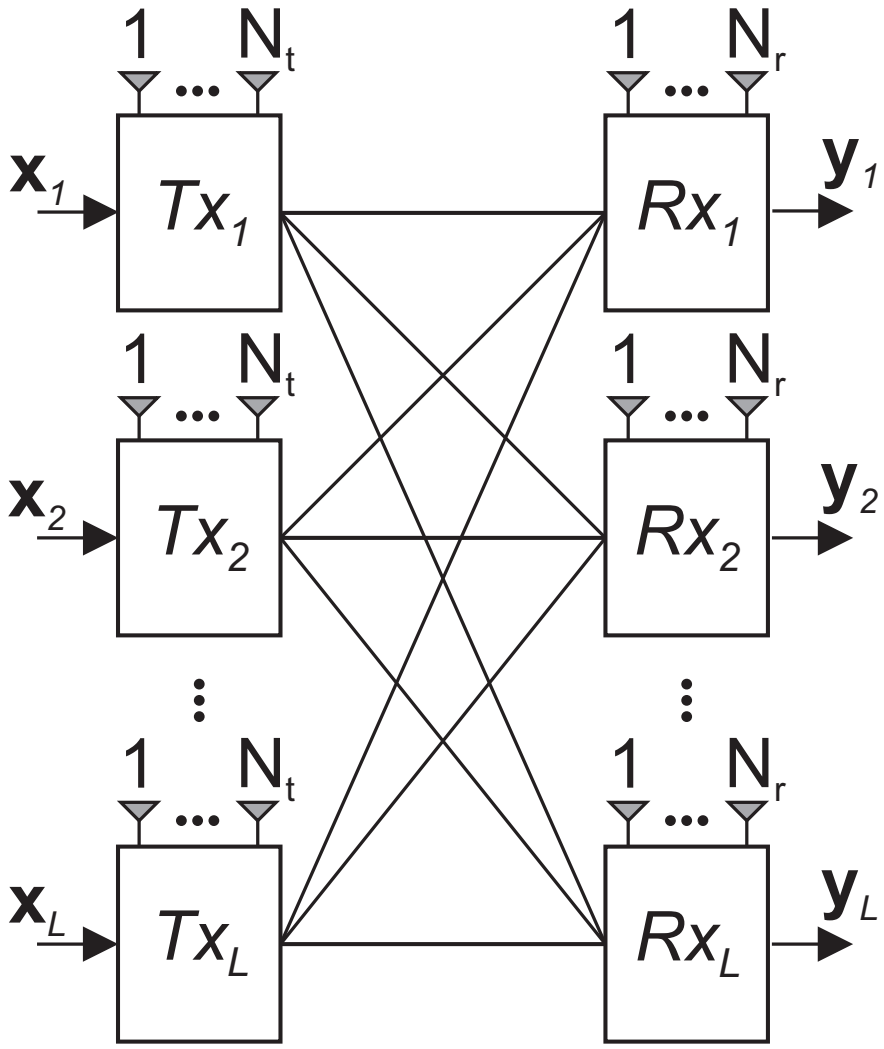

Figure 4.1. The $L-$user point-to-point MIMO network.

then, after beamforming at the receiver side, the received signal in (4.1) can be rewritten as

$$\tilde{\mathbf{y}}_j = \underbrace{\mathbf{U}_j^H \mathbf{H}_{j,j} \mathbf{V}_j \mathbf{s}_j}_{\text{desired signal}} + \underbrace{\mathbf{U}_j^H \sum_{i=1, i\neq j}^{L} \mathbf{H}_{j,i} \mathbf{V}_i \mathbf{s}_i}_{\text{interference}} + \tilde{\mathbf{n}}_j, \ \forall j \in L, \tag{4.3}$$

where $\mathbf{U}_j \in \mathbb{C}^{N_r \times d_s}$ and $\mathbf{V}_i \in \mathbb{C}^{N_t \times d_s}$ denote the beamforming matrices at receiver j and transmitter i, respectively. $\mathbf{H}_{j,i} \in \mathbb{C}^{N_r \times N_t}$ and $\tilde{\mathbf{n}}_j = \mathbf{U}_j^H \mathbf{n}_j \in \mathbb{C}^{d_s \times 1}$ indicate the channel between transmitter i and receiver j and the effective zero-mean AWGN vector, with $\mathbb{E}\{\tilde{\mathbf{n}}_j \tilde{\mathbf{n}}_j^H\} = \sigma_{\tilde{n}}^2 \mathbf{I}$. And finally, d_s stands for the number of data streams in $\mathbf{s}_i$.

To decode the required signal successfully in the case of the MIMO interference channel, the "desired" signal should be aligned into a subspace at the receiver side such that the interfering signals are aligned into the subspace that is orthogonal to $\mathbf{U}_j$. Therefore, the following conditions must be satisfied at receiver j

$$\mathbf{U}_j^H \mathbf{H}_{j,i} \mathbf{V}_i = \mathbf{0},\ \forall i, j \in L,\ i \neq j, \tag{4.4}$$

$$\text{rank}\left(\mathbf{U}_j^H \mathbf{H}_{j,j} \mathbf{V}_j\right) = d_j,\ \forall j \in L, \tag{4.5}$$

where d_j is the number of resolvable interference-free data streams at user j.

4.1.2 The MIMO X- and Z-channel Models

In the MIMO X-channel scenario, [75, 76, 121, 122, 123], the received signal $\mathbf{y}_j$ (Fig. 4.1) can be expressed as

$$\mathbf{y}_j = \sum_{i=1}^{L} \mathbf{H}_{j,i} \mathbf{x}_i + \mathbf{n}_j,\ \forall j \in L, \tag{4.6}$$

where $\mathbf{H}_{j,i} \in \mathbb{C}^{N_r \times N_t}$ indicates the channel link that carries both the desired signal and interference simultaneously from transmitter i to receiver j. $\mathbf{x}_i \in \mathbb{C}^{N_t \times 1}$ is the transmitted signal vector from $Tx\ i$ and $\mathbf{n}_j \in \mathbb{C}^{N_r \times 1}$ stands for the zero-mean AWGN vector, with $\mathbb{E}\{\mathbf{n}_j \mathbf{n}_j^H\} = \sigma_n^2 \mathbf{I}$.

For the case of the MIMO X-channel, it is assumed that transmitter i intends to send data to user j by exploiting the precoding matrix $\mathbf{V}_i^{[j]}$, and subsequently receiver j zero-forces all the interference by multiplying the received signal with the receive beamforming matrix $\mathbf{U}_j$. Thus, to decode the required signal successfully, the following conditions must be satisfied at the user of interest

$$\mathbf{U}_j^H \mathbf{H}_{j,i} \mathbf{V}_i^{[k]} = \mathbf{0},\ j \neq k,\ \forall i, j \in L, \tag{4.7}$$

$$\sum_{i=1}^{L} \text{rank}\left(\mathbf{U}_j^H \mathbf{H}_{j,i} \mathbf{V}_i\right) = \sum_{i=1}^{L} d_{[j,i]} = d_j,\ \forall j \in L, \tag{4.8}$$

where $\mathbf{V}_i^{[k]} \in \mathbb{C}^{N_t \times d_{[k,i]}}$ denotes the transmit beamforming matrix at $Tx\ i$ which intends to deliver the $d_{[k,i]}$ data streams to receiver k. Moreover, any data delivered to receiver j along the $\mathbf{V}_i^{[k]}$ direction causes intra-stream interference. $d_{[j,i]}$ indicates the number of data streams desired to be decoded at receiver j from

transmitter i while d_j is the maximum number of decodable data streams at receiver j, with $d_j = \sum_{\forall i} d_{[j,i]}$.

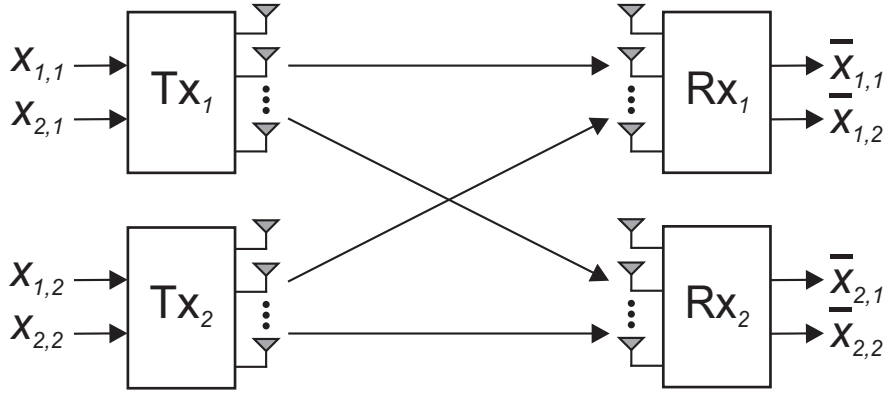

(a) The two-user MIMO X-channel.

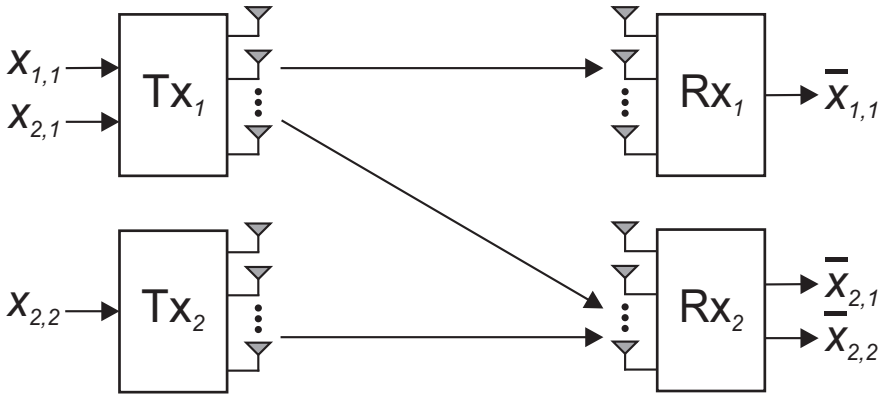

(b) The two-user MIMO Z-channel with $\mathbf{H}_{1,2} = \mathbf{0}$.

Figure 4.2. The point-to-point MIMO models.

Now it is worth considering a two-user MIMO X-channel system as shown in Fig. 4.2(a). With respect to each receiver, the received signal $\mathbf{y}_j \in \mathbb{C}^{N_r \times 1}$ in (4.6) can be expressed as

$$\mathbf{y}_1 = \mathbf{H}_{1,1}\mathbf{x}_1 + \mathbf{H}_{1,2}\mathbf{x}_2 + \mathbf{n}_1,$$
$$\mathbf{y}_2 = \mathbf{H}_{2,1}\mathbf{x}_1 + \mathbf{H}_{2,2}\mathbf{x}_2 + \mathbf{n}_2,$$

where $\mathbf{x}_i = \left[\mathbf{x}_{1,i}^T \; \mathbf{x}_{2,i}^T\right]^T$ where the first digit within the subscripts refers to the receiver which aims to decode the desired message, and $\mathbf{x}_{j,i} \in \mathbb{C}^{d_{[j,i]} \times 1}$ is the data vector which transmitter i desires to deliver to receiver j.

The total DoF η_X is defined as

$$\eta_X \triangleq \max_{\mathcal{D}^X} \left(d_{[1,1]} + d_{[1,2]} + d_{[2,1]} + d_{[2,2]}\right), \tag{4.9}$$

where $\mathcal{D}^X$ denotes the DoF region over the X-channel and $d_{[j,i]}$ indicates the number of data streams transmitted from $Tx\ i$ and successfully detected by receiver j. In [123], the authors proved that under the MIMO X-channel scenario it is feasible to achieve $\lfloor \frac{4}{3}M \rfloor$ degrees of freedom with M antennas at each node. It implies that the number of DoF can be non-integer. For the case when each node has a different number of deployed antennas, the authors provided Theorem 4, [123], which gives the total number of DoF achievable within the network scenario. All considered cases were bounded by the 2×2 MIMO X-channel.

The MIMO Z-channel presented in Fig. 4.2(b) can be characterized as the MIMO X-channel (Fig. 4.2(a)) and described by (4.6). The distinction between the X-channel and Z-channel is related to the constraints on the message such that $\mathbf{x}_{1,2} = \emptyset$ and $\mathbf{H}_{1,2} = \mathbf{0}$, i.e., there is no message or channel from transmitter 2 to receiver 1.

Similar to the MIMO X-channel, the number of DoF for the MIMO Z-channel can be defined as

$$\eta_{Z_{(1,2)}} \triangleq \max_{\mathcal{D}^{Z_{(1,2)}}} \left(d_{[1,1]} + d_{[2,1]} + d_{[2,2]}\right). \tag{4.10}$$

Lemma 1 ([123])

$$\max_{\mathcal{D}^X} \left(d_{[1,1]} + d_{[2,1]} + d_{[2,2]}\right) \leq \max_{\mathcal{D}^{Z_{(1,2)}}} \left(d_{[1,1]} + d_{[2,1]} + d_{[2,2]}\right) = \eta_{Z_{(1,2)}}. \tag{4.11}$$

Outline of the proof. In [123], it is supposed to have a certain coding scheme that is able to obtain $(d_{[1,1]}, d_{[2,1]}, d_{[2,2]})$ in the MIMO X-channel. It is also assumed that $\mathbf{x}_{1,2}$ is known for all nodes *a priori*. Since receiver 1 is provided by $\mathbf{x}_{2,2}$, it is aware of all the information available at transmitter 2 and can subtract the signal of $Tx\ 2$ from its received signal. This implies $\mathbf{H}_{1,2} = \mathbf{0}$. As a result, we conclude that the MIMO X-channel is identical to the MIMO Z-channel. Moreover, the same DoF of $(d_{[1,1]}, d_{[2,1]}, d_{[2,2]})$ are also attainable in the MIMO Z-channel.

4.1.3 The Design of the Compounded MIMO BC Model

Next, we consider a MIMO cellular network with L cells and multiple users as shown in Fig. 3.1 ($L = 3$ cells). For simplicity, it is assumed that all the

base stations have identical coverage area and cell configuration and thus serve the same number of users per cell, K, randomly distributed. In terms of the network coverage, the combined area can be designated as non-overlapping and overlapping areas; moreover, the overlapping area can be further determined as the totally and partially overlapped areas, [131, 132, 139], or the corresponding areas presented in Table 3.1.

Then, under a dense network scenario, it is feasible to assume that each base station serves $\mathcal{K}$ ($\mathcal{K} \leq K$) users per cell in Area 3 (Table 3.1). Since the amounts of power received from the serving and non-serving BSs are comparable it is reasonable to assume that the user of interest may want to obtain messages from several BSs and hence it experiences a multi-source transmission strategy. For the defined multi-source transmission from $\mathcal{L}$ BSs ($1 < \mathcal{L} < L$), then the user of interest observes the network as a set of $(L - \mathcal{L})$ ICs and $\mathcal{L}$ X-channels, and the corresponding types of interference are given by ICI and XCI. And we refer to this scenario as a compounded MIMO BC network scenario, [139]. Under the multi-source transmission ($\mathcal{L}$), the data vector $\mathbf{s}_i$ in (4.2) can be defined as

$$\mathbf{s}_i = \begin{bmatrix} \mathbf{c}^{[i,i]T} & \mathbf{c}^{[i+1,i]T} & \cdots & \mathbf{c}^{[i+\mathcal{L}-1,i]T} \end{bmatrix}^T, \ \forall i \in L. \tag{4.12}$$

For simplicity, but without loss of generality, it is assumed that each BS serves $\mathcal{K} = 1$ user per cell in the totally overlapped area, and then the received signal at user j can be written as

$$\begin{aligned} \mathbf{y}_j &= \sum_{i=1}^{L} \mathbf{H}_{j,i}\mathbf{V}_i\mathbf{s}_i + \mathbf{n}_j \\ &= \underbrace{\sum_{i=j-\mathcal{L}+1}^{j} \mathbf{H}_{j,i}\mathbf{V}_i\mathbf{s}_i}_{\text{desired+XCI signals}} + \underbrace{\sum_{l=1,l\neq i}^{L} \mathbf{H}_{j,l}\mathbf{V}_l\mathbf{s}_l}_{\text{ICI}} + \mathbf{n}_j, \ \forall j \in L, \end{aligned} \tag{4.13}$$

where the first and second terms denote the "desired+XCI" signal and ICI component, respectively. And accordingly, it is feasible to split the transmit BF matrices into two parts as shown in (3.6) as follows

$$\mathbf{V}_i = \mathbf{V}_i^{[ICI]} \times \mathbf{V}_i^{[XCI]}, \ \forall i \in L,$$

where $\mathbf{V}_i \in \mathbb{C}^{N_t \times d_s}$, $\mathbf{V}_i^{[ICI]} \in \mathbb{C}^{N_t \times D}$ and $\mathbf{V}_i^{[XCI]} \in \mathbb{C}^{D \times d_s}$ are the complete and

partial transmit BF matrices. D, as the number of columns in $\mathbf{V}_i^{[ICI]}$, as well as the number of rows in $\mathbf{V}_i^{[XCI]}$, depends on the number of data streams at each BS ($D \geq d_s$). In more details, the value of D is generalised in Section 4.2.6.

Therefore, the received signal (4.13) can be rewritten as

$$\mathbf{y}_j = \underbrace{\sum_{i=j-\mathcal{L}+1}^{j} \mathbf{H}_{j,i}\mathbf{V}_i^{[ICI]}\mathbf{V}_i^{[XCI]}\mathbf{s}_i}_{\text{desired+XCI signals}} + \underbrace{\sum_{l=1,l\neq i}^{L} \mathbf{H}_{j,l}\mathbf{V}_l^{[ICI]}\mathbf{V}_l^{[XCI]}\mathbf{s}_l}_{\text{ICI}} + \mathbf{n}_j,\ \forall j \in L, \quad (4.14)$$

where BS i utilizes the transmit BF matrix $\mathbf{V}_i$, with $\text{trace}\left(\mathbf{V}_i\mathbf{V}_i^H\right) = 1$, and $\mathbf{n}_j \in \mathbb{C}^{N_r \times 1}$ is the zero-mean AWGN vector, with $\mathbb{E}\{\mathbf{n}_j\mathbf{n}_j^H\} = \sigma_n^2\mathbf{I}$. Since $\mathbf{s}_i$ is the vector containing the symbols drawn from i.i.d. Gaussian input and chosen from a desired constellation, we have $\mathbb{E}\{\mathbf{s}_i\mathbf{s}_i^H\} = \mathbf{I}$. All these conditions satisfy the average power constraint at BS i.

We define DoF for the multi-cell network as the pre-log factor of the sum-rate, [17, 18], as in (3.7) as follows

$$\eta = \lim_{\text{SNR}\to\infty} \frac{\mathcal{I}_\Sigma\left(\text{SNR}\right)}{\log_2\left(\text{SNR}\right)} = \sum_{k=1}^{L} d_k,$$

where $\mathcal{I}_\Sigma\left(\text{SNR}\right)$ is the sum rate that can be achieved for a given SNR, and d_k is the number of resolvable interference-free data streams in cell k. The sum rate can be defined as $\mathcal{I}_\Sigma\left(\text{SNR}\right) = \sum_{k=1}^{L} \mathcal{I}_k$, where $\mathcal{I}_k$ denotes the data rate achievable in cell k.

In the following sections, we explain how to mitigate the interference under the compounded MIMO network scenario and then define the constraints on the design of the transmit beamforming matrices for achieving maximum DoF.

4.2 The Achievable DoF Region Analysis

4.2.1 The Compounded MIMO BC scenario with $L = 3$ cells

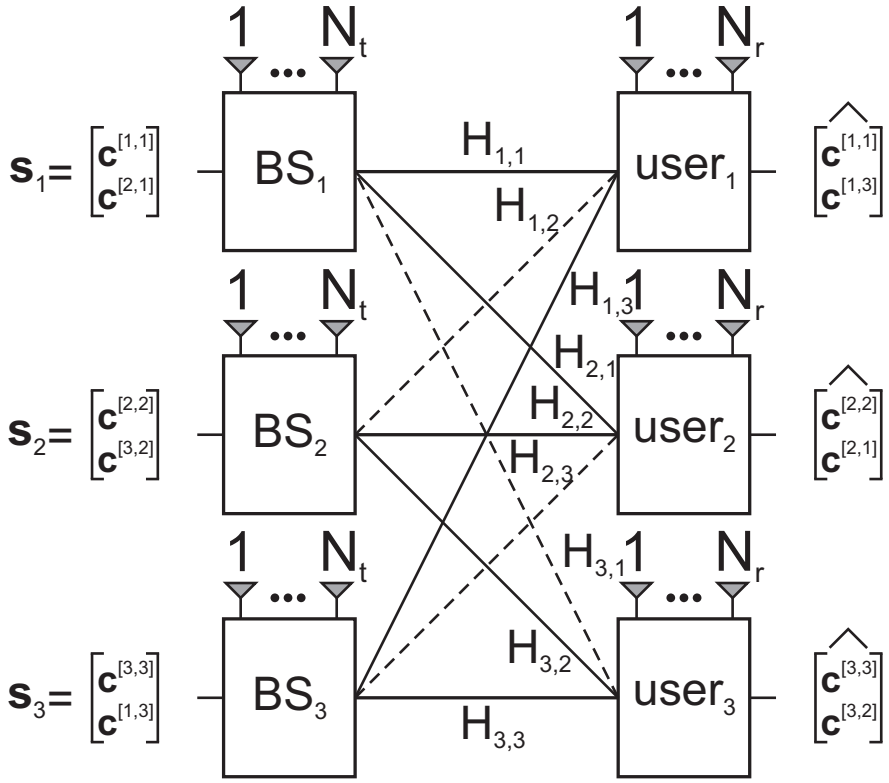

Figure 4.3. The compounded MIMO BC network with $L = 3$ cells and $\mathcal{K} = 1$ user per cell. Solid lines denote the channel links carrying the desired and XCI signals while the dashed lines indicate the ICI links.

Since the DoF region is achievable via the MIMO X- and Z- channels, we consider the compounded MIMO BC model. For simplicity, it is assumed that the cellular network consists of three base stations and three corresponding users as shown in Fig. 4.3, and thus the set of sources $\mathcal{L}$ constituting the multi-source transmission for each user can be defined, according to $1 < \mathcal{L} < L$, as $\mathcal{L} = 2$ base stations. Hereinafter, it is assumed that BS i and user j are deployed with M_i and N_j antennas, respectively, unless it is restated. Then the data vector $\mathbf{s}_i$ (4.12) can be written as

$$\mathbf{s}_i = \begin{bmatrix} \mathbf{c}^{[i,i]} \\ \mathbf{c}^{[i+1,i]} \end{bmatrix}, \ \forall i \in L, \tag{4.15}$$

where the first superscript denotes the user of interest while the second superscript stands for the transmitting BS. Equation (4.15) means that the first data vector transmitted from BS i is dedicated to the user located in the cell i (user i), while the second stream is designated to the $(i+1)^{th}$ cell (or user $(i+1)$). The numeration of users/cells changes circularly, i.e., if $i = L \Rightarrow (i+1) = 4 \rightarrow = 1$.

To give a detailed explanation, please refer to Fig. 4.3, where BS 1 transmits the signal $\mathbf{s}_1 = \left[\mathbf{c}^{[1,1]T} \;\; \mathbf{c}^{[2,1]T}\right]^T$ which is of interest to users 1 and 2 and causes interference to user 3. The signal $\mathbf{s}_2 = \left[\mathbf{c}^{[2,2]T} \;\; \mathbf{c}^{[3,2]T}\right]^T$ from BS 2 is required at users 2 and 3, and regarded as interference at user 1. Analogously, BS 3 with the signal $\mathbf{s}_3 = \left[\mathbf{c}^{[3,3]T} \;\; \mathbf{c}^{[1,3]T}\right]^T$ causes interference to user 2 and tends to deliver the signal to the users belonging to cells 1 and 3. Thus, all the channel links that cause interference can be regarded as IC channels (dotted lines in Fig. 4.3). In contrast, the other channels, shown in Fig. 4.3 as solid lines, convey the useful data to the defined users. User 1 is interested only in $\left[\mathbf{c}^{[1,1]T} \; \mathbf{c}^{[1,3]T}\right]^T$ while users 2 and 3 desire to decode $\left[\mathbf{c}^{[2,2]T} \; \mathbf{c}^{[2,1]T}\right]^T$ and $\left[\mathbf{c}^{[3,3]T} \; \mathbf{c}^{[3,2]T}\right]^T$ signals, respectively. Hence, with respect to (4.15), apart from the ICI, each user observes not only its corresponding symbols that are transmitted from the desired BSs, but also other inter-cell interfering signals (also known as the XCI). Therefore, the received signal (4.14) at the user of interest can be simply written as

$$\begin{aligned}\mathbf{y}_j &= \underbrace{\sum_{i=j-1}^{j} \mathbf{H}_{j,i}\mathbf{V}_i^{[ICI]}\mathbf{V}_i^{[XCI]}\mathbf{s}_i}_{\text{desired+XCI signals}} + \underbrace{\sum_{l=1,l\neq i}^{L=3} \mathbf{H}_{j,l}\mathbf{V}_l^{[ICI]}\mathbf{V}_l^{[XCI]}\mathbf{s}_l}_{\text{ICI}} + \mathbf{n}_j \\ &= \underbrace{\sum_{i=1,i\neq j+1}^{L=3} \mathbf{H}_{j,i}\mathbf{V}_i^{[ICI]}\mathbf{V}_i^{[XCI]}\mathbf{s}_i}_{\text{desired+XCI signals}} + \underbrace{\mathbf{H}_{j,j+1}\mathbf{V}_{j+1}^{[ICI]}\mathbf{V}_{j+1}^{[XCI]}\mathbf{s}_{j+1}}_{\text{ICI}} + \mathbf{n}_j, \qquad (4.16)\end{aligned}$$

$\forall j \in L.$

4.2.2 The ICI Cancellation Scheme

Although, lots of work was done on IA for the MIMO IC model, [2, 79, 104, 105, 118, 113], the ZF technique proved itself as a promising and powerful approach in different wireless network scenarios in terms of the interference mitigation perspective, [140, 141, 142, 143, 144].

From (4.16), it is obvious that the channels causing the ICI to user j are presented by $\mathbf{H}_{j,j+1} \in \mathbb{C}^{N_j \times M_{j+1}}$. Hence, the ICI component can be simply mitigated by utilizing ZF. Then, each $\mathbf{V}_{j+1}^{[ICI]}$ can be calculated as follows

$$\mathbf{V}_{j+1}^{[ICI]} = \text{null}\left(\mathbf{H}_{j,j+1}\right), \ \forall j \in L. \tag{4.17}$$

This expression is only feasible if $M_{j+1} > N_j$, and, consequently, $\mathbf{V}_{j+1}^{[ICI]}$ has a dimension of $M_{j+1} \times (M_{j+1} - N_j)$. We denote the number of columns of the $\mathbf{V}_{j+1}^{[ICI]}$ as $D_{j+1} = (M_{j+1} - N_j)^+$. The numeration across the equation changes circularly as in (4.15).

Hence, after applying $\mathbf{V}^{[ICI]}$ the system model can be regarded as the ICI-free network as shown in Fig. 4.3 without the dashed ICI links presented by $\mathbf{H}_{j,j+1}$. Therefore, from the user's perspective, the observed network can be regarded as a set of the MIMO Z-channels.

4.2.3 The XCI Cancellation Scheme and DoF Characterization

After applying the ICI cancellation scheme, each user sees two effective channel observations given by $\bar{\mathbf{H}}_{j,i} = \mathbf{H}_{j,i}\mathbf{V}_i^{[ICI]}$, $i \neq (j+1)$. Therefore, the received signal (4.16) can be expressed as

$$\begin{aligned}
\mathbf{y}_j &= \underbrace{\sum_{i=1, i\neq j+1}^{L=3} \mathbf{H}_{j,i}\mathbf{V}_i^{[ICI]}\mathbf{V}_i^{[XCI]}\mathbf{s}_i}_{\text{desired+XCI signals}} + \underbrace{\cancel{\mathbf{H}_{j,j+1}\mathbf{V}_{j+1}^{[ICI]}\mathbf{V}_{j+1}^{[XCI]}\mathbf{s}_{j+1}}}_{\text{ICI}=0} + \mathbf{n}_j \\
&= \underbrace{\sum_{i=1, i\neq j+1}^{L=3} \mathbf{H}_{j,i}\mathbf{V}_i^{[ICI]}\mathbf{V}_i^{[XCI]}\mathbf{s}_i}_{\text{desired+XCI signals}} + \mathbf{n}_j \\
&= \underbrace{\sum_{i=1, i\neq j+1}^{L=3} \bar{\mathbf{H}}_{j,i}\mathbf{V}_i^{[XCI]}\mathbf{s}_i}_{\text{desired+XCI signals}} + \mathbf{n}_j, \ \forall j \in L,
\end{aligned} \tag{4.18}$$

where, among the rest of the channel observations, from the viewpoint of the data intended to user j, $\bar{\mathbf{H}}_{j,j}$ denotes the channel carrying the first data vector from BS j to user j, while $\bar{\mathbf{H}}_{j,i}$ $(i \neq j)$ is the collateral channel conveying the second data vector from BS i desired by user j. The absence of the channel matrix given

by $\bar{\mathbf{H}}_{j,i}$ $(i = j + 1)$ implies a successive cancellation of the IC interference.

The partial transmit BF matrix $\mathbf{V}_i^{[XCI]}$ in (4.18) can be presented as

$$\mathbf{V}_i^{[XCI]} = \left[\underbrace{\mathbf{V}_i^{[i,i][XCI]}}_{D_i \times d_{[i,i]}} \quad \underbrace{\mathbf{V}_i^{[i+1,i][XCI]}}_{D_i \times d_{[i+1,i]}}\right], \ \forall i \in L, \tag{4.19}$$

where $\mathbf{V}_m^{[n,m][XCI]}$ consists of $d_{[n,m]}$ columns with D_i elements, $\mathbf{v}_l^{[n,m][XCI]}$, $\forall l \in d_{[n,m]}$. Since this section is devoted to the XCI cancellation, the notation $[XCI]$ in the superscripts of (4.19) is omitted for brevity.

Considering (4.15), it is feasible to assume that each base station i tends to transmit more than one symbol to each of the users of interest (users i and $(i+1)$), and, according to (4.18), the transmitted signal from BS i can be redefined as follows

$$\mathbf{x}_1 = \mathbf{V}_1^{[XCI]}\mathbf{s}_1 = \sum_{i=1}^{d_{[1,1]}} \mathbf{v}_i^{[1,1]} c_i^{[1,1]} + \sum_{i=1}^{d_{[2,1]}} \mathbf{v}_i^{[2,1]} c_i^{[2,1]}, \tag{4.20}$$

$$\mathbf{x}_2 = \mathbf{V}_2^{[XCI]}\mathbf{s}_2 = \sum_{i=1}^{d_{[2,2]}} \mathbf{v}_i^{[2,2]} c_i^{[2,2]} + \sum_{i=1}^{d_{[3,2]}} \mathbf{v}_i^{[3,2]} c_i^{[3,2]}, \tag{4.21}$$

$$\mathbf{x}_3 = \mathbf{V}_3^{[XCI]}\mathbf{s}_3 = \sum_{i=1}^{d_{[3,3]}} \mathbf{v}_i^{[3,3]} c_i^{[3,3]} + \sum_{i=1}^{d_{[1,3]}} \mathbf{v}_i^{[1,3]} c_i^{[1,3]}, \tag{4.22}$$

where $c_l^{[j,i]}$ is the l^{th} input of $\mathbf{c}^{[j,i]}$ used to transmit the codeword for message $\mathbf{x}_{j,i}$. This assumption implies that no constraint is imposed on the antenna configuration which will be further defined in order to deliver the data streams in (4.20)–(4.22).

The transmit beamforming vectors $\mathbf{v}_1^{[1,1]}, \ldots, \mathbf{v}_{d_{1,1}}^{[1,1]}$, $\mathbf{v}_1^{[1,3]}, \ldots, \mathbf{v}_{d_{1,3}}^{[1,3]}$, $\mathbf{v}_1^{[2,1]}, \ldots,$ $\mathbf{v}_{d_{2,1}}^{[2,1]}, \mathbf{v}_1^{[2,2]}, \ldots, \mathbf{v}_{d_{2,2}}^{[2,2]}$, $\mathbf{v}_1^{[3,2]}, \ldots, \mathbf{v}_{d_{3,2}}^{[3,2]}$, $\mathbf{v}_1^{[3,3]}, \ldots, \mathbf{v}_{d_{3,3}}^{[3,3]}$ are drawn from the formulation of the null spaces of the concatenated channel matrices $\bar{\mathbf{H}}^{[1]} \triangleq \left[\bar{\mathbf{H}}_{1,1}\ \bar{\mathbf{H}}_{1,3}\right]$, $\bar{\mathbf{H}}^{[2]} \triangleq \left[\bar{\mathbf{H}}_{2,2}\ \bar{\mathbf{H}}_{2,1}\right]$, and $\bar{\mathbf{H}}^{[3]} \triangleq \left[\bar{\mathbf{H}}_{3,3}\ \bar{\mathbf{H}}_{3,2}\right]$ as shown for $\bar{\mathbf{H}}^{[1]}$ in (4.23), where

$$r_1^{[1]} = (D_1 - N_1)^+, \tag{4.24}$$

$$r_2^{[1]} = (D_3 - N_1)^+, \tag{4.25}$$

$$r^{[1]} = (D_1 + D_3 - N_1)^+ - r_1^{[1]} - r_2^{[1]}. \tag{4.26}$$

In (4.23), vectors $\mathbf{v}_1^{[2,1]}, \ldots, \mathbf{v}_{r_1^{[1]}}^{[2,1]}$ are the orthonormal basis vectors for the

$$\underbrace{\begin{bmatrix}\bar{\mathbf{H}}_{1,1} & \bar{\mathbf{H}}_{1,3}\end{bmatrix}}_{N_1 \times (D_1+D_3)} \underbrace{\left[\begin{array}{ccc|ccc|ccc} | & \cdots & | & | & \cdots & | & | & \cdots & | \\ \mathbf{v}_1^{[2,1]} & \cdots & \mathbf{v}_{r_1^{[1]}}^{[2,1]} & \mathbf{0} & \cdots & \mathbf{0} & \mathbf{v}_{r_1^{[1]}+1}^{[2,1]} & \cdots & \mathbf{v}_{r_1^{[1]}+r^{[1]}}^{[2,1]} \\ | & \cdots & | & | & \cdots & | & | & \cdots & | \\ \hline | & \cdots & | & | & \cdots & | & | & \cdots & | \\ \mathbf{0} & \cdots & \mathbf{0} & \mathbf{v}_1^{[3,3]} & \cdots & \mathbf{v}_{r_2^{[1]}}^{[3,3]} & \mathbf{v}_{r_2^{[1]}+1}^{[3,3]} & \cdots & \mathbf{v}_{r_2^{[1]}+r^{[1]}}^{[3,3]} \\ | & \cdots & | & | & \cdots & | & | & \cdots & | \end{array}\right]}_{(D_1+D_3)\times(D_1+D_3-N_1)^+ \text{ matrix } \mathbf{V}^{[1]} \text{ with orthonormal columns}}$$

$$= \underbrace{\begin{bmatrix} | & \cdots & | \\ \mathbf{0} & \cdots & \mathbf{0} \\ | & \cdots & | \end{bmatrix}}_{N_1 \times (r_1^{[1]}+r_2^{[1]}+r^{[1]})} \tag{4.23}$$

null space of the channel matrix $\bar{\mathbf{H}}_{1,1}$. Analogously, vectors $\mathbf{v}_1^{[3,3]}, \ldots, \mathbf{v}_{r_2^{[1]}}^{[3,3]}$ are the orthonormal basis vectors for the null space of the channel matrix $\bar{\mathbf{H}}_{1,3}$. The last $r^{[1]}$ columns of $\mathbf{V}^{[1]}$ are the rest of the null space basis vectors for the combined matrix $\bar{\mathbf{H}}^{[1]}$. The product of $\bar{\mathbf{H}}^{[1]}$ with $\mathbf{V}^{[1]}$ produces a zero-matrix which has a size of $N_1 \times \left(r_1^{[1]} + r_2^{[1]} + r^{[1]}\right)$.

Note that each pair of vectors such as $\mathbf{v}_i^{[1,1]}$ and $\mathbf{v}_j^{[1,3]}$, $\mathbf{v}_i^{[2,2]}$ and $\mathbf{v}_j^{[2,1]}$, $\mathbf{v}_i^{[3,3]}$ and $\mathbf{v}_j^{[3,2]}$ are the transmit BF vectors for the messages designated to users 1, 2, and 3, respectively. The above design chooses these vectors from the null spaces of the corresponding user's channel matrices to zero-force interference as much as possible. The derivation of the first $r_1^{[1]}$ vectors for $\mathbf{v}_i^{[2,1]}$ and the first $r_2^{[1]}$ for $\mathbf{v}_j^{[3,3]}$ is explicit. The $r^{[1]}$ vectors are chosen such that

$$\bar{\mathbf{H}}_{1,1}\mathbf{v}_{r_1^{[1]}+i}^{[2,1]} = -\bar{\mathbf{H}}_{1,3}\mathbf{v}_{r_2^{[1]}+i}^{[3,3]}, \ \forall i \in \{1, \ldots, r^{[1]}\}. \tag{4.27}$$

Thus, the two interfering signals arriving along the direction given in (4.27) span a one-dimensional space at user 1. The remaining vectors $\mathbf{v}_{r_1^{[1]}+r^{[1]}+1,\ldots,r_{d_{21}}^{[1]}}^{[2,1]}$ and $\mathbf{v}_{r_2^{[1]}+r^{[1]}+1,\ldots,r_{d_{33}}^{[1]}}^{[3,3]}$ are picked randomly to ensure that they are linearly independent with probability one.

In a similar way, the transmit BF matrices for the messages designated to users 2 and 3 are derived in Section 4.2.4.

With this in mind, all the generated signals at the BSs are linearly independent

$$
\begin{aligned}
I^{[1]} &= \sum_{i=1}^{d_{[2,1]}} \bar{\mathbf{H}}_{1,1}\mathbf{v}_i^{[2,1]}c_i^{[2,1]} + \sum_{i=1}^{d_{[3,3]}} \bar{\mathbf{H}}_{1,3}\mathbf{v}_i^{[3,3]}c_i^{[3,3]} \\
&= \overbrace{\sum_{i=1}^{\min(d_{[2,1]},r_1^{[1]})} \bar{\mathbf{H}}_{1,1}\mathbf{v}_i^{[2,1]}c_i^{[2,1]} + \sum_{i=1}^{\min(d_{[3,3]},r_2^{[1]})} \bar{\mathbf{H}}_{1,3}\mathbf{v}_i^{[3,3]}c_i^{[3,3]}}^{=0} \\
&\quad + \overbrace{\sum_{i=r_1^{[1]}+r^{[1]}+1}^{d_{[2,1]}} \bar{\mathbf{H}}_{1,1}\mathbf{v}_i^{[2,1]}c_i^{[2,1]}}^{\text{space dimension range}=(d_{[2,1]}-r_1^{[1]})^+-r^{[1]}} + \overbrace{\sum_{i=r_2^{[1]}+r^{[1]}+1}^{d_{[3,3]}} \bar{\mathbf{H}}_{1,3}\mathbf{v}_i^{[3,3]}c_i^{[3,3]}}^{\text{space dimension range}=(d_{[3,3]}-r_2^{[1]})^+-r^{[1]}} \\
&\quad + \overbrace{\sum_{i=1}^{r^{[1]}} \left(\bar{\mathbf{H}}_{1,1}\mathbf{v}_{r_1^{[1]}+i}^{[2,1]}c_{r_1^{[1]}+i}^{[2,1]} + \bar{\mathbf{H}}_{1,3}\mathbf{v}_{r_2^{[1]}+i}^{[3,3]}c_{r_2^{[1]}+i}^{[3,3]}\right)}^{\text{space dimension range}=1}
\end{aligned} \tag{4.32}
$$

with probability one, if

$$D_1 \geq d_{[1,1]} + d_{[2,1]}, \tag{4.28}$$

$$D_2 \geq d_{[2,2]} + d_{[3,2]}, \tag{4.29}$$

$$D_3 \geq d_{[3,3]} + d_{[1,3]}. \tag{4.30}$$

Obtaining $\left(d_{[1,1]}, d_{[1,3]}, d_{[2,1]}, d_{[2,2]}, d_{[3,2]}, d_{[3,3]}\right)$ is now determined by the ability of the users to have enough space to decode the desired symbols. Consider user 1 which desires to receive messages $\mathbf{x}_{1,1}$ and $\mathbf{x}_{1,3}$. These desired messages are propagated along the $d_{[1,1]}$ and $d_{[1,3]}$ linearly independent directions from transmitters 1 and 3, respectively. If the interference at user 1 spans the $d_{I^{[1]}}$ dimensions, then we need to have the following number of receive antennas

$$N_1 \geq d_{[1,1]} + d_{[1,3]} + d_{I^{[1]}}. \tag{4.31}$$

If the above condition is satisfied, user 1 can suppress $I^{[1]}$, formulated in (4.32), by discarding the $d_{I^{[1]}}$ dimensions containing interference.

According to the different interference terms shown earlier, the conditions to achieve $\left(d_{[1,1]}, d_{[1,3]}, d_{[2,1]}, d_{[2,2]}, d_{[3,2]}, d_{[3,3]}\right)$ are determined in (4.33)–(4.35).

Each condition in (4.33)–(4.35) has three cases due to the min terms.

$$
\begin{aligned}
N_1 \geq\ & d_{[1,1]} + d_{[1,3]} + \left(d_{[2,1]} - (D_1 - N_1)^+\right)^+ + \left(d_{[3,3]} - (D_3 - N_1)^+\right)^+ \\
& - \min\Big[\left(d_{[2,1]} - (D_1 - N_1)^+\right)^+,\quad \left(d_{[3,3]} - (D_3 - N_1)^+\right)^+, \\
& \qquad (D_1 + D_3 - N_1)^+ - (D_1 - N_1)^+ - (D_3 - N_1)^+\Big], \qquad (4.33) \\
N_2 \geq\ & d_{[2,1]} + d_{[2,2]} + \left(d_{[1,1]} - (D_1 - N_2)^+\right)^+ + \left(d_{[3,2]} - (D_2 - N_2)^+\right)^+ \\
& - \min\Big[\left(d_{[1,1]} - (D_1 - N_2)^+\right)^+,\quad \left(d_{[3,2]} - (D_2 - N_2)^+\right)^+, \\
& \qquad (D_1 + D_2 - N_2)^+ - (D_1 - N_2)^+ - (D_2 - N_2)^+\Big], \qquad (4.34) \\
N_3 \geq\ & d_{[3,2]} + d_{[3,3]} + \left(d_{[2,2]} - (D_2 - N_3)^+\right)^+ + \left(d_{[1,3]} - (D_3 - N_3)^+\right)^+ \\
& - \min\Big[\left(d_{[3,2]} - (D_2 - N_3)^+\right)^+,\quad \left(d_{[1,3]} - (D_3 - N_3)^+\right)^+, \\
& \qquad (D_2 + D_3 - N_3)^+ - (D_2 - N_3)^+ - (D_3 - N_3)^+\Big] \qquad (4.35)
\end{aligned}
$$

Regarding (4.33), the subspace enabling the interference suppression at user 1 can be described in the following ways.

Case 1:

$$
\begin{aligned}
& \min\Big[\left(d_{[2,1]} - (D_1 - N_1)^+\right)^+,\quad \left(d_{[3,3]} - (D_3 - N_1)^+\right)^+, \\
& \qquad (D_1 + D_3 - N_1)^+ - (D_1 - N_1)^+ - (D_3 - N_1)^+\Big] \\
& = \left(d_{[2,1]} - (D_1 - N_1)^+\right)^+ \\
& \Leftrightarrow\ N_1 \geq d_{[1,1]} + d_{[1,3]} + d_{[2,1]} - (D_1 - N_1)^+ \\
& \Leftrightarrow\ \max(N_1, D_1) \geq d_{[1,1]} + d_{[1,3]} + d_{[2,1]}.
\end{aligned}
$$

Case 2:

$$
\begin{aligned}
& \min\Big[\left(d_{[2,1]} - (D_1 - N_1)^+\right)^+,\quad \left(d_{[3,3]} - (D_3 - N_1)^+\right)^+, \\
& \qquad (D_1 + D_3 - N_1)^+ - (D_1 - N_1)^+ - (D_3 - N_1)^+\Big] \\
& = \left(d_{[3,3]} - (D_3 - N_1)^+\right)^+ \\
& \Leftrightarrow\ N_1 \geq d_{[1,1]} + d_{[1,3]} + d_{[3,3]} - (D_3 - N_1)^+ \\
& \Leftrightarrow\ \max(N_1, D_3) \geq d_{[1,1]} + d_{[1,3]} + d_{[3,3]}.
\end{aligned}
$$

Case 3:

$$
\begin{aligned}
& \min\Big[\left(d_{[2,1]} - (D_1 - N_1)^+\right)^+,\quad \left(d_{[3,3]} - (D_3 - N_1)^+\right)^+, \\
& \qquad (D_1 + D_3 - N_1)^+ - (D_1 - N_1)^+ - (D_3 - N_1)^+\Big]
\end{aligned}
$$

$$
\begin{aligned}
&= (D_1 + D_3 - N_1)^+ - (D_1 - N_1)^+ - (D_3 - N_1)^+ \\
&\Leftrightarrow \; N_1 \geq d_{[1,1]} + d_{[1,3]} + d_{[2,1]} + d_{[3,3]} - (D_1 + D_3 - N_1)^+ \\
&\Leftrightarrow \; \max(N_1, D_1 + D_3) \geq d_{[1,1]} + d_{[1,3]} + d_{[2,1]} + d_{[3,3]}.
\end{aligned}
$$

With $D_{j+1} = (M_{j+1} - N_j)^+$ and repeating the same operations with conditions (4.34)–(4.35), the outer bound on the DoF region can be defined as follows

$$
\begin{aligned}
&\mathcal{D}_{out}^{M-X} \\
&\triangleq \{\max(d_{[1,1]} + d_{[1,3]} + d_{[2,1]} + d_{[2,2]} + d_{[3,2]} + d_{[3,3]}) \in \mathbb{R}_+^6 : \\
&\qquad d_{[1,1]} + d_{[1,3]} + d_{[2,1]} \leq \max(N_1, D_1), \\
&\qquad d_{[1,1]} + d_{[1,3]} + d_{[3,3]} \leq \max(N_1, D_3), \\
&\qquad d_{[2,1]} + d_{[2,2]} + d_{[1,1]} \leq \max(N_2, D_1), \\
&\qquad d_{[2,1]} + d_{[2,2]} + d_{[3,2]} \leq \max(N_2, D_2), \\
&\qquad d_{[3,2]} + d_{[3,3]} + d_{[2,2]} \leq \max(N_3, D_2), \\
&\qquad d_{[3,2]} + d_{[3,3]} + d_{[1,3]} \leq \max(N_3, D_3), \\
&\qquad d_{[1,1]} + d_{[1,3]} \leq N_1, \\
&\qquad d_{[2,1]} + d_{[2,2]} \leq N_2, \\
&\qquad d_{[3,2]} + d_{[3,3]} \leq N_3, \\
&\qquad d_{[1,1]} + d_{[2,1]} \leq D_1, \\
&\qquad d_{[2,2]} + d_{[3,2]} \leq D_2, \\
&\qquad d_{[1,3]} + d_{[3,3]} \leq D_3\}.
\end{aligned}
$$

The common scheme to define the DoF region for any L is given as (4.67) in Section 4.2.7.

While the set $\mathcal{D}_{out}^{M-X}$ provides an outer limit for all obtainable $d_{[j,i]}$ on the compounded multi-cell MIMO network, maximizing any weighted sum of $d_{[j,i]}$ over $\mathcal{D}_{out}^{M-X}$ is a linear programming (LP) problem. The following presents an upper limit for the total number of DoF in a closed-form by explicitly solving the above linear programming problem.

$$
\begin{aligned}
&\textit{Conjecture } 1: \\
&\eta_{out} \triangleq \max_{\mathcal{D}_{out}^{M-X}} \left(d_{[1,1]} + d_{[1,3]} + d_{[2,1]} + d_{[2,2]} + d_{[3,2]} + d_{[3,3]}\right)
\end{aligned}
$$

$$
\begin{aligned}
=\min\{&D_1+D_2+D_3,\ \ N_1+N_2+N_3,\ \ \max(N_3,D_3)+\max(N_2,D_1),\\
&\max(N_1,D_1)+\max(N_3,D_2),\ \ \max(N_2,D_2)+\max(N_1,D_3),\\
&\frac{\max(N_1,D_1)+\max(N_1,D_3)+\max(N_2,D_2)+\max(N_3,D_2)}{2},\\
&\frac{\max(N_1,D_3)+\max(N_2,D_1)+\max(N_3,D_3)+\max(N_2,D_2)}{2},\\
&\frac{\max(N_1,D_1)+\max(N_2,D_1)+\max(N_3,D_2)+\max(N_3,D_3)}{2},\\
&\frac{\max(N_3,D_3)+\max(N_2,D_1)+D_1+D_3+N_3}{2},\\
&\frac{\max(N_3,D_2)+\max(N_3,D_3)+D_1+N_1+N_2}{2},\\
&\frac{\max(N_2,D_2)+\max(N_3,D_2)+D_1+D_3+N_1}{2},\\
&\frac{\max(N_2,D_1)+\max(N_3,D_3)+D_1+D_2+D_3}{2},\\
&\frac{\max(N_2,D_1)+\max(N_3,D_3)+N_1+N_2+N_3}{2},\\
&\frac{\max(N_2,D_1)+\max(N_2,D_2)+D_3+N_1+N_3}{2},\\
&\frac{\max(N_1,D_1)+\max(N_3,D_2)+D_1+D_2+D_3}{2},\\
&\frac{\max(N_1,D_1)+\max(N_2,D_1)+D_2+D_3+N_3}{2},\\
&\frac{\max(N_1,D_1)+\max(N_3,D_2)+N_1+D_2+D_3}{2},\\
&\frac{\max(N_1,D_1)+\max(N_3,D_2)+N_1+N_2+N_3}{2},\\
&\frac{\max(N_1,D_3)+\max(N_2,D_2)+D_1+D_2+D_3}{2},\\
&\frac{\max(N_1,D_3)+\max(N_2,D_2)+N_1+N_2+N_3}{2},\\
&\frac{\max(N_1,D_3)+\max(N_1,D_1)+D_2+N_2+N_3}{2},\\
&\frac{\max(N_1,D_3)+\max(N_3,D_3)+D_1+D_2+N_2}{2},\\
&\frac{\max(D_1,N_1)+\max(D_3,N_1)+\max(D_1,N_2)}{3}\\
&+\frac{\max(D_2,N_2)+\max(D_2,N_3)+\max(D_3,N_3)}{3}\}.
\end{aligned}
$$

$$2\max\left(D_1, N_1, D_2, N_2, D_3, N_3\right) \geq \left(\frac{\max(D_1, N_1) + \max(D_3, N_1) + \max(D_1, N_2)}{3} + \frac{\max(D_2, N_2) + \max(D_2, N_3) + \max(D_3, N_3)}{3}\right) \quad (4.36)$$

Outline of the proof : The theorem is proved by solving the dual problem for the linear program

$$\max\left(d_{[1,1]} + d_{[1,3]} + d_{[2,1]} + d_{[2,2]} + d_{[3,2]} + d_{[3,3]}\right).$$

We explicitly estimate all the extreme points of the feasible space, calculate the objective value at the extreme points, and, finally, eliminate the redundant limits. The solution for Conjecture 1 can be found using the fundamental theorem of linear programming, [145, 146].

Note that all twenty three terms in the min expression of Conjecture 1 are important in general. The examples shown at the top of the page explain this point, and only one of the twenty three limits is tight in each case.

As shown, the number of transmit antennas per node is always greater than the number of receive antennas per node. This condition can be written as $M_i > N_j,\ \forall i, j \in L\ (L = 3)$. Otherwise, the transmitters are not able to zero-force the IC interference. After zero-forcing the ICI, the rest of transmit antennas (D_i) are exploited to mitigate the XCI to gain the maximum DoF.

Comparing these results to the provided outer bound of the compounded three-cell MIMO network, it should be noted that it is feasible to achieve $2N$ DoF by substituting $D_1 = D_2 = D_3 = N_1 = N_2 = N_3 = N$ into the upper bound η_{out} as in (4.36).

4.2.4 The Design of the Transmit Beamforming Matrices

This section presents the rest part of the proposed algorithm which was omitted in the main body of the Chapter. Since the transmit beamforming matrices responsible for the ICI can be calculated by (4.17), the effective channel matrices can be derived as $\bar{\mathbf{H}}_{j,i} = \mathbf{H}_{j,i}\mathbf{V}_i^{[ICI]},\ \forall i, j \in L\ (L = 3)$, where each $\bar{\mathbf{H}}_{j,j+1} = \mathbf{0}$ implies the successive ICI cancellation.

$$\text{Example 1: } (N_1, N_2, N_3) = (2, 4, 6),\ (D_1, D_2, D_3) = (4, 6, 4)$$
$$\Leftrightarrow (M_1, M_2, M_3) = (10, 8, 8) \Rightarrow \eta_{out} = 10, \tag{4.37}$$
$$\text{Example 2: } (N_1, N_2, N_3) = (2, 2, 2),\ (D_1, D_2, D_3) = (1, 1, 1)$$
$$\Leftrightarrow (M_1, M_2, M_3) = (3, 3, 3) \Rightarrow \eta_{out} = 3, \tag{4.38}$$
$$\text{Example 3: } (N_1, N_2, N_3) = (3, 3, 3),\ (D_1, D_2, D_3) = (3, 3, 3)$$
$$\Leftrightarrow (M_1, M_2, M_3) = (6, 6, 6) \Rightarrow \eta_{out} = 6 \tag{4.39}$$

Now it is worth considering users 2 and 3. Hence, it needs to concatenate the rest of the channel matrices with respect to these users such that $\bar{\mathbf{H}}^{[2]} \triangleq \left[\bar{\mathbf{H}}_{2,2}\ \bar{\mathbf{H}}_{2,1}\right]$ and $\bar{\mathbf{H}}^{[3]} \triangleq \left[\bar{\mathbf{H}}_{3,3}\ \bar{\mathbf{H}}_{3,2}\right]$. Therefore, after substitution (4.18) and (4.20)–(4.22), the received signals at users 2 and 3 can be written as follows

$$\begin{aligned}\mathbf{y}_2 = \bar{\mathbf{H}}_{2,1} &\left(\sum_{i=1}^{d_{1,1}} \mathbf{v}_i^{[1,1]} c_i^{[1,1]} + \sum_{i=1}^{d_{2,1}} \mathbf{v}_i^{[2,1]} c_i^{[2,1]}\right) \\ &+ \bar{\mathbf{H}}_{2,2} \left(\sum_{i=1}^{d_{2,2}} \mathbf{v}_i^{[2,2]} c_i^{[2,2]} + \sum_{i=1}^{d_{3,2}} \mathbf{v}_i^{[3,2]} c_i^{[3,2]}\right) + \mathbf{n}_2, \end{aligned} \tag{4.40}$$

$$\begin{aligned}\mathbf{y}_3 = \bar{\mathbf{H}}_{3,2} &\left(\sum_{i=1}^{d_{2,2}} \mathbf{v}_i^{[2,2]} c_i^{[2,2]} + \sum_{i=1}^{d_{3,2}} \mathbf{v}_i^{[3,2]} c_i^{[3,2]}\right) \\ &+ \bar{\mathbf{H}}_{3,3} \left(\sum_{i=1}^{d_{3,3}} \mathbf{v}_i^{[3,3]} c_i^{[3,3]} + \sum_{i=1}^{d_{1,3}} \mathbf{v}_i^{[1,3]} c_i^{[1,3]}\right) + \mathbf{n}_3. \end{aligned} \tag{4.41}$$

The transmit direction vectors $\mathbf{v}_1^{[1,1]}, \ldots, \mathbf{v}_{d_{1,1}}^{[1,1]}$, $\mathbf{v}_1^{[1,3]}, \ldots, \mathbf{v}_{d_{1,3}}^{[1,3]}$, $\mathbf{v}_1^{[2,1]}, \ldots, \mathbf{v}_{d_{2,1}}^{[2,1]}$, $\mathbf{v}_1^{[2,2]}, \ldots, \mathbf{v}_{d_{2,2}}^{[2,2]}$, $\mathbf{v}_1^{[3,2]}, \ldots, \mathbf{v}_{d_{3,2}}^{[3,2]}$, $\mathbf{v}_1^{[3,3]}, \ldots, \mathbf{v}_{d_{3,3}}^{[3,3]}$ are drawn from the formulation of the null spaces of the concatenated matrices $\bar{\mathbf{H}}^{[2]} \triangleq \left[\bar{\mathbf{H}}_{2,2}\ \bar{\mathbf{H}}_{2,1}\right]$ and $\bar{\mathbf{H}}^{[3]} \triangleq \left[\bar{\mathbf{H}}_{3,3}\ \bar{\mathbf{H}}_{3,2}\right]$ as shown in (4.42)–(4.43), where

$$r_1^{[2]} = (D_2 - N_2)^+, \tag{4.44}$$
$$r_2^{[2]} = (D_1 - N_2)^+, \tag{4.45}$$
$$r^{[2]} = (D_1 + D_2 - N_2)^+ - r_1^{[2]} - r_2^{[2]}, \tag{4.46}$$
$$r_1^{[3]} = (D_3 - N_3)^+, \tag{4.47}$$
$$r_2^{[3]} = (D_2 - N_3)^+, \tag{4.48}$$
$$r^{[3]} = (D_2 + D_3 - N_3)^+ - r_1^{[3]} - r_2^{[3]}. \tag{4.49}$$

$$\underbrace{\left[\bar{\mathbf{H}}_{2,2}\ \bar{\mathbf{H}}_{2,1}\right]}_{N_2 \times (D_1+D_2)} \underbrace{\left[\begin{array}{c|c|c} \begin{array}{ccc} | & \cdots & | \\ \mathbf{v}_1^{[3,2]} & \cdots & \mathbf{v}_{r_1^{[2]}}^{[3,2]} \\ | & \cdots & | \end{array} & \begin{array}{ccc} | & \cdots & | \\ \mathbf{0} & \cdots & \mathbf{0} \\ | & \cdots & | \end{array} & \begin{array}{ccc} | & \cdots & | \\ \mathbf{v}_{r_1^{[2]}+1}^{[3,2]} & \cdots & \mathbf{v}_{r_1^{[2]}+r^{[2]}}^{[3,2]} \\ | & \cdots & | \end{array} \\ \hline \begin{array}{ccc} | & \cdots & | \\ \mathbf{0} & \cdots & \mathbf{0} \\ | & \cdots & | \end{array} & \begin{array}{ccc} | & \cdots & | \\ \mathbf{v}_1^{[1,1]} & \cdots & \mathbf{v}_{r_2^{[2]}}^{[1,1]} \\ | & \cdots & | \end{array} & \begin{array}{ccc} | & \cdots & | \\ \mathbf{v}_{r_2^{[2]}+1}^{[1,1]} & \cdots & \mathbf{v}_{r_2^{[2]}+r^{[2]}}^{[1,1]} \\ | & \cdots & | \end{array} \end{array}\right]}_{(D_1+D_2) \times (D_1+D_2-N_2)^+ \text{ matrix } \mathbf{V}^{[2]} \text{ with orthonormal columns}}$$

$$= \underbrace{\left[\begin{array}{ccc} | & \cdots & | \\ \mathbf{0} & \cdots & \mathbf{0} \\ | & \cdots & | \end{array}\right]}_{N_2 \times (r_1^{[2]}+r_2^{[2]}+r^{[2]})} \tag{4.42}$$

$$\underbrace{\left[\bar{\mathbf{H}}_{3,3}\ \bar{\mathbf{H}}_{3,2}\right]}_{N_3 \times (D_2+D_3)} \underbrace{\left[\begin{array}{c|c|c} \begin{array}{ccc} | & \cdots & | \\ \mathbf{v}_1^{[1,3]} & \cdots & \mathbf{v}_{r_1^{[3]}}^{[1,3]} \\ | & \cdots & | \end{array} & \begin{array}{ccc} | & \cdots & | \\ \mathbf{0} & \cdots & \mathbf{0} \\ | & \cdots & | \end{array} & \begin{array}{ccc} | & \cdots & | \\ \mathbf{v}_{r_1^{[3]}+1}^{[1,3]} & \cdots & \mathbf{v}_{r_1^{[3]}+r^{[3]}}^{[1,3]} \\ | & \cdots & | \end{array} \\ \hline \begin{array}{ccc} | & \cdots & | \\ \mathbf{0} & \cdots & \mathbf{0} \\ | & \cdots & | \end{array} & \begin{array}{ccc} | & \cdots & | \\ \mathbf{v}_1^{[2,2]} & \cdots & \mathbf{v}_{r_2^{[3]}}^{[2,2]} \\ | & \cdots & | \end{array} & \begin{array}{ccc} | & \cdots & | \\ \mathbf{v}_{r_2^{[3]}+1}^{[2,2]} & \cdots & \mathbf{v}_{r_2^{[3]}+r^{[3]}}^{[2,2]} \\ | & \cdots & | \end{array} \end{array}\right]}_{(D_2+D_3) \times (D_2+D_3-N_3)^+ \text{ matrix } \mathbf{V}^{[3]} \text{ with orthonormal columns}}$$

$$= \underbrace{\left[\begin{array}{ccc} | & \cdots & | \\ \mathbf{0} & \cdots & \mathbf{0} \\ | & \cdots & | \end{array}\right]}_{N_3 \times (r_1^{[3]}+r_2^{[3]}+r^{[3]})} \tag{4.43}$$

In (4.42), vectors $\mathbf{v}_1^{[3,2]}, \ldots, \mathbf{v}_{r_1^{[2]}}^{[3,2]}$ and $\mathbf{v}_1^{[1,1]}, \ldots, \mathbf{v}_{r_2^{[2]}}^{[1,1]}$ are the orthonormal basis vectors for the null spaces of the channel matrices $\bar{\mathbf{H}}_{2,2}$ and $\bar{\mathbf{H}}_{2,1}$, respectively. The last $r^{[2]}$ columns of $\mathbf{V}^{[2]}$ are the rest of the null space basis vectors for the combined matrix $\bar{\mathbf{H}}^{[2]}$. The product of $\bar{\mathbf{H}}^{[2]}$ with $\mathbf{V}^{[2]}$ produces a zero-matrix which has a size of $N_2 \times \left(r_1^{[2]} + r_2^{[2]} + r^{[2]}\right)$.

Analogously, in (4.43), vectors $\mathbf{v}_1^{[1,3]}, \ldots, \mathbf{v}_{r_1^{[3]}}^{[1,3]}$ and $\mathbf{v}_1^{[2,2]}, \ldots, \mathbf{v}_{r_2^{[3]}}^{[2,2]}$ are the orthonormal basis vectors for the null spaces of the channel matrices $\bar{\mathbf{H}}_{3,3}$ and $\bar{\mathbf{H}}_{3,2}$, respectively. The last $r^{[3]}$ columns of $\mathbf{V}^{[3]}$ are the rest of the null space basis vectors for the combined matrix $\bar{\mathbf{H}}^{[3]}$. The product of $\bar{\mathbf{H}}^{[3]}$ with $\mathbf{V}^{[3]}$ produces a

zero-matrix which has a size of $N_3 \times \left(r_1^{[3]} + r_2^{[3]} + r^{[3]}\right)$.

Note that each pair of vectors such as $\mathbf{v}_i^{[1,1]}$ and $\mathbf{v}_j^{[1,3]}$, $\mathbf{v}_i^{[2,2]}$ and $\mathbf{v}_j^{[2,1]}$, $\mathbf{v}_i^{[3,3]}$ and $\mathbf{v}_j^{[3,2]}$ are the transmit BF vectors for the messages designated to users 1, 2, and 3, respectively. The above design chooses these vectors from the null spaces of the corresponding users channel matrices to zero-force interference as much as possible. The derivation of the first $r_1^{[2]}$ vectors for $\mathbf{v}_i^{[3,2]}$, the first $r_2^{[2]}$ vectors for $\mathbf{v}_i^{[1,1]}$, the first $r_1^{[3]}$ vectors for $\mathbf{v}_i^{[1,3]}$, and the first $r_2^{[3]}$ vectors for $\mathbf{v}_i^{[2,2]}$ are explicit. The $r^{[2]}$ and $r^{[3]}$ are chosen such that

$$\bar{\mathbf{H}}_{2,2}\mathbf{v}^{[3,2]}_{r_1^{[2]}+i} = -\bar{\mathbf{H}}_{2,1}\mathbf{v}^{[1,1]}_{r_2^{[2]}+i},\ \forall i \in \{1,\ldots,r^{[2]}\}, \tag{4.50}$$

$$\bar{\mathbf{H}}_{3,3}\mathbf{v}^{[1,3]}_{r_1^{[3]}+i} = -\bar{\mathbf{H}}_{3,2}\mathbf{v}^{[2,2]}_{r_2^{[3]}+i},\ \forall i \in \{1,\ldots,r^{[3]}\}. \tag{4.51}$$

Thus, each pair of the interfering signals arriving along directions given in (4.50) and (4.51) spans a one-dimensional space at users 2 and 3, respectively. The remaining couples of vectors

$$\left(\mathbf{v}^{[3,2]}_{r_1^{[2]}+r^{[2]}+1,\ldots,r^{[2]}_{d_{3,2}}},\ \mathbf{v}^{[1,1]}_{r_2^{[2]}+r^{[2]}+1,\ldots,r^{[2]}_{d_{1,1}}}\right)$$

and

$$\left(\mathbf{v}^{[1,3]}_{r_1^{[3]}+r^{[3]}+1,\ldots,r^{[3]}_{d_{1,3}}},\ \mathbf{v}^{[2,2]}_{r_2^{[3]}+r^{[3]}+1,\ldots,r^{[3]}_{d_{2,2}}}\right)$$

are picked randomly to ensure that they are linearly independent with probability one.

4.2.5 Case Study and Results Discussion

Next, we consider a compounded three-cell MIMO BC network presented in Fig. 4.3. For simplicity, but without loss of generality, it is feasible to assume that the transmitted signal (4.15) is given as

$$\mathbf{s}_i = \begin{bmatrix} c^{[i,i]} \\ c^{[i+1,i]} \end{bmatrix},\ \forall i \in L\ (L=3), \tag{4.52}$$

where BS i intends to transmit only one symbol to each of the corresponding users. An identical antenna configuration is also assumed where each BS and MS are deployed with M and N antennas, respectively.

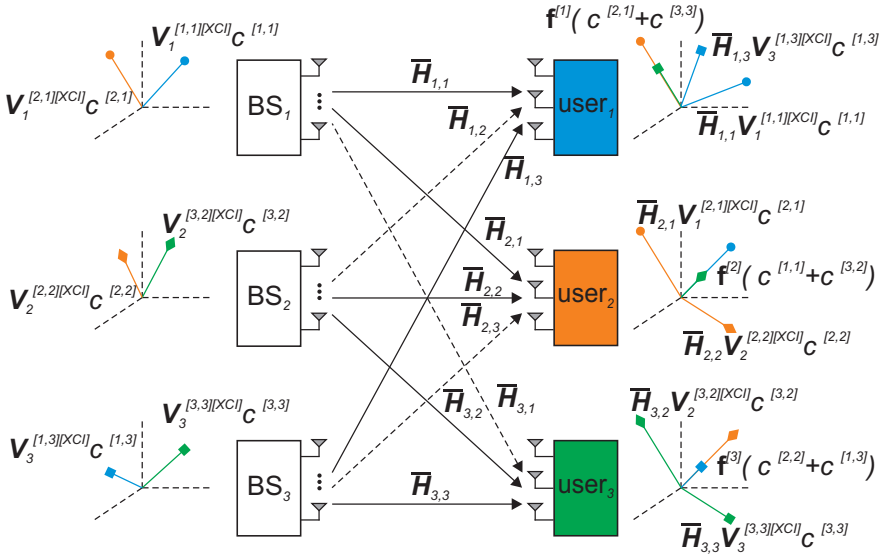

Figure 4.4. Interference alignment in the three-cell compounded MIMO BC network.

To simplify the design of the transmit beamforming matrices responsible for the XCI cancellation, M and N are chosen to ensure that the effective channel matrices $\bar{\mathbf{H}}$ have the dimension of $N \times N$.

Remark. In [121], the authors proposed a MMK coding scheme for the two-user MIMO X-channel. It was shown that with $N = 3$ antennas at each node, a multiplexing gain of 4 is achievable.

Accordingly, to derive an integer number of DoF, each user is equipped with three receive antennas ($N = 3$). Therefore, to successively implement the ICI cancellation (4.17), the base stations are required to be deployed with $M = 6$ antennas per node and $\mathbf{V}^{[ICI]} \in \mathbb{C}^{M \times N}$ can be subsequently derived. Thus, the effective channel matrices $\bar{\mathbf{H}}_{j,i} = \mathbf{H}_{j,i}\mathbf{V}_i^{[ICI]} \in \mathbb{C}^{N \times N}$ $(i \neq j+1)$ meet the above condition and $\bar{\mathbf{H}}_{j,j+1} = \mathbf{H}_{j,j+1}\mathbf{V}_{j+1}^{[ICI]} = \mathbf{0}$.

Once ICI is successively cancelled, the compounded three-cell MIMO network can be regarded as shown in Fig. 4.4 where each user is interested in two symbols (in the corresponding colour). Then, $\mathbf{V}^{[XCI]}$ can be designed according to the alignment conditions in [123] by aligning all the undesired symbols along a vector $\mathbf{f}^{[j]}$ at user j as shown in Fig. 4.4. Then, according to (4.19) and (4.52), $\mathbf{V}_i^{[XCI]} \in \mathbb{C}^{N \times d_s}$ can be defined as follows

$$\mathbf{V}_i^{[XCI]} = \left[\begin{array}{cc} \mathbf{V}_i^{[i,i][XCI]} & \mathbf{V}_i^{[i+1,i][XCI]} \end{array} \right]$$

$$= \left[\begin{array}{cc} \left(\bar{\mathbf{H}}_{i+1,i}\right)^{-1} \mathbf{f}^{[i+1]} & \left(\bar{\mathbf{H}}_{i,i}\right)^{-1} \mathbf{f}^{[i]} \end{array} \right], \ \forall i \in L. \tag{4.53}$$

Therefore, all the undesired symbols at user j are aligned along the vector $\mathbf{f}^{[j]}$ which is picked randomly to be independent from each other. Hence, the received signal (4.18) at user j can be presented as

$$\begin{aligned}
\mathbf{y}_j &= \underbrace{\sum_{i=1, i\neq j+1}^{L=3} \bar{\mathbf{H}}_{j,i} \mathbf{V}_i^{[XCI]} \mathbf{s}_i}_{\text{desired+XCI signals}} + \mathbf{n}_j \\
&= \bar{\mathbf{H}}_{j,j} \mathbf{V}_j^{[XCI]} \mathbf{s}_j + \bar{\mathbf{H}}_{j,j-1} \mathbf{V}_{j-1}^{[XCI]} \mathbf{s}_{j-1} + \mathbf{n}_j \\
&= \bar{\mathbf{H}}_{j,j} \left[\begin{array}{cc} \left(\bar{\mathbf{H}}_{j+1,j}\right)^{-1} \mathbf{f}^{[j+1]} & \left(\bar{\mathbf{H}}_{j,j}\right)^{-1} \mathbf{f}^{[j]} \end{array} \right] \left[\begin{array}{c} x^{[j,j]} \\ x^{[j+1,j]} \end{array} \right] \\
&\quad + \bar{\mathbf{H}}_{j,j-1} \left[\begin{array}{cc} \left(\bar{\mathbf{H}}_{j,j-1}\right)^{-1} \mathbf{f}^{[j]} & \left(\bar{\mathbf{H}}_{j-1,j-1}\right)^{-1} \mathbf{f}^{[j-1]} \end{array} \right] \left[\begin{array}{c} x^{[j-1,j-1]} \\ x^{[j,j-1]} \end{array} \right] + \mathbf{n}_j \\
&= \left[\begin{array}{ccc} \bar{\mathbf{H}}_{j,j} \mathbf{V}_j^{[j,j][XCI]} & \bar{\mathbf{H}}_{j,j-1} \mathbf{V}_{j-1}^{[j,j-1][XCI]} & \mathbf{f}^{[j]} \end{array} \right] \left[\begin{array}{c} x^{[j,j]} \\ x^{[j,j-1]} \\ \left(x^{[j-1,j-1]} + x^{[j+1,j]}\right) \end{array} \right] + \mathbf{n}_j \\
&= \mathbf{T}_j \left[\begin{array}{c} \mathbf{x}^{[j]} \\ \left(x^{[j-1,j-1]} + x^{[j+1,j]}\right) \end{array} \right] + \mathbf{n}_j, \ j \in L \ (L = 3),
\end{aligned} \tag{4.54}$$

where $\mathbf{T}_j \in \mathbb{C}^{N \times N}$ is the resulting channel matrix observed by user j, $\mathbf{x}^{[j]} = \left[x^{[j,j]} \ x^{[j,j-1]}\right]^T$ is the data of interest to user j, and $\mathbf{n}_j \in \mathbb{C}^{N \times 1}$ is the zero-mean AWGN vector.

Finally, the achievable rate by user j can be defined as

$$\mathcal{I}_j = \sum_{i=j-1}^{j} \mathcal{I}_{x^{[j,i]}} = \mathcal{I}_{x^{[j,j]}} + \mathcal{I}_{x^{[j,j-1]}}, \tag{4.55}$$

where $\mathcal{I}_{x^{[j,j]}}$ and $\mathcal{I}_{x^{[j,j-1]}}$ are the individual rates related to each desired symbol defined as

$$\mathcal{I}_{x^{[j,i]}} = \log_2\left(1 + J^{[j,i]}\right), \tag{4.56}$$

where the SINR of the desired symbol $x^{[j,i]}$ can be expressed as

$$J^{[j,i]} = \text{trace}\left(\left(\mathbf{T}_j^{[l,l\neq\{i,3\}]} \mathbf{T}_j^{[l,l\neq\{i,3\}]H} + \mathbf{T}_j^{[3]} \mathbf{T}_j^{[3]H} + \sigma_n^2 \mathbf{I}\right)^{-1} \mathbf{T}_j^{[i]} \mathbf{T}_j^{[i]H}\right), \tag{4.57}$$

$$I_{\Sigma} = \sum_{j=1}^{L=3} \sum_{i=j-1}^{j} \log_2 \left(\det \left[\mathbf{I} + \left(\mathbf{T}_j^{[l,l\neq\{i,3\}]} \mathbf{T}_j^{[l,l\neq\{i,3\}]H} + \mathbf{T}_j^{[3]} \mathbf{T}_j^{[3]H} + \sigma_n^2 \mathbf{I} \right)^{-1} \mathbf{T}_j^{[i]} \mathbf{T}_j^{[i]H} \right] \right) \tag{4.58}$$

where $\mathbf{T}_j^{[l]}$ represents the l^{th} column of $\mathbf{T}_j$.

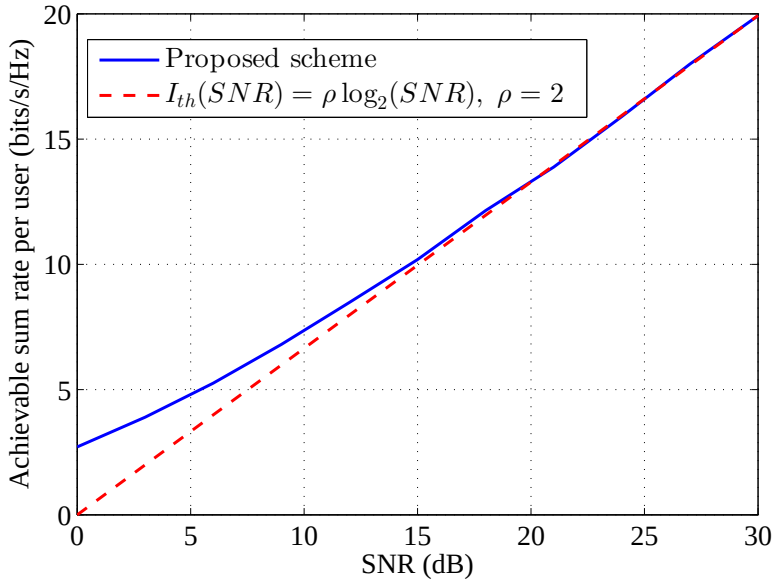

Figure 4.5. Achievable sum rate per user utilizing (4.55)–(4.57).

To validate the proposed scheme and its analysis, the sum rate achievable by user j can be defined by utilizing (4.55)–(4.57). To calculate the received signal (4.54), $\mathbf{H} \in \mathbb{C}^{M \times N}$ is used where each entry of $\mathbf{H}$ is generated using i.i.d. RVs according to $\mathcal{CN}(0,1)$ as in [19, 79]. It is also assumed that each channel is quasi-stationary and frequency flat fading. Therefore, the achievable rate of user j is equal to $\mathcal{I}_j = 19.78$ bits/s/Hz (at 30 dB in Fig. 4.5) that corresponds to two DoF $\left(\frac{\mathcal{I}_j(30 \text{ dB})}{\log_2(30 \text{ dB})} = 1.98 \approx 2 \right)$.

Therefore, in terms of the total DoF achievable for the case study with $L = 3$ cells, we can achieve six DoF which is verified by both simulation (Fig. 4.5) and theoretical results presented in Example 3 on p. 96.

4.2.6 Generalization of the Proposed Scheme

The general expression of the received signal at user j is written as

$$\mathbf{y}_j = \underbrace{\sum_{i=j-\mathcal{L}+1}^{j} \mathbf{H}_{j,i}\mathbf{V}_i^{[ICI]}\mathbf{V}_i^{[XCI]}\mathbf{s}_i}_{\text{desired+XCI signals}} + \underbrace{\sum_{l=1,l\neq i}^{L} \mathbf{H}_{j,l}\mathbf{V}_l^{[ICI]}\mathbf{V}_l^{[XCI]}\mathbf{s}_l}_{\text{ICI}} + \mathbf{n}_j,\ \forall j \in L. \quad (4.59)$$

Identical Antenna Configuration

Under an identical antenna configuration, BSs and users are deployed with M and N antennas per node, respectively. Since we derive the effective channel matrix $\bar{\mathbf{H}} \in \mathbb{C}^{N\times N}$, we have to regard the fact that the number of the ICI channels increases linearly as the number of cells grows. Accordingly, we give the minimum requirements for the numbers of transmit and receive antennas to efficiently realize the proposed scheme.

For the case with more than one ICI channel ($L-\mathcal{L} > 1$), equation (4.17) can be adapted as

$$\mathbf{V}_i^{[ICI]} = \text{null}\left(\left[\ \left(\mathbf{H}_{[i+\mathcal{L},i]}\right)^H \ \ \ldots \ \ \left(\mathbf{H}_{[i+(L-1),i]}\right)^H\ \right]^H\right),\ \forall i \in L, \quad (4.60)$$

where the numeration of the first term in the subscript changes circularly, e.g., for $L = 4$, $\mathcal{L} = 2$ and $i = 3 \Rightarrow i+\mathcal{L} = 3+2 = 5 \triangleq 1$ and $i+(L-1) = 3+3 = 6 \triangleq 2$. In (4.60), for the case of $L \geq 3$, each user observes extra $(L-\mathcal{L})$ IC links that have to be mitigated in order to successively implement the concept of the compounded L-cell MIMO network. Therefore, if all the users are deployed with the same number of antennas, N, the matrix under the null function in (4.60) has dimension of $M \times N(L-\mathcal{L})$. Hence, $\mathbf{V}_i^{[ICI]}$ exists only if $M > N(L-\mathcal{L})$. Therefore, the size of $\mathbf{V}_i^{[ICI]}$ is $M \times M - N(L-\mathcal{L})$. In order to derive $\bar{\mathbf{H}}$, we modify the existence condition of $\mathbf{V}_i^{[ICI]}$ as $N = M - N(L-\mathcal{L})$. Consequently, we have to equip each BS with the number of antennas defined as

$$M = N(L-\mathcal{L}+1), \quad (4.61)$$

and the difference between the numbers of transmit and receive antennas is given by

$$D = M - N = N(L - \mathcal{L}). \tag{4.62}$$

As shown, the provided above condition satisfies the conventional MIMO X-channel with $L = 2$ cells and three antennas per node, [121], and hence the condition simply reduces to $M = N = 3$ because the BSs do not cause any ICI ($\mathcal{L} = 0$), and $D = 0$.

Different Antenna Configuration

For the case when users are equipped with different number of antennas, we have to calculate the $\mathbf{V}^{[ICI]}$ matrix as a function of the number of receive antennas. As defined earlier, within the proposed L-cell MIMO network each receiving node experiences $(L - \mathcal{L})$ ICI channels. Hence, the size of the matrix $\mathbf{V}_i^{[ICI]}$ can be given as

$$M_i \times \left(M_i - \sum_{k=i+\mathcal{L}, k\neq i,\ldots,i+\mathcal{L}-1}^{L} N_k \right)^+.$$

The positive difference between the numbers of antennas should satisfy the condition on the number of data streams to transmit (see (4.28)–(4.30)) and can be calculated as

$$D_i \geq \sum_{k=i}^{i+\mathcal{L}-1} d_{[k,i]},\ \forall i \in L, \tag{4.63}$$

where $d_{[k,i]}$ denotes the number of data streams transmitted from BS i to user k under a multi-source transmission scenario.

Hence, the minimum number of antennas at BS i can be calculated as follows

$$\begin{aligned} M_i &\geq \sum_{k=i+\mathcal{L}, k\neq\{i,\ldots,i+\mathcal{L}-1\}}^{L} N_k + D_i \\ &= \sum_{k=i+\mathcal{L}, k\neq\{i,\ldots,i+\mathcal{L}-1\}}^{L} N_k + \sum_{k=i}^{i+\mathcal{L}-1} d_{[k,i]},\ \forall i \in L. \end{aligned} \tag{4.64}$$

This condition should by satisfied to ensure that the proposed scheme can be realized and all the interference in the network is captured.

When M is not Sufficient

The case when the number of transmit antennas is not enough to maintain the proposed scheme can be written as

$$M_i < \sum_{k=i+\mathcal{L},k\neq\{i,\ldots,i+\mathcal{L}-1\}}^{L} N_k + \sum_{k=i}^{i+\mathcal{L}-1} d_{[k,i]},\ \forall i \in L. \tag{4.65}$$

For simplicity, it is assumed that BS i aims to transmit a similar number of the data streams $d_{[(\cdot),i]}$ to each of the interested users. Then, (4.65) can be rewritten as

$$M_i < \sum_{k=i+\mathcal{L},k\neq\{i,\ldots,i+\mathcal{L}-1\}}^{L} N_k + \mathcal{L}d_{[(\cdot),i]},\ \forall i \in L. \tag{4.66}$$

According to (4.66), we consider several cases under the assumption of

$$\sum_{k=i+\mathcal{L},k\neq\{i,\ldots,i+\mathcal{L}-1\}}^{L} N_k > \mathcal{L}d_{[(\cdot),i]}.$$

$M_i < \mathcal{L}d_{[(\cdot),i]}$ This case is the worst network scenario because BS i does not have enough antennas to transmit all the desired data streams to the intended users.

$M_i = \mathcal{L}d_{[(\cdot),i]}$ This antenna configuration implies that all the unwanted users suffer from the ICI caused by BS i. Since the received signal at user j is given by (4.59), the second ICI term in this equation degrades the SNR metric.

$\mathcal{L}d_{[(\cdot),i]} < M_i \leq \sum_{k=i+\mathcal{L},k\neq\{i,\ldots,i+\mathcal{L}-1\}}^{L} N_k + \mathcal{L}d_{[(\cdot),i]}$ This case consists of two possibilities given by

$$\mathcal{L}d_{[(\cdot),i]} < M_i \leq \sum_{k=i+\mathcal{L},k\neq\{i,\ldots,i+\mathcal{L}-1\}}^{L} N_k$$

and

$$\sum_{k=i+\mathcal{L},k\neq\{i,\ldots,i+\mathcal{L}-1\}}^{L} N_k < M_i < \mathcal{L}d_{[(\cdot),i]} + \sum_{k=i+\mathcal{L},k\neq\{i,\ldots,i+\mathcal{L}-1\}}^{L} N_k.$$

Both of them stand for the scenario when the ICI (caused by BS i) might be partially or totally present at each user. In particular, it depends on how many antennas, from the total amount of antennas of the unwanted users, are taken

into account to prevent the IC interference as shown in (4.60).

It is also worth mentioning that the results are applicable to the general X-channel in the sense that the receiver is served simultaneously by more than one BS. However, in the case when the channel is purely X-channel (i.e., each the user is served by all the base stations) the part of the BF matrix responsible for the non X-channel interference is replaced by an identity submatrix. In our proposed set up, the system does not receive any less interference, but rather part of the otherwise X-channel interference becomes ICI interference. Hence, by arranging the set up in this way the overall amount of interference is unchanged, but we have more design-flexibility to maximize the DoF.

4.2.7 An Upper Limit of the DoF Region for the Compounded Multi-cell MIMO BC Network

With respect to the number of cells, L, the outer bound on the DoF region can be defined as in (4.67). Thus, for the considered MIMO network with L-cells we have $4L$ constraints that determine the upper limit of the DoF region ($\mathcal{L} = 2$).

While the set $\mathcal{D}_{out}^{M-X}$ provides an outer limit for all attainable $d_{[j,i]}$ on the L-cell MIMO IC-X channel, maximization of the sum of $d_{[j,i]}$ over $\mathcal{D}_{out}^{M-X}$ is a linear programming problem, where it is required to explicitly estimate all the extreme points of the feasible space, to calculate the objective values and, finally, to eliminate all the redundant limits.

$$\begin{aligned}\mathcal{D}_{out}^{M-X} \triangleq \{\max \sum_{i=1}^{L} \left(d_{[i,i]} + d_{[i+1,i]}\right) \in \mathbb{R}_{+}^{2L} :& \\ &\text{sets of constraints with respect to each cell } i : \\ & d_{[i,i]} + d_{[i-1,i-1]} + d_{[i,i-1]} \leq \max(D_{i-1}, N_i) \\ & d_{[i,i]} + d_{[i+1,i]} + d_{[i,i-1]} \leq \max(D_i, N_i) \\ & d_{[i,i]} + d_{[i,i-1]} \leq N_i \\ & d_{[i,i]} + d_{[i+1,i]} \leq D_i\}. \end{aligned} \tag{4.67}$$

4.3 Chapter Summary

This Chapter proposed an interference alignment and cancellation scheme for a downlink network with multiple cells and MIMO users under a compounded MIMO BC network scenario. The joint transmit BF matrices were designed using a closed-form expression to capture all the interference. We then characterized the DoF region and provided an explicit upper limit for the achievable DoF. Moreover, the analytical and numerical results validated that the proposed scheme achieves the promised number of DoF. Finally, the proposed scheme and its analysis for different antenna configurations were generalized. Moreover, the results demonstrated that it is feasible to achieve more DoF by carefully designing the network downlink transmission.

Chapter 5

Interference Alignment in Compounded MIMO Broadcast Channels with Antenna Correlation and Mixed User Classes

This Chapter considers a compounded MIMO BC network scenario with MIMO mixed users classes and presents a beamforming technique that can achieve the maximum degree of freedom. Chapter 3 considered the network scenario comprising of all the aforementioned cases and proposed a closed-form IA scheme dealing with a mitigation of the corresponding types of interference. Due to limited physical space, resulting in small separations between the antenna elements, each channel is affected by antenna correlation which hinders further enhancements of the transmission rate. In contrast to Chapters 3 and 4, this Chapter considers the compounded MIMO BC network scenario when the users require different classes of data. In particular, the Chapter focusses on the achievable sum rate and DoF region under various scenarios of CSI mismatch and spatial correlations. A beamforming algorithm to define the minimum required antenna configuration to achieve the maximum realizable DoF is proposed. The performance of this technique is evaluated in conventional and Large-scale MIMO systems under different channel conditions. Finally, the complexity of this technique is studied and compared to well-known benchmark techniques. The results demonstrate

the effectiveness of the proposed technique particularly under highly correlated channels. It is shown that this technique is not only associated with relatively lower computational requirement, but also can still achieve the maximum DoF even when the multiplexed users belong to different classes.

5.1 System Model

The system model considered here presents a compounded MIMO broadcast channel network scenario comprising of L cells with multiple users located in the totally overlapped area, [131, 132]. Accordingly, the network configuration is defined as (M, N, K, L, d), where M and N indicate the number of transmit and receive antennas, respectively, K is the number of users per cell, and d denotes the number of data streams transmitted from each BS. As in Chapter 3, this Chapter focuses only on the users located in Area 3 defined in Table (3.1); hence, we specify these receivers as a subset of the total number of users per cell ($\mathcal{K} \leq K$). For the sake of brevity, it is assumed that each BS serves only one user in the totally overlapped area ($\mathcal{K} = 1$), and, according to Chapter 3, the received signal of the user of interest can be then written as

$$\tilde{\mathbf{y}}_j = \underbrace{\mathbf{U}_j^H \sum_{i=j-\mathcal{L}+1}^{j} \mathbf{H}_{j,i}\mathbf{V}_i\mathbf{s}_i}_{\text{desired + XCI signals}} + \underbrace{\mathbf{U}_j^H \sum_{l=1,l\neq i}^{L} \mathbf{H}_{j,l}\mathbf{V}_l\mathbf{s}_l}_{\text{ICI}} + \tilde{\mathbf{n}}_j, \ \forall j \in L, \tag{5.1}$$

where $\mathbf{U}_j \in \mathbb{C}^{N\times d}$ denotes the receive beamforming matrix of the user of interest, and $\tilde{\mathbf{n}}_j = \mathbf{U}_j^H\mathbf{n}_j \in \mathbb{C}^{d\times 1}$ is the effective zero-mean AWGN vector, with $\mathbb{E}\left\{\tilde{\mathbf{n}}_j\tilde{\mathbf{n}}_j^H\right\} = \sigma_{\tilde{n}}^2\mathbf{I}$. $\mathbf{H}_{j,i} \in \mathbb{C}^{N\times M}$ is the channel matrix between base station i and the user of interest. $\mathcal{L}$ is the number of cells which are interested in the data transmitted from BS i ($1 < \mathcal{L} < L$). Regarding the design of the transmit beamforming matrix, it is feasible to split it into two parts as in (3.6) as follows

$$\mathbf{V}_i = \mathbf{V}_i^{[ICI]} \times \mathbf{V}_i^{[XCI]}, \ \forall i \in L,$$

where $\mathbf{V}_i^{[ICI]} \in \mathbb{C}^{M\times Q}$ and $\mathbf{V}_i^{[XCI]} \in \mathbb{C}^{Q\times d}$ are the BF matrices responsible for mitigating the ICI and XCI terms in (5.1), respectively. $\mathbf{V}_i \in \mathbb{C}^{M\times d}$ is the transmit BF matrix at BS i, with trace $\left\{\mathbf{V}_i\mathbf{V}_i^H\right\} = 1$. It is assumed that $\mathbf{s}_i \in \mathbb{C}^{d\times 1}$ is the data vector comprising of the symbols drawn from i.i.d. Gaussian input

signaling and chosen from a desired constellation, with $\mathbb{E}\left\{\mathbf{s}_i\mathbf{s}_i^H\right\} = \mathbf{I}$. Then, all these conditions sufficiently meet the average power constraint at the BS.

With this in mind and due to the nature of broadcast transmission, it can be assumed that the users within one cell desire to receive the same data, thus the transmitted signal can be expressed as

$$\mathbf{s}_i = \left[\mathbf{c}^{[i,i]T} \quad \mathbf{c}^{[i,i+1]T} \quad \cdots \quad \mathbf{c}^{[i,l]T} \quad \cdots \quad \mathbf{c}^{[i,i+\mathcal{L}-1]T}\right]^T, \ \forall i \in L, \tag{5.2}$$

where $\mathbf{c}^{[j,l]} \in \mathbb{C}^{P\times 1}$ is the l^{th} part of the message vector transmitted from base station i and designed to be delivered to the user belonging to cell j. More specifically, (5.2) implies that BS i dedicates the first part of the data to its corresponding user, while the second part of the data is transmitted to the user belonging to the neighbouring cell $(i+1)$, and so on. The superscript numeration $(i + \mathcal{L} - 1)$ changes circularly, e.g., for $i = 3$ and $L = 3$ ($\mathcal{L} = 2$), we have $(i + \mathcal{L} - 1) = 4 \rightarrow 1$.

5.1.1 Imperfect CSI

Since the CSI acquisition in practice is presented by imperfect estimates of the channel parameters, the system performance is likely to be degraded compared with the assumption of perfect CSI. Accordingly, to understand the impact of CSI mismatch on the system performance, the CSI acquisition model given by (2.7)–(2.8) is redefined in order to facilitate the following derivations related to antenna correlation as

$$\mathbf{G} = \hat{\mathbf{H}} + \hat{\mathbf{E}}, \tag{5.3}$$

where $\hat{\mathbf{H}} \sim \mathcal{CN}\left(0, \frac{1}{\tau+1}\mathbf{I}\right)$ indicates the mismatched channel, and $\hat{\mathbf{E}} \sim \mathcal{CN}\left(0, \frac{\tau}{\tau+1}\mathbf{I}\right)$ is independent of $\hat{\mathbf{H}}$. τ is given by $\tau = \beta\rho^{-\alpha}$ $(\alpha \geq 0, \beta > 0)$, where ρ stands for a nominal SNR, and α and β represent the constants used to define various CSI scenarios, [19, 24, 25, 26, 27].

5.1.2 Kronecker Product based Channel Modeling with Antenna Correlation

The downlink channel $\mathbf{H}_{j,i}$ in (5.1) is modeled as a correlated Rayleigh flat fading channel. Since the system model in Chapter 3 presumes that both transmitter and receiver nodes are deployed with multiple antennas, it is feasible to assume

that the fading is correlated at both sides.

The general model of the correlated channel is given as, [148, 149, 150],

$$\mathrm{vec}\left(\mathbf{H}\right) = \mathbf{R}^{1/2}\mathrm{vec}\left(\mathbf{G}\right), \tag{5.4}$$

where $\mathbf{G}$ is the i.i.d. MIMO channel with either perfect CSI or CSI mismatch as in (5.3), and $\mathbf{R}$ is the covariance matrix defined as

$$\mathbf{R} \triangleq \mathbb{E}\left\{\mathrm{vec}\left(\mathbf{G}\right)\mathrm{vec}\left(\mathbf{G}\right)^{H}\right\}, \tag{5.5}$$

where $\mathrm{vec}\left(\cdot\right)$ indicates the vector operator.

A popular MIMO channel model is called the Kronecker model, [150, 151, 152], which is based on the assumption of a separability of the transmit and receive correlation coefficients, that is, the transmitter does not affect the spatial properties of the received signal.

The Kronecker model is limited because it does not take into account the coupling between the direction of departure (DoD) at the transmitter and the direction of arrival (DoA) at the receiver, which is typical in MIMO channels. Thus, the Kronecker model can be applied only in certain environments. In small 2×2 and 3×3 MIMO systems, because of reduced spatial resolution involved, the Kronecker model was shown to be a good fit to the measured channel, [153, 154]. However, application of the Kronecker model to a measured 8×8 non-line-of-sight (NLOS) MIMO channel resulted in discrepancies in the modeled capacity and the joint spatial DoD-DoA spectra, [155]. Similar results were provided in outdoor-to-indoor office MIMO channel measurements, [156]; while the Kronecker model was found to be a good fit in a 2×8 line-of-sight (LOS) setup, the fit was found to be not as good in a 16×8 NLOS setup. In [157, 158], the authors studied the suitability of the Kronecker model in the two-ring and elliptical models. It was shown that the Kronecker model is suitable for use in the two-ring model (for some outdoor environments) and not applicable in the elliptical model (for some indoor environments) due to non-separability and separability of the correlation structures in the latter and former models, respectively.

Despite the limitation of ignoring the coupling between the DoD and DoA at transmit and receive ends, the Kronecker model is widely used in information theoretic capacity analysis and simulation studies, [159, 160, 161, 162]. Though the Kronecker model is expected to be increasingly inaccurate for increasing array

size and angular resolution, it still finds use in large MIMO system studies because of its simplicity. Therefore, the Kronecker model is found to be sufficient to analyse the effect of spatial correlation on the network performances for the case of Large-scale MIMO model.

With all this in mind, the Kronecker-based correlation matrix is given as

$$\mathbf{R} = \mathbf{R}_r \otimes \mathbf{R}_t, \tag{5.6}$$

where the notation $\otimes$ stands for the Kronecker product operator, $\mathbf{R}_r \in \mathbb{C}^{N\times N}$ and $\mathbf{R}_t \in \mathbb{C}^{M\times M}$ are the receive and transmit correlation matrices defined as

$$\mathbf{R}_r = \frac{1}{M}\mathbb{E}\left\{\mathbf{G}\mathbf{G}^H\right\}, \tag{5.7}$$

$$\mathbf{R}_t = \frac{1}{N}\mathbb{E}\left\{\mathbf{G}^H\mathbf{G}\right\}. \tag{5.8}$$

Then, the channel realization, with respect to imperfect CSI (5.3), can be modeled as, [163, 164],

$$\begin{aligned}\mathbf{H} &= \mathbf{R}_r^{1/2}\mathbf{G}\mathbf{R}_t^{1/2}\\ &= \mathbf{R}_r^{1/2}\left(\hat{\mathbf{H}} + \hat{\mathbf{E}}\right)\mathbf{R}_t^{1/2}\\ &= \mathbf{R}_r^{1/2}\hat{\mathbf{H}}\mathbf{R}_t^{1/2} + \mathbf{R}_r^{1/2}\hat{\mathbf{E}}\mathbf{R}_t^{1/2}\\ &= \tilde{\mathbf{H}} + \tilde{\mathbf{E}},\end{aligned} \tag{5.9}$$

where $\tilde{\mathbf{H}} = \mathbf{R}_r^{1/2}\hat{\mathbf{H}}\mathbf{R}_t^{1/2} \sim \mathcal{CN}(\mathbf{0}, \mathbf{R}_r \otimes \frac{1}{\tau+1}\mathbf{I} \otimes \mathbf{R}_t)$ is the estimated channel matrix, and $\tilde{\mathbf{E}} = \mathbf{R}_r^{1/2}\hat{\mathbf{E}}\mathbf{R}_t^{1/2} \sim \mathcal{CN}(\mathbf{0}, \mathbf{R}_r \otimes \frac{\tau}{\tau+1}\mathbf{I} \otimes \mathbf{R}_t)$ is the estimation error which is uncorrelated with $\tilde{\mathbf{H}}$. In the above $\mathcal{CN}(\mu, \mathbf{\Sigma})$ denotes the multivariate complex normal distribution with mean vector μ and covariance matrix $\mathbf{\Sigma}$.

With this in mind, we refer to [165], where, for the case of both-end correlation, the authors showed that the Kronecker-based exponential and uniform models are empirically reasonable to apply at transmitter and receiver sides, respectively. Moreover, these simple single-parameter models allow one to investigate the effects of both-end correlation on the achievable sum rate and DoF to achieve clearer insights in an explicit way.

Exponential Correlation Coefficient Model

The most common and easy model that accounts for the potential antenna correlation is the exponential model, [150, 152], which can be accordingly utilized at the transmitter side as follows

$$\mathbf{R}_{t_{[m,n]}} = \begin{cases} r^{|m-n|}, & \text{if } m \geq n, \\ (r^{\dagger})^{|m-n|}, & \text{if } m < n, \end{cases} \tag{5.10}$$

where the subscript notation $[m, n]$ indicates the matrix element located in the m^{th} row and n^{th} column. $(\cdot)^{\dagger}$ denotes a complex conjugate and $r = ae^{j\theta}$ is the complex correlation coefficient with $0 \leq a < 1$. For simplicity, $r = a$ is assumed throughout the Chapter, unless it is restated.

Uniform Correlation Coefficient Model

The uniform coefficient model, [166], is the worst case scenario where all the correlation coefficients are defined as

$$\mathbf{R}_{r_{[m,n]}} = \begin{cases} r^{|m-n|}, & \text{if } m = n, \\ r, & \text{if } m \neq n, \end{cases} \tag{5.11}$$

where the coefficients of all neighbouring subchannels are assumed to be equal to those of the distant channels.

5.2 The DoF and Sum Rate Analysis

As stated in Chapters 3 and 4, the compounded MIMO BC scenario represents the network model where each user located in the totally overlapped area experiences a multi-source transmission from $\mathcal{L}$ base stations. In particular, Chapter 3 focused on the scenario when each Tx-Rx pair has an identical antenna configuration with an equal number of data streams transmitted to the users of interest. In contrast to Chapter 3, here we consider the network scenario when the BSs serve different classes of users deployed with various numbers of antennas. For this reason, the network configuration is restated (given in the previous section) as $(M_i, N_i, \mathcal{K}, L, d_i)$. To analyse how the proposed IA scheme performs under the modified transmission strategy, the same three-cell network scenario is utilized as

in Chapter 3. For the sake of simplicity, it is assumed that each cell consists of one BS serving a single user in the totally overlapped area in a similar fashion as in Fig. 3.2. Thus, each BS aims to send data to two users of interest ($\mathcal{L} = 2$). Accordingly, the transmitted signal in (5.2) can be rewritten as

$$\mathbf{s}_i = \begin{bmatrix} \mathbf{c}^{[i,i]} \\ \mathbf{c}^{[i,i+1]} \end{bmatrix}, \ \forall i \in L, \tag{5.12}$$

where $\mathbf{c}^{[i,1]} \in \mathbb{C}^{d^{[i,i]} \times 1}$ is the data vector transmitted from BS i to the corresponding user belonging the same cell, while $\mathbf{c}^{[i+1,2]} \in \mathbb{C}^{d^{[i,i+1]} \times 1}$ indicates the data transmitted to a desired user in the neighbouring cell. Since we want to examine different classes of users, it can be assumed that BS i transmits i data streams to the corresponding user i and only one data stream to a desired user in the neighbouring cell.

In the following sections, we show how to define the antenna configuration for each Tx-Rx pair for the case of three-cell MIMO network and to determine the performance metrics taking into account antenna correlations.

5.2.1 The Beamforming Design

Since the transmit beamforming matrix is decoupled into two parts, it needs to start with the design of the part responsible for the IC interference mitigation. For the sake of brevity, we refer to Section 3.4.1, where the given scheme is also applicable for the case with a single user per cell.

After applying that scheme, we come up with $\mathbf{V}_i^{[ICI]}$ with dimension of $M_i \times (M_i - N_{i-1})$. Hence, the matrix dimension leads to the following condition

$$(M_i - N_{i-1})^+ \geq d_i, \ \forall i \in L \tag{5.13}$$

to be satisfied for a successful transmission of all the desired data to the interested users, and d_i is the number of data streams transmitted from BS i and defined with respect to (5.12) as

$$d_i = \sum_{j=i}^{i+1} d_{[i,j]}, \ \forall i \in L. \tag{5.14}$$

For simplicity of the following derivations, a new variable is introduced that indicates the number of columns in $\mathbf{V}_i^{[ICI]}$, as well as the number of non-occupied

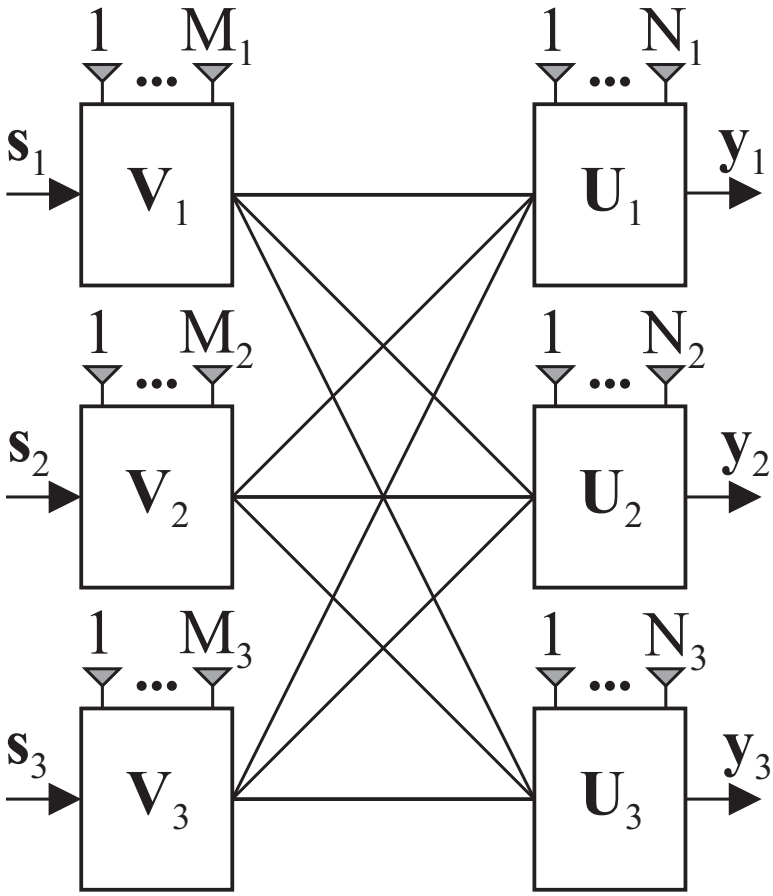

Figure 5.1. The three-cell compounded MIMO BC scenario with $\mathcal{K} = 1$ user per cell with various numbers of antennas at each Tx-Rx pair.

antennas at the transmitter side, and can be defined as

$$Q_i = (M_i - N_{i-1})^+, \ \forall i \in L. \tag{5.15}$$

Finally, the condition of the successive ICI cancellation in (5.13) is restated as

$$\text{rank}\left(\mathbf{V}_i^{[ICI]}\right) \geq Q_i, \ \forall i \in L. \tag{5.16}$$

Since we have different classes of receivers and BSs that aim to transmit different numbers of data streams to the users of interest, we need to define the number of data streams desired to be decoded at user j as

$$d^{[j]} = \sum_{\forall i} d_{[i,j]}, \ \forall j \in L, \tag{5.17}$$

where $d_{[i,j]}$ indicates the number of data streams transmitted from BS i to the particular user j. In general, the number of transmitted data streams from BS i is not equal to the number of data streams desired to be received by the corresponding user i, $d_i \neq d^{[i]}$; nevertheless, the total number of streams at the transmitter side always matches the one at the receiver side as

$$\sum_{i=1}^{L=3} d_i = \sum_{j=1}^{L=3} d^{[j]}. \tag{5.18}$$

With this in mind, the received signal $\tilde{\mathbf{y}}_j$ at user j can be written as

$$\begin{aligned}
\tilde{\mathbf{y}}_j &= \underbrace{\mathbf{U}_j^H \sum_{i=j-1}^{j} \mathbf{H}_{j,i}\mathbf{V}_i^{[ICI]}\mathbf{V}_i^{[XCI]}\mathbf{s}_i}_{\text{desired + XCI signals}} + \underbrace{\cancel{\mathbf{U}_j^H \sum_{l=1,l\neq i}^{L=3} \mathbf{H}_{j,l}\mathbf{V}_l^{[ICI]}\mathbf{V}_l^{[XCI]}\mathbf{s}_l}}_{\text{ICI=0}} + \tilde{\mathbf{n}}_j \\
&= \sum_{i=j-1}^{j} \mathbf{U}_j^H \mathbf{H}_{j,i}\mathbf{V}_i^{[ICI]}\mathbf{V}_i^{[XCI]}\mathbf{s}_i + \tilde{\mathbf{n}}_j \\
&= \sum_{i=j-1}^{j} \bar{\mathbf{H}}_{j,i}\mathbf{V}_i^{[XCI]}\mathbf{s}_i + \tilde{\mathbf{n}}_j \\
&= \sum_{i=j-1}^{j} \bar{\mathbf{H}}_{j,i} \underbrace{\left[\mathbf{V}^{[i,i]XCI}\right.}_{Q_i \times d_{[i,i]}} \underbrace{\left.\mathbf{V}^{[i,i+1]XCI}\right]}_{Q_i \times d_{[i,i+1]}} \begin{bmatrix} \mathbf{c}^{[i,i]} \\ \mathbf{c}^{[i,i+1]} \end{bmatrix} + \tilde{\mathbf{n}}_j, \ \forall j \in L,
\end{aligned} \tag{5.19}$$

where $\bar{\mathbf{H}}_{j,i} = \mathbf{U}_j^H \mathbf{H}_{j,i}\mathbf{V}_i^{[ICI]}$ indicates the effective channel matrix. The underbraced terms represent the $Q_i \times d_{[m,n]}$ matrices responsible for the XCI cancellation of the undesired data, $\mathbf{c}^{[m,n]}$. Then, the user of interest no longer experiences the ICI, but the interference arriving along the desired directions presented by the $\mathbf{c}^{[j-1,j-1]}$ and $\mathbf{c}^{[j,j+1]}$ data vectors with $d_{[j-1,j-1]}$ and $d_{[j,j+1]}$ data streams, respectively. Hence, the minimum and maximum numbers of the interfering data streams is defined as

$$k_i = \min\left\{d_{[j-1,j-1]}, d_{[j,j+1]}\right\}, \tag{5.20}$$

$$r_i = \max\left\{d_{[j-1,j-1]}, d_{[j,j+1]}\right\}, \tag{5.21}$$

and the corresponding difference as

$$w_i = r_i - k_i. \tag{5.22}$$

To be more specific, the received signal at user 1 with respect to (5.12) can be presented as

$$\begin{aligned}\tilde{\mathbf{y}}_1 &= \bar{\mathbf{H}}_{1,1}\left[\mathbf{V}^{[1,1]XCI} \quad \mathbf{V}^{[1,2]XCI}\right]\begin{bmatrix}\mathbf{c}^{[1,1]}\\ \mathbf{c}^{[1,2]}\end{bmatrix} \\ &\quad + \bar{\mathbf{H}}_{1,3}\left[\mathbf{V}^{[3,3]XCI} \quad \mathbf{V}^{[3,1]XCI}\right]\begin{bmatrix}\mathbf{c}^{[3,3]}\\ \mathbf{c}^{[3,1]}\end{bmatrix} + \tilde{\mathbf{n}}_1 \\ &= \underbrace{\bar{\mathbf{H}}_{1,1}\mathbf{V}^{[1,1]XCI}\mathbf{c}^{[1,1]} + \bar{\mathbf{H}}_{1,3}\mathbf{V}^{[3,1]XCI}\mathbf{c}^{[3,1]}}_{\text{desired signal}} \\ &\quad + \underbrace{\bar{\mathbf{H}}_{1,1}\mathbf{V}^{[1,2]XCI}\mathbf{c}^{[1,2]} + \bar{\mathbf{H}}_{1,3}\mathbf{V}^{[3,3]XCI}\mathbf{c}^{[3,3]}}_{\text{interference}} + \tilde{\mathbf{n}}_1. \end{aligned} \tag{5.23}$$

Since it is assumed that user 1 is deployed with N_1 antennas, this number has to be enough to allocate the desired signal into a subspace separate from the interference, and can be then defined as

$$N_1 \geq d^{[1]} + d_{I^{[1]}}, \tag{5.24}$$

where $d_{I^{[1]}}$ is the subspace spanning the interfering $\mathbf{c}^{[1,2]}$ and $\mathbf{c}^{[1,2]}$ vectors present at user 1 and can be expressed as

$$I^{[1]} = \sum_{i=1}^{d_{[1,2]}} \bar{\mathbf{H}}_{1,1}\mathbf{v}_i^{[1,2]}c_i^{[1,2]} + \sum_{i=1}^{d_{[3,3]}} \bar{\mathbf{H}}_{1,3}\mathbf{v}_i^{[3,3]}c_i^{[3,3]}. \tag{5.25}$$

Therefore, the number of receive antennas has to be enough to decode the received signal and consequently needs to satisfy the following requirement

$$N_1 \geq d^{[1]} + d_{[1,2]} + d_{[3,3]},$$

which is not always possible to provide at the receive side due to the physical space limitation.

We define the k_1 and r_1 variables given in (5.20)–(5.21) as

$$\begin{aligned} k_1 &= \min\left(d_{[1,2]}, d_{[3,3]}\right), \\ r_1 &= \max\left(d_{[1,2]}, d_{[3,3]}\right). \end{aligned}$$

$$I^{[1]} = \sum_{i=1}^{d_{[1,2]}} \bar{\mathbf{H}}_{1,1}\mathbf{v}_i^{[1,2]}c_i^{[1,2]} + \sum_{i=1}^{d_{[3,3]}} \bar{\mathbf{H}}_{1,3}\mathbf{v}_i^{[3,3]}c_i^{[3,3]}$$
$$= \underbrace{\sum_{i=1}^{k_1}\left(\bar{\mathbf{H}}_{1,1}\mathbf{v}_i^{[1,2]}c_i^{[1,2]} + \bar{\mathbf{H}}_{1,3}\mathbf{v}_i^{[3,3]}c_i^{[3,3]}\right)}_{\text{space dimension range = 1}} + \underbrace{\sum_{l=k_1+1}^{k_1+w_1} \bar{\mathbf{H}}_{1,1}\mathbf{v}_l^{[1,2]}c_l^{[1,2]}}_{\text{space dimension range = 0}} \tag{5.27}$$

Accordingly, the corresponding difference between $d_{[1,2]}$ and $d_{[3,3]}$ is given as

$$w_1 = r_1 - k_1,$$

where w_1 indicates the number of the interfering data streams that can not be aligned with the other interfering signal, and, therefore, these w_1 vectors need to be mitigated at the receiver.

To reduce the subspace spanning the $I^{[1]}$, it needs to ensure that these interfering signals span a one-dimensional space, and determine the k_1 pairs of precoding vectors such that

$$\bar{\mathbf{H}}_{1,1}\mathbf{v}_i^{[1,2]} = -\bar{\mathbf{H}}_{1,3}\mathbf{v}_i^{[3,3]},\ \forall i \in \{1, 2, \ldots, k_1\}, \tag{5.26}$$

where $\mathbf{v}_i^{[m,n]}$ is the i^{th} column of the $\mathbf{V}^{[m,n]XCI}$ matrix from (5.23), and the XCI notation is omitted for brevity. We pick randomly the $\mathbf{v}_{1,\ldots,k_1}^{[1,2]}$ and $\mathbf{v}_{1,\ldots,k_1}^{[3,3]}$ vectors to guarantee that they are linearly independent with probability one. This can be presented as shown in (5.27), where it is assumed that $r_1 = d_{[1,2]}$.

Since user 1 obtains the $\mathbf{c}^{[1,2]}$ and $\mathbf{c}^{[3,3]}$ data vectors with $d_{[1,2]}$ and $d_{[3,3]}$ data streams, respectively, for $d_{[1,2]} \neq d_{[3,3]}$, we then need to define which effective channel matrix, $\bar{\mathbf{H}}_{1,x}$, needs to be cancelled, where x can be derived from

$$[x, y] = \begin{cases} [1, 2], \text{ if } r_1 = d_{[1,2]}, \\ [3, 3], \text{ if } r_1 = d_{[3,3]}. \end{cases}$$

Therefore, we have the w_1 interfering beamforming vectors, $\mathbf{V}_{\{k_1+1:k_1+w_1\}}^{[x,y]} =$

$$\underbrace{\begin{bmatrix}\bar{\mathbf{H}}_{1,1} & \bar{\mathbf{H}}_{1,3}\end{bmatrix}}_{N_1\times(Q_1+Q_3)} \underbrace{\left[\begin{array}{ccc|ccc|c} | & \cdots & | & | & \cdots & | & | \;\; \cdots \;\; | \\ \mathbf{v}_1^{[1,2]} & \cdots & \mathbf{v}_{k_1}^{[1,2]} & \mathbf{v}_{k_1+1}^{[1,2]} & \cdots & \mathbf{v}_{k_1+w_1}^{[1,2]} & \boxed{\begin{array}{ccc} | & \cdots & | \\ \mathbf{0} & \cdots & \mathbf{0} \\ | & \cdots & | \end{array}} \\ | & \cdots & | & | & \cdots & | & \\ \hline | & \cdots & | & | & \cdots & | & | \;\; \cdots \;\; | \\ \mathbf{v}_1^{[3,3]} & \cdots & \mathbf{v}_{k_1}^{[3,3]} & \mathbf{0} & \cdots & \mathbf{0} & \mathbf{v}_{k_1+1}^{[3,3]} \;\; \cdots \;\; \mathbf{v}_{k_1+w_1}^{[3,3]} \\ | & \cdots & | & | & \cdots & | & | \;\; \cdots \;\; | \end{array}\right]}_{(Q_1+Q_3)\times(k_1+w_1)}$$

$$= \underbrace{\begin{bmatrix} | & \cdots & | \\ \mathbf{0} & \cdots & \mathbf{0} \\ | & \cdots & | \end{bmatrix}}_{N_1\times\max(d_{[1,2]},d_{[3,3]})} \tag{5.31}$$

$\left\{\mathbf{v}_{k_1+1}^{[x,y]},\ldots,\mathbf{v}_{k_1+w_1}^{[x,y]}\right\}$, that are obtained by finding the null space of the corresponding effective channel as follows

$$\mathbf{V}_{\{k_1+1:k_1+w_1\}}^{[x,y]} = \text{null}\left(\bar{\mathbf{H}}_{1,x}\right), \tag{5.28}$$

where $\mathbf{V}_{\{k_1+1:k_1+w_1\}}^{[x,y]}$ denotes the part of the BF matrix with a range from the $(k_1+1)^{th}$ up to the $(k_1+w_1)^{th}$ column. This leads to the following condition to be satisfied

$$w_1 \leq (Q_1 - N_1)^+ \text{ or } w_1 \leq (Q_3 - N_1)^+. \tag{5.29}$$

As a result, the interference observed by user 1 can be mitigated as shown in (5.31), where it is assumed $d_{[1,2]} > d_{[3,3]}$ and the boxed term is redundant, unless $d_{[1,2]} < d_{[3,3]}$. According to (5.27), the interference at the user of interest spans a one-dimensional space, thus the number of receive antennas given in (5.24) can be redefined as

$$N_1 = d^{[1]} + 1. \tag{5.30}$$

Finally, if all the conditions above are satisfied, user 1 experiences the interference-free data transmission.

Similar to cell 1, the conditions satisfying the ability to maintain the proposed scheme for the rest of cells are defined as follows

$$\begin{aligned} \mathcal{D}_{out} \triangleq \text{maximize} \quad & \left(d_{[1,1]} + d_{[1,2]} + d_{[2,2]} + d_{[2,3]} + d_{[3,1]} + d_{[3,3]}\right) \in \mathbb{R}_+^6 \\ \text{subject to} \quad & d_{[1,1]} + d_{[1,2]} \leq Q_1, \end{aligned} \tag{5.32.1}$$

$$d_{[2,2]} + d_{[2,3]} \leq Q_2, \tag{5.32.2}$$

$$d_{[3,1]} + d_{[3,3]} \leq Q_3, \tag{5.32.3}$$

$$d_{[1,1]} + d_{[3,1]} + 1 \leq N_1, \tag{5.32.4}$$

$$d_{[1,2]} + d_{[2,2]} + 1 \leq N_2, \tag{5.32.5}$$

$$d_{[2,3]} + d_{[3,3]} + 1 \leq N_3, \tag{5.32.6}$$

$$D_1 = d_{[1,1]} + d_{[3,1]} + d_{[1,2]} \leq \max(N_1, Q_1), \tag{5.32.7}$$

$$D_2 = d_{[2,2]} + d_{[1,2]} + d_{[1,1]} \leq \max(N_2, Q_1), \tag{5.32.8}$$

$$D_3 = d_{[2,2]} + d_{[1,2]} + d_{[2,3]} \leq \max(N_2, Q_2), \tag{5.32.9}$$

$$D_4 = d_{[3,3]} + d_{[2,3]} + d_{[2,2]} \leq \max(N_3, Q_2), \tag{5.32.10}$$

$$D_5 = d_{[1,1]} + d_{[3,1]} + d_{[3,3]} \leq \max(N_1, Q_3), \tag{5.32.11}$$

$$D_6 = d_{[3,3]} + d_{[2,3]} + d_{[3,1]} \leq \max(N_3, Q_3), \tag{5.32.12}$$

$$\overline{Q}_t = w_j + N_j, \ \forall j \in L, \tag{5.32.13}$$

$$t = m \leftarrow d_{[m,n]} = r_j \text{ in (5.21)}, \tag{5.32.14}$$

where t indicates the first subscript index, and $(\cdot)^+$ represents a function that returns a non-negative value. The case of $w_j = 0$ implies that at this particular user the numbers of interfering streams are identical.

Although at a glance it might seem that the DoF region above is not too different from the one defined in Section 4.2.3, it is worth mentioning that Chapter 4 focused on the network case with an identical antenna configuration leading to identical numbers of data streams causing the interference at the receiver side, that is, only one class of users is considered. Thus, considering different classes of users entails more conditions related to the XCI mitigation shown by the second term in (5.27), which spans a zero-dimensional space.

The set $\mathcal{D}_{out}$ provides the conditions defining the outer limit for all the attainable $d_{[j,i]}$ under the compounded MIMO BC by maximizing a weighted sum of $d_{[j,i]}$ which is a linear programming problem. At the same time, this set of conditions is suitable either to analyse the achievable DoF region under a given network antenna configuration or to calculate the minimum number of antennas at each node in order to obtain the required DoF. Subsequently, we provide the algorithm that allows us to compute the minimum required number of antennas at each Tx-Rx pair with maximum DoF.

The following provides the total number of DoF by explicitly solving the LP

Algorithm 1 Defining the Antenna Configuration

Require:
inputs $\left\{d_{[i,j]}\right\},\ \forall i,j \in L$
Q_1 from (5.32.1)
Q_2 from (5.32.2)
Q_3 from (5.32.3)
N_1 from (5.32.4)
N_2 from (5.32.5)
N_3 from (5.32.6)
Ensure:
if (5.32.7) or (5.32.8) is not valid **then**
  update $Q_1 \leftarrow D_1$ or $Q_1 \leftarrow D_2$
else if (5.32.9) or (5.32.10) is not valid **then**
  update $Q_2 \leftarrow D_3$ or $Q_2 \leftarrow D_4$
else if (5.32.11) or (5.32.12) is not valid **then**
  update $Q_3 \leftarrow D_5$ or $Q_3 \leftarrow D_6$
end if
return Q_1, Q_2, Q_3.
for $j = 1:3$ **do**
  calculate w_j, according to (5.22).
  find the value of t with respect to (5.32.14).
  if $t = j$ **then**
    $\overline{Q}_t := \overline{Q}_j$
    if $\overline{Q}_j > Q_j$ **then**
      update $Q_j \leftarrow \overline{Q}_j$
    end if
  else
    $\overline{Q}_t := \overline{Q}_{j-1}$
    if $\overline{Q}_{j-1} > Q_{j-1}$ **then**
      update $Q_{j-1} \leftarrow \overline{Q}_{j-1}$
    end if
  end if
  return Q_{j-1} or Q_j (if updated only).
  This derived value will be used in the next iteration
end for
utilize Q_1, Q_2, Q_3, N_1, N_2, N_3 to calculate the numbers of transmit antennas as in (5.15).

problem.

Conjecture 2 :

$$
\begin{aligned}
\eta &\triangleq \max_{\mathcal{D}_{out}} \left(d_{[1,1]} + d_{[1,2]} + d_{[2,2]} + d_{[2,3]} + d_{[3,1]} + d_{[3,3]}\right) \\
&= \min \{Q_1 + Q_2 + Q_3, N_1 + N_2 + N_3 - 3, \\
&\qquad \max(N_1, Q_1) + \max(N_3, Q_2), \\
&\qquad \max(N_1, Q_3) + \max(N_2, Q_2), \\
&\qquad \max(N_2, Q_1) + \max(N_3, Q_3), \\
&\qquad \frac{\max(N_1, Q_1) + \max(N_1, Q_3) + \max(N_2, Q_2) + \max(N_3, Q_2)}{2}, \\
&\qquad \frac{\max(N_1, Q_3) + \max(N_2, Q_1) + \max(N_3, Q_3) + \max(N_2, Q_2)}{2}, \\
&\qquad \frac{\max(N_1, Q_1) + \max(N_2, Q_1) + \max(N_3, Q_2) + \max(N_3, Q_3)}{2}, \\
&\qquad \frac{\max(N_1, Q_1) + \max(N_1, Q_3) + Q_2 + N_2 + N_3}{2} - 1, \\
&\qquad \frac{\max(N_1, Q_1) + \max(N_2, Q_1) + Q_2 + Q_3 + N_3 - 1}{2}, \\
&\qquad \frac{\max(N_1, Q_1) + \max(N_3, Q_2) + Q_1 + Q_2 + Q_3}{2}, \\
&\qquad \frac{\max(N_1, Q_1) + \max(N_3, Q_2) + N_1 + N_2 + N_3 - 1}{2} - 1, \\
&\qquad \frac{\max(N_1, Q_3) + \max(N_2, Q_2) + Q_1 + Q_2 + Q_3}{2}, \\
&\qquad \frac{\max(N_1, Q_3) + \max(N_2, Q_2) + N_1 + N_2 + N_3 - 1}{2} - 1, \\
&\qquad \frac{\max(N_1, Q_3) + \max(N_3, Q_3) + Q_1 + Q_2 + N_2 - 1}{2}, \\
&\qquad \frac{\max(N_2, Q_1) + \max(N_2, Q_2) + Q_3 + N_1 + N_3}{2} - 1, \\
&\qquad \frac{\max(N_2, Q_1) + \max(N_3, Q_3) + Q_1 + Q_2 + Q_3}{2}, \\
&\qquad \frac{\max(N_2, Q_1) + \max(N_3, Q_3) + N_1 + N_2 + N_3 - 1}{2} - 1, \\
&\qquad \frac{\max(N_2, Q_2) + \max(N_3, Q_2) + Q_1 + Q_3 + N_1 - 1}{2}, \\
&\qquad \frac{\max(N_3, Q_2) + \max(N_3, Q_3) + Q_1 + N_1 + N_2}{2} - 1, \\
&\qquad \frac{\max(N_1, Q_1) + \max(N_1, Q_3) + \max(N_2, Q_1)}{3}
\end{aligned}
$$

$$+\frac{\max(N_2,Q_2)+\max(N_3,Q_2)+\max(N_3,Q_3)}{3}\Bigg\}.$$

Outline of the proof : Conjecture 2 can be verified by solving the dual problem by linear programming

$$\max\left(d_{[1,1]}+d_{[1,2]}+d_{[2,2]}+d_{[2,3]}+d_{[3,3]}+d_{[3,1]}\right).$$

Since all the extreme points of the feasible space can be directly evaluated, we compute the objective value at these points and eliminate the limits that can be regarded redundant. Using the fundamental theorem of LP, [145, 146], we find the solution.

It is worth noting that all the terms given in Conjecture 2 are essential because any of them is valid for a certain antenna configuration.

We define the achievable DoF for our multi-cell network as the pre-log factor of the sum rate, [17, 18]. This is one of the key metrics used for assessing the performance of a multiple antenna system in the high SNR region defined as

$$\eta=\lim_{SNR\to\infty}\frac{\mathcal{I}_{\sum}(SNR)}{\log_2(SNR)}=\sum_{j=1}^{L}d^{[j]},$$

where $\mathcal{I}_{\sum}(SNR)$ denotes the sum rate that can be achieved at a given SNR defined as $\mathcal{I}_{\sum}(SNR)=\sum_{j=1}^{L}\mathcal{I}_j(SNR)$, where $\mathcal{I}_j$ and $d^{[j]}$ are the data rate and the number of the successfully decoded data streams at user j, respectively.

Therefore, the received signal at user j, with respect to the considered channel model in (5.9), can be rewritten as

$$\begin{aligned}\tilde{\mathbf{y}}_j&=\mathbf{U}_j^H\sum_{i=1}^{L=3}\mathbf{H}_{j,i}\mathbf{V}_i\mathbf{s}_i+\tilde{\mathbf{n}}_j\\&=\underbrace{\mathbf{U}_j^H\sum_{i=1,\ i\neq j+1}^{L=3}\mathbf{H}_{j,i}\mathbf{V}_i\mathbf{s}_i}_{\text{desired signal + XCI}}+\underbrace{\mathbf{U}_j^H\mathbf{H}_{j,j+1}\mathbf{V}_{j+1}\mathbf{s}_{j+1}}_{\text{ICI}}+\tilde{\mathbf{n}}_j\\&=\underbrace{\mathbf{U}_j^H\sum_{i=1,\ i\neq j+1}^{L=3}\left(\tilde{\mathbf{H}}_{j,i}+\tilde{\mathbf{E}}_{j,i}\right)\mathbf{V}_i\mathbf{s}_i}_{\text{desired signal + XCI}}+\underbrace{\mathbf{U}_j^H\left(\tilde{\mathbf{H}}_{j,j+1}+\tilde{\mathbf{E}}_{j,j+1}\right)\mathbf{V}_{j+1}\mathbf{s}_{j+1}}_{\text{ICI}}+\tilde{\mathbf{n}}_j\end{aligned}$$

$$\mathcal{I}_{\Sigma} = \sum_{j=1}^{L=3} \mathcal{I}_j$$
$$= \sum_{j=1}^{L=3} \log_2 \det \left(\mathbf{I} + \frac{\sum_{i=j-1}^{j} \left| \mathbf{U}_j^H \tilde{\mathbf{H}}_{j,i} \mathbf{V}^{[i,j]} \right|^2}{\sum_{i=j-1}^{j} \left| \mathbf{U}_j^H \tilde{\mathbf{H}}_{j,i} \mathbf{V}^{[i,l\{l\neq j\}]} \right|^2 + \sum_{k=1}^{L=3} \left| \mathbf{U}_j^H \tilde{\mathbf{E}}_{j,k} \mathbf{V}_k \right|^2 + \sigma_{\tilde{n}}^2 \mathbf{I}} \right) \tag{5.34}$$

$$= \underbrace{\mathbf{U}_j^H \sum_{i=j-1}^{j} \tilde{\mathbf{H}}_{j,i} \mathbf{V}^{[i,j]} \mathbf{c}^{[i,j]}}_{\text{desired signal}} + \underbrace{\mathbf{U}_j^H \sum_{i=j-1}^{j} \tilde{\mathbf{H}}_{j,i} \mathbf{V}^{[i,l\{l\neq j\}]} \mathbf{c}^{[i,l\{l\neq j\}]}}_{\text{XCI}}$$
$$+ \underbrace{\cancel{\mathbf{U}_j^H \tilde{\mathbf{H}}_{j,j+1} \mathbf{V}_{j+1} \mathbf{s}_{j+1}}}_{\text{ICI} = 0} + \underbrace{\mathbf{U}_j^H \sum_{i=1}^{L=3} \tilde{\mathbf{E}}_{j,i} \mathbf{V}_i \mathbf{s}_i}_{\text{CSI mismatch}} + \tilde{\mathbf{n}}_j, \ \forall j \in L. \tag{5.33}$$

With this in mind, the data rate achievable at the user of interest can be determined as shown in (5.34).

5.3 Computational complexity

For a given $m \times n$ matrix, the required arithmetic operations to determine its singular values and corresponding singular vectors are given by $\mathcal{O}(\min\{mn^2, m^2n\})$, [138]. Moreover, the multiplication of two $m \times n$ and $n \times p$ matrices requires mnp operations.

We analyse the computational complexity of the proposed scheme from the perspective of each receiver. Since the BF matrix consists of two parts, we start from the BF responsible for ICI cancellation. The derivation of $\mathbf{V}^{[ICI]}$ given in (3.16) mainly involves SVD and matrix multiplication.

In general, we define $\mathbf{D}_i$, the null space of $\mathbf{C}_i$ in (3.12), which requires a computational complexity of

$$\mathcal{O}\left(\min\left\{(M_i^3 + 2M_iN_{i-1} + M_iN_{i-1}^2); (M_i^3 + M_i^2N_{i-1})\right\}\right).$$

$$\mathcal{O}(Y) = k_i \left\{ \begin{array}{l} \prod_{n=1}^{L=3} N_n + N_i^3 + N_{i-2}N_{i-1} - N_{i-1}N_i + 2M_{i-1}M_i - M_iN_{i-2} \\ + M_iN_i\left(M_{i-1} - N_{i-2} + 2\right) - M_{i-1}N_{i-1}\left(N_i + 1\right) \end{array} \right\} + X, \tag{5.35}$$

$$\text{where } X = \left\{ \begin{array}{ll} \min\left\{\left(M_i - N_{i-1}\right)^2 N_i; \left(M_i - N_{i-1}\right) N_i^2\right\}, & \text{if } r_i = d_{[i,i+1]}, \\ \min\left\{\left(M_{i-1} - N_{i-2}\right)^2 N_i; \left(M_{i-1} - N_{i-2}\right) N_i^2\right\}, & \text{if } r_i = d_{[i-1,i-1]}. \end{array} \right.$$

The next operation related to SVD involves the effective interference direction caused by base station i with dimension of $M_i \times N_{i-1}$ and correspondingly requires $\mathcal{O}\left(\min\left\{M_iN_{i-1}^2; M_i^2N_{i-1}\right\}\right)$, where the minimum is $M_iN_{i-1}^2$. Then the overall complexity needed to calculate $V_i^{[ICI]}$ equals $\mathcal{O}\left(M_i^3 + 2M_iN_{i-1} + 2M_iN_{i-1}^2\right)$, which can be bounded by $(M_i^3 + 2M_i^2N_{i-1})$.

Now we consider the second part of the precoding matrix responsible for $\mathbf{V}^{[XCI]}$, whose structure is given in (5.27). Since two interfering signals are presented at the receiver, the minimum value is defined as in (5.20). To make sure that the k_1 vectors of these two interfering signals with $d_{[i,i+1]}$ and $d_{[i-1,i-1]}$ data streams span a zero-dimensional subspace, we have the complexity $\mathcal{O}(Y)$ based on the value of k_i as in (5.35). For the case when the numbers of data streams interfering at the user of interest are not identical ($d_{[i,i+1]} \neq d_{[i-1,i-1]}$), we require the additional operations given by X as in (5.35).

The last operation is the matrix multiplication of two $\mathbf{V}_i^{[ICI]}$ and $\mathbf{V}^{[XCI]}$ matrices with the corresponding complexity of $\mathcal{O}\left(M_i^3 - 2M_i^2N_{i-1} + M_iN_{i-1}^2\right)$. Therefore, the overall computational complexity of the proposed BF design is $\mathcal{O}\left(2M_i^3 + M_iN_{i-1}^2 + Y\right)$. However, due to the different numbers of transmitted data streams to each of the users, we have different antenna settings for each specific Tx-Rx pair; for the sake of comparison fairness, we consider the equal antenna configuration ($X = 0$) and $k_i = 1$.

Since the proposed technique offers spatial multiplexing over multi-antenna wireless communication systems, its computation complexity is compared with a benchmark algorithm such as V-BLAST which complexity can be given by $\mathcal{O}\left(2NM^3 + 4NM^2 + 2NM\right)$ (only the arithmetic operations responsible for multiplication and division are taken into account), [167]. For the sake of fairness, we set up the same interrelation between of the number of transmit and receive antennas for both techniques as $M = 2N + 1$. As a result, it can be seen in Fig.

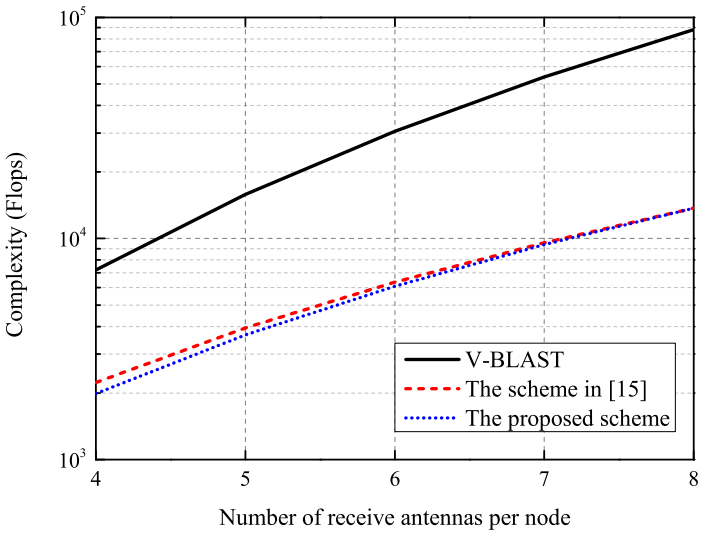

Figure 5.2. The computational complexities of the proposed scheme and V-BLAST.

5.2 that the proposed scheme requires much less computation operations than the V-BLAST technique.

5.4 Simulation Results

This section presents our results using Monte Carlo simulations to investigate the effect of antenna correlation and CSI mismatch on the network performances. The simulations assume QPSK modulation and frequency flat fading which is designed according to (5.3). To make a fair comparison, the total transmit power at the BS is constrained to unity irrespective of the number of transmit antennas. To create different classes of users with various numbers of antennas, it is assumed that BS i transmits the i data streams to the corresponding user i, and only one data stream to the collateral user of interest. Therefore, we have three receivers deployed with three, four and five antennas, respectively.

According to [168], we examine three correlation regimes, the low, medium and high correlations. The low correlation mode indicates the scenario with no correlation with sufficient spacing ($\geq \lambda/2$) between the antennas. According to (5.9), the medium and high correlation regimes at the transmitter side can be modeled by $r = 0.3$ and $r = 0.9$, respectively; however, the same modes at the receiver side can be presented by $r = 0.9$.

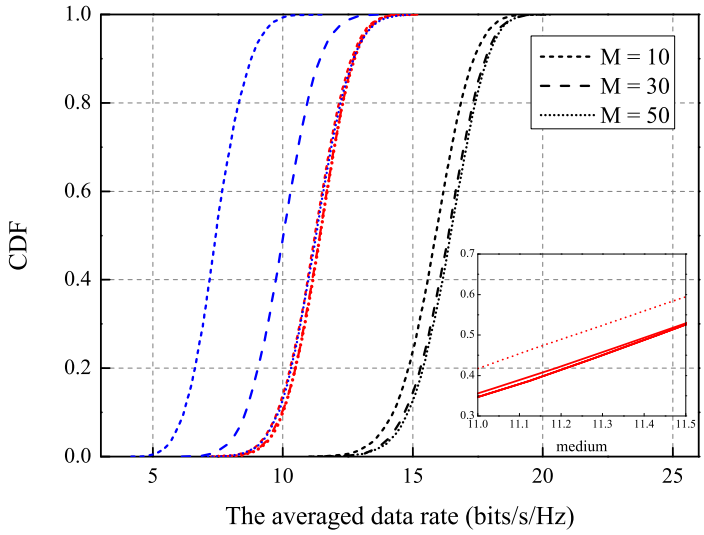

Figure 5.3. CDF curves with low (black), medium (red) and high (blue) correlations for different numbers of transmit antennas at 30 dB.

In Fig. 5.3, we evaluate a cumulative distribution function (CDF) of the achievable data rate for every user in the assumed system model. The data rates are calculated using the proposed scheme under different antenna correlation modes. For the sake of clarity, we consider the averaged data rate achievable by the network. The observation point is 30 dB. We deploy transmitters with ten, thirty and fifty antennas to estimate the potential benefit attainable from the Large-Scale MIMO scenario. As it can be seen, for the case of low correlation, the probability of attaining a higher data rate increases as the number of antennas at the BS goes up. Regarding the medium correlation case, we observe severe degradation in the achievable data rate, and the various numbers of transmit antennas do not seem to have much difference; however, a different antenna deployment still matters as it is shown in the inset figure (Fig. 5.3). Finally, we consider the high correlation mode presented in blue lines with which produces a significant loss in the achievable data rate. For $M = 10$, $M = 30$ and $M = 50$ antennas deployed at the transmitter side, the averaged data rate of 8.8, 11.4 and 12.75 bits/s/Hz are achievable with a probability of 90%. It is worth to note that the deployment of more antennas allow us to overcome the high correlation, and accordingly, the system can be treated as though it is experiencing the medium correlation. With this in mind, in the next simulation, we consider only the

network case where all the BSs are equipped with fifty antennas.

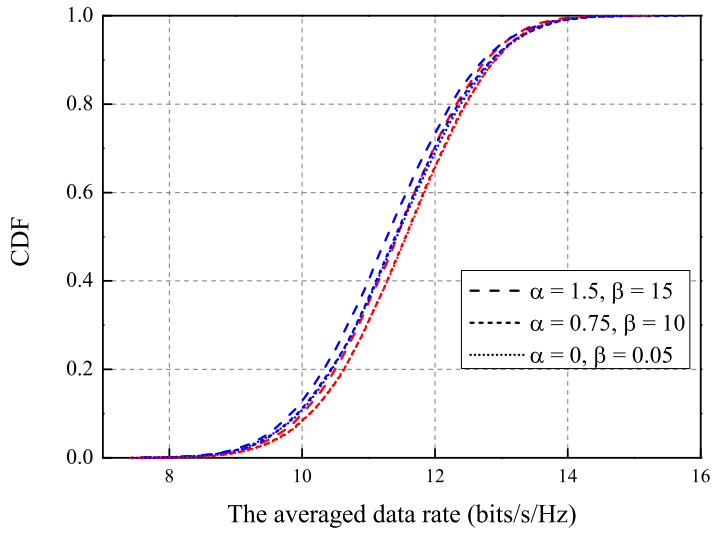

Figure 5.4. CDF curves with low (black), medium (red) and high (blue) correlations for different CSI mismatch cases with $M = 50$ antennas per BS at 30 dB.

Next, we want to investigate the combined effect of CSI mismatch and antenna correlation on the achievable data rates. The observation point is 30 dB. As shown in Fig. 5.4, the case of $(\alpha = 1.5, \beta = 15)$ performs worse than the other two scenarios of the CSI acquisition. The CSI mismatch cases given by $(\alpha = 0.75, \beta = 10)$ and $(\alpha = 0, \beta = 0.05)$ act in a similar way under the medium and high correlation regimes; however, for low correlation, the network with $(\alpha = 0, \beta = 0.05)$ slightly outperforms the one modeled by $(\alpha = 0.75, \beta = 10)$. This result leads to the realization that the SNR-dependent and SNR-independent CSI acquisition scenarios, $(\alpha = 0, \beta = 0.05)$ and $(\alpha = 0.75, \beta = 10)$, do not differ from each other in the cases of medium and high antenna correlations.

Finally, we provide a 3D plot presenting the data rate achievable at 30 dB as a function of the number of transmit antennas and correlation coefficient. The correlation at the transmitter side is assumed to be high and modeled by using the exponential model as in (5.10) ($r = 0.9$). Accordingly, the antenna correlation at the receiver side is given as in (5.11) and simulated within the range $[0, 1]$. As it can be seen, the achievable data rate increases as the number of transmit antennas goes up, while the data rate decreases as the correlation coefficient increases.

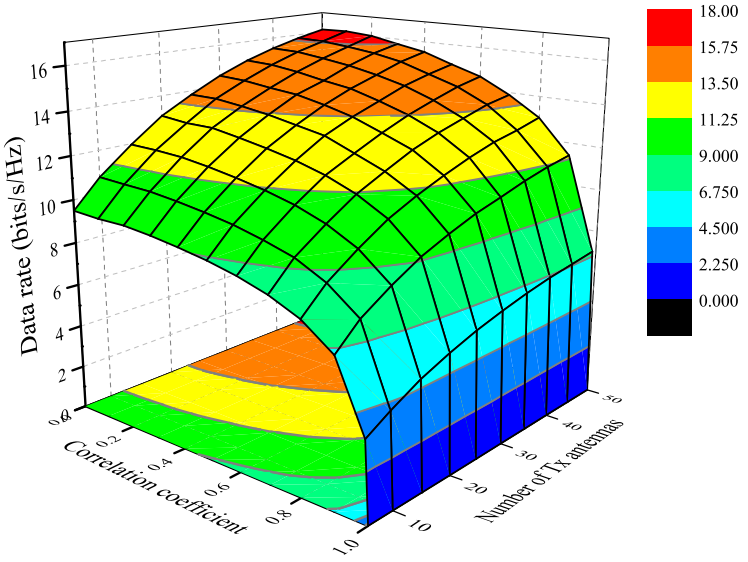

Figure 5.5. The achievable data rate as a function of the correlation coefficient and number of transmit antennas.

5.5 Chapter Summary

This Chapter considered the compounded MIMO BC network case and proposed a tailored transmit BF design that accounts for different classes of users. We also presented the DoF region analysis and provided an algorithm to define the minimum antenna configuration to achieve a required number of data streams in the network. Moreover, we calculated the computational complexity of the proposed scheme and investigated the impact of spatial antenna correlation under various CSI acquisition scenarios. Finally, the proposed scheme was examined in traditional and Large-scale MIMO systems. It was shown that the performance obtained for the latter case demonstrated that the deployment of more antennas allows us to overcome the effect of high correlation by a careful utilization of the available transmit antennas.

Chapter 6

A Closed-form Interference Alignment Cancellation for the Multi-user MIMO X-channel Model

This Chapter proposes a non-iterative IA scheme for the MIMO X-channel network consisting of three transmitter-receiver pairs without symbol extension. First it demonstrates the basic principle of how to design the beamforming matrices for this set-up. Then the achievable sum rate is estimated under perfect and imperfect channel state information. Moreover, it will be shown that applying the proposed scheme allows one to achieve over 58 bits/s/Hz. Finally, the computational complexity of the proposed scheme will be calculated.

6.1 System Model

The system model considered here presents a MIMO system with L Tx-Rx pairs under the X-channel scenario which is defined by a message set when each transmitter sends independent data symbols to all the receivers. Therefore, the signal from transmitter i can be expressed as

$$\mathbf{s}_i = \left[s_i^{[1]} \ \cdots \ s_i^{[l]} \ \cdots \ s_i^{[L]} \right]^T, \forall i, l \in L, \tag{6.1}$$

where $s_i^{[l]}$ is a symbol transmitted from $Tx\ i$ to $Rx\ l$ such that each receiving node treats all the transmitters as the information and interference sources simultaneously.

Each receiver decodes the received signal by multiplying it with a receive beamforming matrix; thus, this can be written as

$$\tilde{\mathbf{y}}_j = \mathbf{U}_j^H \mathbf{y}_j = \mathbf{U}_j^H \sum_{i=1}^{L} \mathbf{H}_{j,i}\mathbf{V}_i\mathbf{s}_i + \tilde{\mathbf{n}}_j,\ \forall j \in L, \tag{6.2}$$

where $\mathbf{U}_j \in \mathbb{C}^{N_r \times d_s}$ denotes the receive beamforming matrix for the user of interest, and $\tilde{\mathbf{n}}_j = \mathbf{U}_j^H \mathbf{n}_j \in \mathbb{C}^{d_s \times 1}$ is the effective zero-mean AWGN vector at the output of the beamformer, with $\mathbb{E}\{\tilde{\mathbf{n}}_j \tilde{\mathbf{n}}_j^H\} = \sigma_{\tilde{n}}^2 \mathbf{I}$. $\mathbf{H}_{j,i} \in \mathbb{C}^{N_r \times N_t}$ denotes the channel between $Tx\ i$ and $Rx\ j$. It is assumed that each channel is quasi-stationary and frequency flat fading. $\mathbf{V}_i \in \mathbb{C}^{N_t \times d_s}$ is a transmit BF matrix, with $\text{trace}\{\mathbf{V}_i \mathbf{V}_i^H\} = 1$, where d_s is the number of data streams transmitted from each Tx. Since it is assumed that $\mathbf{s}_i$ is the vector containing the symbols drawn from i.i.d. Gaussian input signaling and chosen from a desired constellation, we have $\mathbb{E}\{\mathbf{s}_i \mathbf{s}_i^H\} = \mathbf{I}$. All these conditions imply that the average power constraint at the transmitter is satisfied.

To decode the required signal successfully, it needs to be linearly independent of interference, which can be attained by aligning the interfering signals into the subspace that is orthogonal to $\mathbf{U}_j$. Therefore, the following conditions must be satisfied at receiver j

$$\mathbf{U}_j^H \mathbf{H}_{j,i} \mathbf{V}_i^{[l]} = \mathbf{0},\ l \neq j, \forall i, j \in L, \tag{6.3}$$

$$\sum_{k=1}^{L} \text{rank}\left(\mathbf{U}_j^H \mathbf{H}_{j,k} \mathbf{V}_k^{[j]}\right) = d_j,\quad \forall j \in L, \tag{6.4}$$

where d_j is the maximum number of the resolvable interference-free data streams at receiver j, and $\mathbf{V}_i^{[l]}$ indicates the l^{th} column of the transmit beamforming matrix at transmitter i.

According to (6.2), the achievable sum rate is evaluated as follows, [113],

$$\mathcal{I}_\Sigma = \sum_{j=1}^{L} \log_2 \left(\det \left(\mathbf{I} + \frac{\sum\limits_{i=1}^{L} \left| \mathbf{U}_j^H \mathbf{H}_{j,i} \mathbf{V}_i^{[j]} \right|^2}{\sum\limits_{i=1}^{L} \sum\limits_{l=1, l\neq j}^{L} \left| \mathbf{U}_j^H \mathbf{H}_{j,i} \mathbf{V}_i^{[l]} \right|^2 + \sigma_{\tilde{n}}^2 \mathbf{I}} \right) \right). \tag{6.5}$$

The following sections show how to design the closed-form beamforming technique for the three-user MIMO network and provide the sum rate achievable under different CSI acquisition scenarios.

6.2 Transmit Beamforming Design

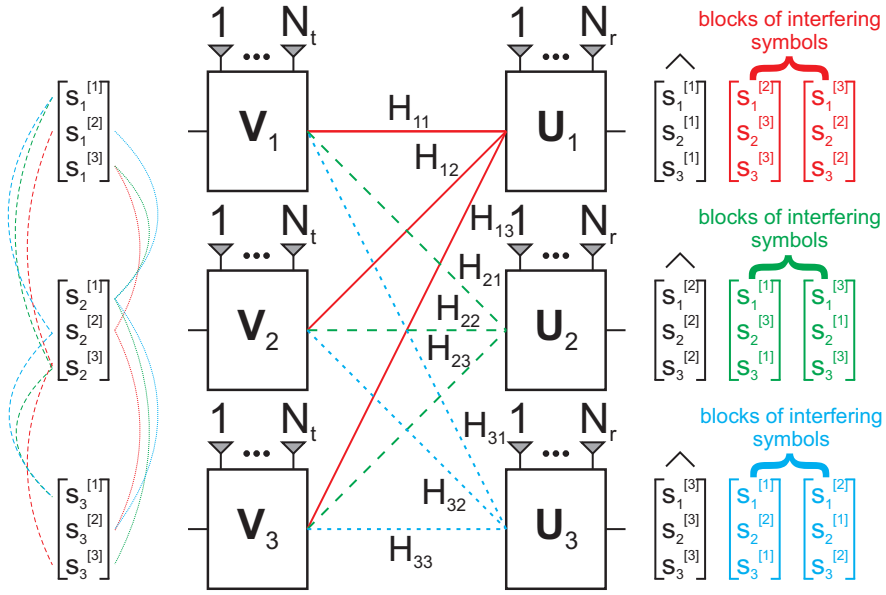

Figure 6.1. The three-user MIMO X-channel network with blocks of the interfering symbols.

To give a detailed explanation, we refer to Fig. 6.1 where each node is deployed with N antennas ($N = N_t = N_r$). Each transmitter i sends the signal $\mathbf{s}_i = \left[s_i^{[1]}\ s_i^{[2]}\ s_i^{[3]}\right]^T$ such that symbol $s_i^{[l]}$ is of interest to receiver l ($l \in L$), while receiver j desires to decode $\mathbf{s}^{[j]} = \left[s_1^{[j]}\ s_2^{[j]}\ s_3^{[j]}\right]^T$. Therefore, the received signal $\mathbf{y}_j$ at the user of interest can be written as

$$\begin{aligned}\mathbf{y}_j &= \sum_{i=1}^{L=3} \mathbf{H}_{j,i}\mathbf{V}_i\mathbf{s}_i + \mathbf{n}_j \\ &= \sum_{i=1}^{L=3} \mathbf{H}_{j,i}\left[\mathbf{V}_i^{[1]},\ \mathbf{V}_i^{[2]},\ \mathbf{V}_i^{[3]}\right]\begin{bmatrix} s_i^{[1]} \\ s_i^{[2]} \\ s_i^{[3]} \end{bmatrix} + \mathbf{n}_j\end{aligned}$$

$$= \underbrace{\sum_{i=1}^{L=3} \mathbf{H}_{j,i}\mathbf{V}_i^{[j]}s_i^{[j]}}_{\text{desired signal}} + \underbrace{\sum_{i=1}^{L=3}\sum_{k=1,k\neq j}^{L=3} \mathbf{H}_{j,i}\mathbf{V}_i^{[k]}s_i^{[k]}}_{\text{interference from all transmitters}} + \mathbf{n}_j, \ \forall j \in L. \tag{6.6}$$

6.2.1 Grouping Method at Rx 1

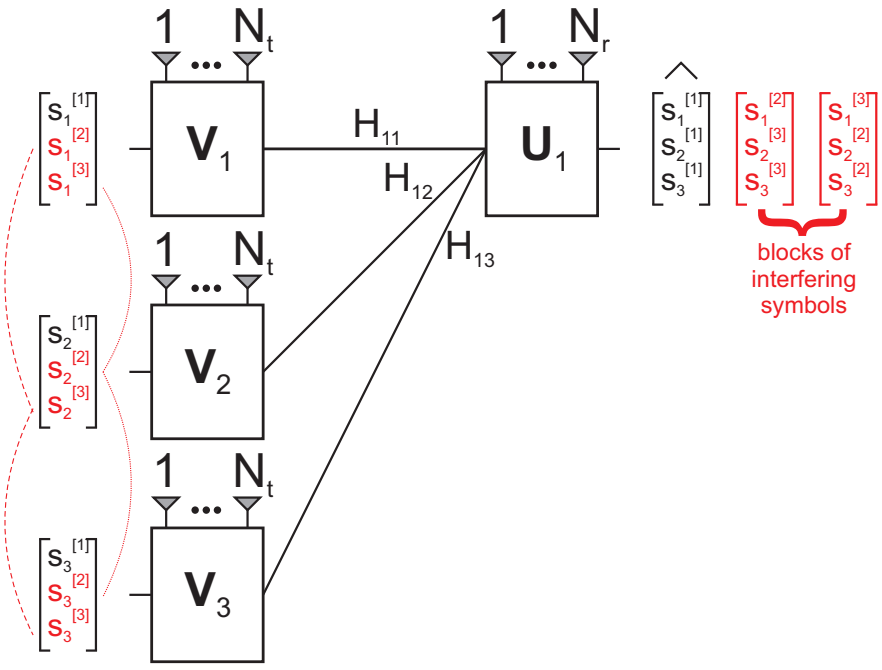

Figure 6.2. The grouping method of the interfering signals at receiver 1.

Receiver 1 aims to decode $\mathbf{s}^{[1]}$ transmitted from all the sources and the rest of the symbols arriving from the same directions are seen as interference (red symbols). Thus, the interfering symbols can be grouped into several blocks as shown on the receiver side (Fig. 6.2). It results in two blocks of interfering symbols that can be spanned by two subspaces $\mathbf{A}_1$ and $\mathbf{A}_2$ as

$$\mathbf{A}_1 :\Rightarrow \text{span}\left\{\mathbf{H}_{1,1}\mathbf{V}_1^{[2]},\ \mathbf{H}_{1,2}\mathbf{V}_2^{[3]},\ \mathbf{H}_{1,3}\mathbf{V}_3^{[3]}\right\},$$
$$\mathbf{A}_2 :\Rightarrow \text{span}\left\{\mathbf{H}_{1,1}\mathbf{V}_1^{[3]},\ \mathbf{H}_{1,2}\mathbf{V}_2^{[2]},\ \mathbf{H}_{1,3}\mathbf{V}_3^{[2]}\right\}.$$

Therefore, $\mathbf{A}_1$ can be written as

$$\mathbf{A}_1 = \mathbf{H}_{1,1}\mathbf{V}_1^{[2]} = \mathbf{H}_{1,2}\mathbf{V}_2^{[3]} = \mathbf{H}_{1,3}\mathbf{V}_3^{[3]}.$$

Considering $\mathbf{V}_1^{[2]}$, we have

$$\mathbf{A}_1 - \mathbf{H}_{1,1}\mathbf{V}_1^{[2]} = [\mathbf{I} \quad -\mathbf{H}_{1,1}] \begin{bmatrix} \mathbf{A}_1 \\ \mathbf{V}_1^{[2]} \end{bmatrix} = \mathbf{0}. \tag{6.7}$$

Further applying this approach to the rest of precoding vectors results in the following matrix equation

$$\begin{bmatrix} \mathbf{I} & -\mathbf{H}_{1,1} & \mathbf{0} & \mathbf{0} \\ \mathbf{I} & \mathbf{0} & -\mathbf{H}_{1,2} & \mathbf{0} \\ \mathbf{I} & \mathbf{0} & \mathbf{0} & -\mathbf{H}_{1,3} \end{bmatrix} \begin{bmatrix} \mathbf{A}_1 \\ \mathbf{V}_1^{[2]} \\ \boxed{\mathbf{V}_2^{[3]}} \\ \mathbf{V}_3^{[3]} \end{bmatrix} = \mathbf{C}_{A_1}\mathbf{D}_{A_1} = \mathbf{0}. \tag{6.8}$$

To obtain distinct precoding matrices $\mathbf{V}_1^{[3]}$, $\mathbf{V}_2^{[2]}$ and $\mathbf{V}_3^{[2]}$, the channel matrices in (6.8) need to be reshuffled in terms of their position as follows

$$\begin{bmatrix} \mathbf{I} & -\mathbf{H}_{1,2} & \mathbf{0} & \mathbf{0} \\ \mathbf{I} & \mathbf{0} & -\mathbf{H}_{1,3} & \mathbf{0} \\ \mathbf{I} & \mathbf{0} & \mathbf{0} & -\mathbf{H}_{1,1} \end{bmatrix} \begin{bmatrix} \mathbf{A}_2 \\ \boxed{\mathbf{V}_2^{[2]}} \\ \boxed{\mathbf{V}_3^{[2]}} \\ \boxed{\mathbf{V}_1^{[3]}} \end{bmatrix} = \mathbf{C}_{A_2}\mathbf{D}_{A_2} = \mathbf{0}. \tag{6.9}$$

The dimension of $\mathbf{C}_{A_{k,k\in\{1,2\}}}$ is $3N \times 4N$, and thus the SVD-based nullspace $\mathbf{D}_{A_{k,k\in\{1,2\}}}$ always exists with the dimension of $4N \times N$. Accordingly, it is feasible to obtain square $N \times N$ $\mathbf{V}_k^{[l,l\neq 1]}$ matrices. These square matrices are required to provide the precoding design due to the fact that their inverses are always obtainable. These inverses will be further utilized in (6.11)–(6.15). Any column vector of $\mathbf{V}_k^{[l,l\neq 1]}$ derived in (6.8)–(6.9) will be utilized as the required beamforming vector in (6.6).

Regarding the reshuffle, both $\mathbf{C}_{A_1}$ and $\mathbf{C}_{A_2}$ are independent matrices if and only if the row vectors of them are linearly independent from each other. To prove their independence, it is sufficient to build a matrix by row-by-row assignment from both $\mathbf{C}_{A_1}$ and $\mathbf{C}_{A_2}$ matrices as

$$\mathbf{W} = \begin{bmatrix} \mathbf{C}_{A_1}(i,:) \\ \mathbf{C}_{A_2}(j,:) \end{bmatrix}, \ \forall i,j \in \{1,2,\ldots,3N\}, \tag{6.10}$$

where $\mathbf{C}_{A_k}(l,:)$ denotes the l^{th} row of the $\mathbf{C}$ matrix related to the subspace

spanned by $\mathbf{A}_k$. By computing row reduced echelon form $(rref)$ of the $\mathbf{W}$ matrix, one can calculate its rank and verify that

$$\text{rank}\left(rref\left(\mathbf{W}\right)\right) = 2,$$

which is always valid for any combination of these rows. This leads to the fact that the row vectors are linearly independent from each other, and thus the derived beamforming $\mathbf{V}_k^{[l,l\neq 1]}$ matrices can be treated as distinct ones.

6.2.2 Grouping Method at Rx 2

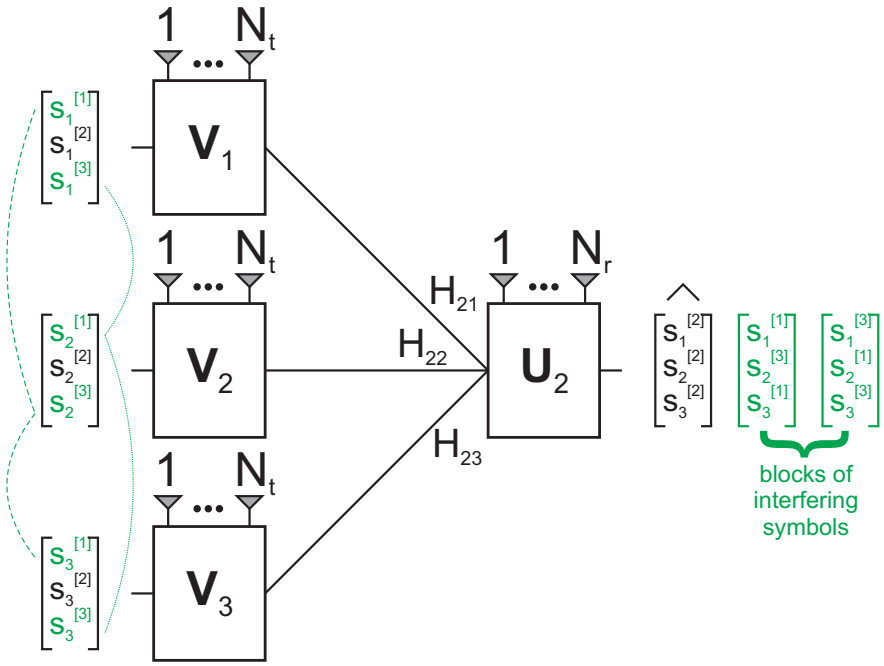

Figure 6.3. The grouping method of the interfering signals at receiver 2.

So far, the precoding matrices $\mathbf{V}_i^{[1]}$ have not been determined yet. In Fig. 6.3, receiver 2 observes two blocks of the interfering symbols (in green) spanned by the subspaces $\mathbf{B}_1$ and $\mathbf{B}_2$, and these spaces can be respectively defined as

$$\mathbf{B}_1 :\Rightarrow \text{span}\left\{\mathbf{H}_{2,1}\mathbf{V}_1^{[1]},\ \mathbf{H}_{2,2}\mathbf{V}_2^{[3]},\ \mathbf{H}_{2,3}\mathbf{V}_3^{[1]}\right\},$$
$$\mathbf{B}_2 :\Rightarrow \text{span}\left\{\mathbf{H}_{2,1}\mathbf{V}_1^{[3]},\ \mathbf{H}_{2,2}\mathbf{V}_2^{[1]},\ \mathbf{H}_{2,3}\mathbf{V}_3^{[3]}\right\}.$$

Hence, $\mathbf{B}_1$ can be utilized to find $\mathbf{V}_1^{[1]}$ and $\mathbf{V}_3^{[1]}$ as

$$\mathbf{V}_1^{[1]} = \mathbf{H}_{2,1}^{-1}\mathbf{H}_{2,2}\mathbf{V}_2^{[3]},$$
$$\mathbf{V}_3^{[1]} = \mathbf{H}_{2,3}^{-1}\mathbf{H}_{2,2}\mathbf{V}_2^{[3]}.$$

Considering $\mathbf{B}_2$, two beamforming matrices $\mathbf{V}_1^{[3]}$ and $\mathbf{V}_3^{[3]}$ have been already defined. Thus, $\mathbf{V}_2^{[1]}$ is chosen to align with $\mathbf{V}_1^{[3]}$ as

$$\mathbf{V}_2^{[1]} = \mathbf{H}_{2,2}^{-1}\mathbf{H}_{2,1}\mathbf{V}_1^{[3]}.$$

Therefore, receiver 2 needs to align $\mathbf{H}_{2,3}\mathbf{V}_3^{[3]}$ with $\mathbf{H}_{2,1}\mathbf{V}_1^{[3]}$ which can be implemented by determining a complementary matrix $\mathbf{T}_{B_2}$ as

$$\begin{aligned} &\mathbf{H}_{2,1}\mathbf{V}_1^{[3]} = \mathbf{H}_{2,3}\mathbf{V}_3^{[3]}\mathbf{T}_{B_2} \\ \Rightarrow &\mathbf{T}_{B_2} = \left(\mathbf{H}_{2,3}\mathbf{V}_3^{[3]}\right)^{-1}\mathbf{H}_{2,1}\mathbf{V}_1^{[3]} \\ \Rightarrow &\boxed{\tilde{\mathbf{V}}_3^{[3]}} = \mathbf{V}_3^{[3]}\mathbf{T}_{B_2}. \end{aligned} \tag{6.11}$$

6.2.3 Grouping Method at Rx 3

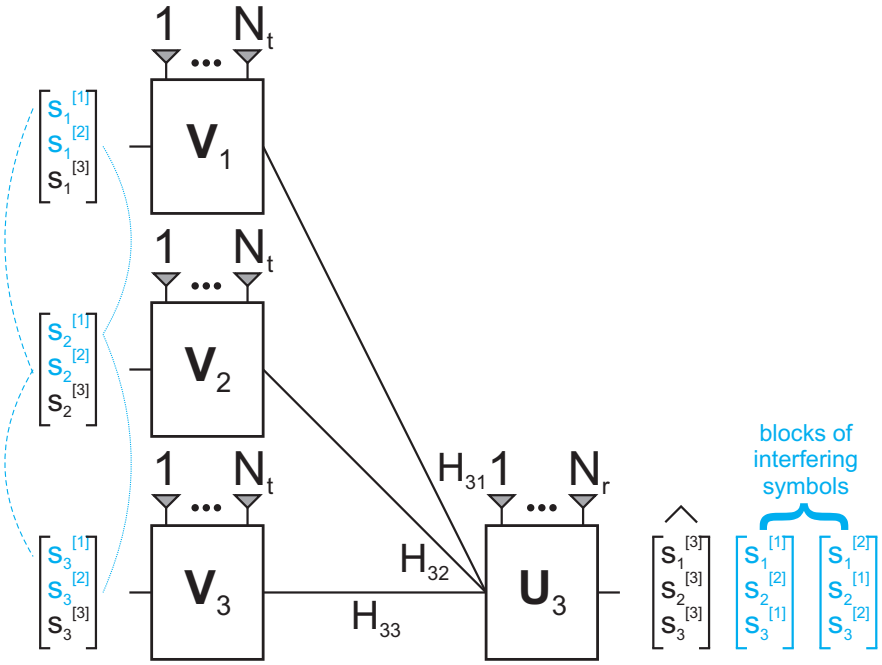

Figure 6.4. The grouping method of the interfering signals at receiver 3.

Next, we consider receiver 3 with the interfering symbols (in blue) spanned by $\mathbf{F}_1$ and $\mathbf{F}_2$ as

$$\begin{aligned}\mathbf{F}_1 :\Rightarrow &\text{span}\left\{\mathbf{H}_{3,1}\mathbf{V}_1^{[1]},\ \mathbf{H}_{3,2}\mathbf{V}_2^{[2]},\ \mathbf{H}_{3,3}\mathbf{V}_3^{[1]}\right\},\\ \mathbf{F}_2 :\Rightarrow &\text{span}\left\{\mathbf{H}_{3,1}\mathbf{V}_1^{[2]},\ \mathbf{H}_{3,2}\mathbf{V}_2^{[1]},\ \mathbf{H}_{3,3}\mathbf{V}_3^{[2]}\right\}.\end{aligned}$$

The precoding matrix $\mathbf{V}_2^{[2]}$ from (6.9) is chosen to be aligned with the interfering symbols given in $\mathbf{F}_1$ by defining complimentary matrices as

$$\begin{aligned}&\mathbf{H}_{3,2}\mathbf{V}_2^{[2]} = \mathbf{H}_{3,1}\mathbf{V}_1^{[1]}\mathbf{T}_{F_{11}}\\ \Rightarrow&\mathbf{T}_{F_{11}} = \left(\mathbf{H}_{3,1}\mathbf{V}_1^{[1]}\right)^{-1}\mathbf{H}_{3,2}\mathbf{V}_2^{[2]}\\ \Rightarrow&\boxed{\tilde{\mathbf{V}}_1^{[1]}} = \mathbf{V}_1^{[1]}\mathbf{T}_{F_{11}}, \qquad (6.12)\\ &\mathbf{H}_{3,2}\mathbf{V}_2^{[2]} = \mathbf{H}_{3,3}\mathbf{V}_3^{[1]}\mathbf{T}_{F_{12}}\\ \Rightarrow&\mathbf{T}_{F_{12}} = \left(\mathbf{H}_{3,3}\mathbf{V}_3^{[1]}\right)^{-1}\mathbf{H}_{3,2}\mathbf{V}_2^{[2]}\\ \Rightarrow&\boxed{\tilde{\mathbf{V}}_3^{[1]}} = \mathbf{V}_3^{[1]}\mathbf{T}_{F_{12}}. \qquad (6.13)\end{aligned}$$

Similar to $\mathbf{F}_2$, we have

$$\begin{aligned}&\mathbf{H}_{3,3}\mathbf{V}_3^{[2]} = \mathbf{H}_{3,2}\mathbf{V}_2^{[1]}\mathbf{T}_{F_{21}}\\ \Rightarrow&\mathbf{T}_{F_{21}} = \left(\mathbf{H}_{3,2}\mathbf{V}_2^{[1]}\right)^{-1}\mathbf{H}_{3,3}\mathbf{V}_3^{[2]}\\ \Rightarrow&\boxed{\tilde{\mathbf{V}}_2^{[1]}} = \mathbf{V}_2^{[1]}\mathbf{T}_{F_{21}}, \qquad (6.14)\\ &\mathbf{H}_{3,3}\mathbf{V}_3^{[2]} = \mathbf{H}_{3,1}\mathbf{V}_1^{[2]}\mathbf{T}_{F_{22}}\\ \Rightarrow&\mathbf{T}_{F_{22}} = \left(\mathbf{H}_{3,1}\mathbf{V}_1^{[2]}\right)^{-1}\mathbf{H}_{3,3}\mathbf{V}_3^{[2]}\\ \Rightarrow&\boxed{\tilde{\mathbf{V}}_1^{[2]}} = \mathbf{V}_1^{[2]}\mathbf{T}_{F_{22}}. \qquad (6.15)\end{aligned}$$

All the beamforming matrices enclosed in boxes represent the $N \times N$ square matrices. Since only one column vector is required from each beamforming matrix to implement interference-free data transmission, their first columns can be simply chosen to build the final precoding matrices $\mathbf{V}_1$, $\mathbf{V}_2$ and $\mathbf{V}_3$. To prevent misunderstanding of which matrices are utilized in transmit beamforming design, a different notation for the precoding vectors is introduced as $\mathbf{f}_i^{[l]}$ as shown in

$\mathbf{f}_1^{[1]} = \tilde{\mathbf{V}}_1^{[1]}(:,1)$ from (6.12)	$\mathbf{f}_1^{[2]} = \tilde{\mathbf{V}}_1^{[2]}(:,1)$ from (6.15)
$\mathbf{f}_2^{[1]} = \tilde{\mathbf{V}}_2^{[1]}(:,1)$ from (6.14)	$\mathbf{f}_2^{[2]} = \mathbf{V}_2^{[2]}(:,1)$ from (6.9)
$\mathbf{f}_3^{[1]} = \tilde{\mathbf{V}}_3^{[1]}(:,1)$ from (6.13)	$\mathbf{f}_3^{[2]} = \mathbf{V}_3^{[2]}(:,1)$ from (6.9)

$\mathbf{f}_1^{[3]} = \mathbf{V}_1^{[3]}(:,1)$ from (6.9)
$\mathbf{f}_2^{[3]} = \mathbf{V}_2^{[3]}(:,1)$ from (6.8)
$\mathbf{f}_3^{[3]} = \tilde{\mathbf{V}}_3^{[3]}(:,1)$ from (6.11)

(6.16)

(6.16), where the first columns are chosen to be the precoding vectors.

Furthermore, the subspaces $\mathbf{F}_1$ and $\mathbf{F}_2$ are chosen as

$$\mathbf{F}_1 = \mathbf{H}_{3,2}\mathbf{f}_2^{[2]},$$
$$\mathbf{F}_2 = \mathbf{H}_{3,3}\mathbf{f}_3^{[2]}.$$

With respect to receiver 3, all the interfering symbols are aligned along $\mathbf{F}_1$ and $\mathbf{F}_2$ combined together in $\mathbf{F}$. Then, the interference at receiver j can be suppressed by the receive beamforming matrix $\mathbf{U}_j$ as

$$\mathbf{F} = [\mathbf{F}_1 \;\; \mathbf{F}_2],$$
$$\mathbf{U}_3 = \text{null}\left(\mathbf{F}^H\right); \tag{6.17}$$
$$\mathbf{B} = \left[\mathbf{H}_{2,1}\mathbf{f}_1^{[1]} \;\; \mathbf{H}_{2,2}\mathbf{f}_2^{[1]} \;\; \mathbf{H}_{2,2}\mathbf{f}_2^{[3]} \;\; \mathbf{H}_{2,3}\mathbf{f}_3^{[1]} \;\; \mathbf{H}_{2,3}\mathbf{f}_3^{[3]}\right],$$
$$\mathbf{U}_2 = \text{null}\left(\mathbf{B}^H\right); \tag{6.18}$$
$$\mathbf{A} = \left[\mathbf{A}_1 \;\; \mathbf{A}_2 \;\; \mathbf{H}_{1,1}\mathbf{f}_1^{[2]} \;\; \mathbf{H}_{1,3}\mathbf{f}_3^{[3]}\right],$$
$$\mathbf{U}_1 = \text{null}\left(\mathbf{A}^H\right). \tag{6.19}$$

Since each receiver needs to decode three symbols, $\mathbf{U}_j$ should have a dimension of $N_r \times d_s$, it needs to consider $\mathbf{B} \in \mathbb{C}^{N_r \times 5}$. Therefore, the number of antennas at each node equals eight in this case. Hence, the received signal can be rewritten as

$$\tilde{\mathbf{y}}_j = \mathbf{U}_j^H \sum_{i=1}^{L=3} \mathbf{H}_{j,i}\mathbf{V}_i\mathbf{s}_i + \tilde{\mathbf{n}}_j$$

$$
\begin{aligned}
&= \mathbf{U}_j^H \sum_{i=1}^{L=3} \mathbf{H}_{j,i} \left[\mathbf{f}_i^{[1]} \ \mathbf{f}_i^{[2]} \ \mathbf{f}_i^{[3]} \right] \begin{bmatrix} s_i^{[1]} \\ s_i^{[2]} \\ s_i^{[3]} \end{bmatrix} + \tilde{\mathbf{n}}_j \\
&= \underbrace{\mathbf{U}_j^H \sum_{i=1}^{L=3} \mathbf{H}_{j,i} \mathbf{f}_i^{[j]} s_i^{[j]}}_{\text{desired signal}} + \underbrace{\mathbf{U}_j^H \sum_{i=1}^{L=3} \sum_{l=1, l\neq j}^{L=3} \mathbf{H}_{j,i} \mathbf{f}_i^{[l]} s_i^{[l]}}_{\text{interference} = 0} + \tilde{\mathbf{n}}_j \\
&= \left[\mathbf{U}_j^H \mathbf{H}_{j,1} \mathbf{f}_1^{[j]} \ \ \mathbf{U}_j^H \mathbf{H}_{j,2} \mathbf{f}_2^{[j]} \ \ \mathbf{U}_j^H \mathbf{H}_{j,3} \mathbf{f}_3^{[j]} \right] \begin{bmatrix} s_1^{[j]} \\ s_2^{[j]} \\ s_3^{[j]} \end{bmatrix} + \tilde{\mathbf{n}}_j \\
&= \bar{\mathbf{H}}^{[j]} \mathbf{s}^{[j]} + \tilde{\mathbf{n}}_j, \ \forall j \in L, \qquad (6.20)
\end{aligned}
$$

where $\bar{\mathbf{H}}_j$ and $\tilde{\mathbf{n}}_j$ denote the effective channel matrix and zero-mean AWGN vector observed by receiver j, respectively. $\mathbf{s}^{[j]}$ indicates the received signal intended for user j.

With respect to (6.20), the sum rate (6.5) can be calculated as

$$
\mathcal{I}_\Sigma = \sum_{j=1}^{L=3} \log_2 \left(\det \left(\mathbf{I} + \frac{\bar{\mathbf{H}}^{[j]} \bar{\mathbf{H}}^{[j]H}}{\sigma_{\tilde{n}}^2 \mathbf{I}} \right) \right). \qquad (6.21)
$$

6.2.4 Imperfect CSI

Assuming perfect CSI is highly idealistic, therefore, to understand the impact of CSI mismatch, we exploit the CSI acquisition model defined in (2.7)–(2.8) (Chapter 2).

With this in mind, the received signal (6.20) of the user of interest can be rewritten as

$$
\begin{aligned}
\tilde{\mathbf{y}}_j &= \mathbf{U}_j^H \sum_{i=1}^{L=3} \mathbf{H}_{j,i} \mathbf{V}_i \mathbf{s}_i + \tilde{\mathbf{n}}_j \\
&= \mathbf{U}_j^H \sum_{i=1}^{L=3} \left(\frac{1}{\tau+1} \hat{\mathbf{H}}_{j,i} + \tilde{\mathbf{H}}_{j,i} \right) \left[\mathbf{f}_i^{[1]} \ \mathbf{f}_i^{[2]} \ \mathbf{f}_i^{[3]} \right] \begin{bmatrix} s_i^{[1]} \\ s_i^{[2]} \\ s_i^{[3]} \end{bmatrix} + \tilde{\mathbf{n}}_j \\
&= \underbrace{\frac{1}{\tau+1} \mathbf{U}_j^H \sum_{i=1}^{L=3} \hat{\mathbf{H}}_{j,i} \mathbf{f}_i^{[j]} s_i^{[j]}}_{\text{desired signal}} + \underbrace{\mathbf{U}_j^H \sum_{i=1}^{L=3} \tilde{\mathbf{H}}_{j,i} \mathbf{f}_i^{[j]} s_i^{[j]}}_{\text{CSI mismatch of desired signal}}
\end{aligned}
$$

$$\mathcal{I}_{\Sigma} = \sum_{j=1}^{L=3} \log_2 \left(\det \left(\mathbf{I} + \frac{\sum_{i=1}^{L=3} \left| \frac{1}{\tau+1} \mathbf{U}_j^H \hat{\mathbf{H}}_{j,i} \mathbf{f}_i^{[j]} \right|^2}{\sum_{i=1}^{L=3} \left| \mathbf{U}_j^H \tilde{\mathbf{H}}_{j,i} \mathbf{f}_i^{[j]} \right|^2 + \sum_{i=1}^{L=3} \sum_{l=1, l\neq j}^{L=3} \left| \mathbf{U}_j^H \tilde{\mathbf{H}}_{j,i} \mathbf{f}_i^{[l]} s_i^{[l]} \right|^2 + \sigma_{\tilde{n}}^2 \mathbf{I}} \right) \right). \tag{6.23}$$

$$+ \underbrace{\frac{1}{\tau+1} \mathbf{U}_j^H \sum_{i=1}^{L=3} \sum_{l=1, l\neq j}^{L=3} \hat{\mathbf{H}}_{j,i} \mathbf{f}_i^{[l]} s_i^{[l]}}_{\text{interference} = 0} + \underbrace{\mathbf{U}_j^H \sum_{i=1}^{L=3} \sum_{l=1, l\neq j}^{L=3} \tilde{\mathbf{H}}_{j,i} \mathbf{f}_i^{[l]} s_i^{[l]}}_{\text{CSI mismatch of interference}} + \tilde{\mathbf{n}}_j, \ \forall j \in L. \tag{6.22}$$

Accordingly, the sum rate with respect to imperfect CSI can be calculated as shown in (6.23).

6.2.5 Computational Complexity

Since the beamforming matrices in (6.8)–(6.9) are calculated using the SVD-based nullspace, the corresponding computational complexity of SVD can be written as $\mathcal{O}(pm^2 + m^3)$ for a $m \times p$ matrix with $p < m$, [169]. Then, the overall computational complexity of the proposed scheme is $\mathcal{O}(258N^3)$.

Since each beamforming matrix (boxed one) consists of N vectors, it is feasible to choose the best one that increases the achievable sum rate. This can be simply implemented by choosing the vector corresponding to the largest eigenvalue. The eigenvalue-based search slightly complicates the complexity of the proposed scheme, i.e., the arithmetic complexity of this search for a given $N \times N$ matrix is $\mathcal{O}(N^3)$. Therefore, the overall additional complexity equals $9N^3$. Fig. 6.5 presents the computational complexities of the original and eigenvalue-based methods.

6.3 Simulation Results

We evaluate the overall achievable sum rate for the three-user MIMO X-channel model with Rayleigh fading, [19, 79]. It can be seen from Fig. 6.6 that it allows us to obtain 58.75 bits/s/Hz at SNR = 30 dB by utilizing (6.16). Then we investigate the effect of different CSI conditions on the achievable sum rate that

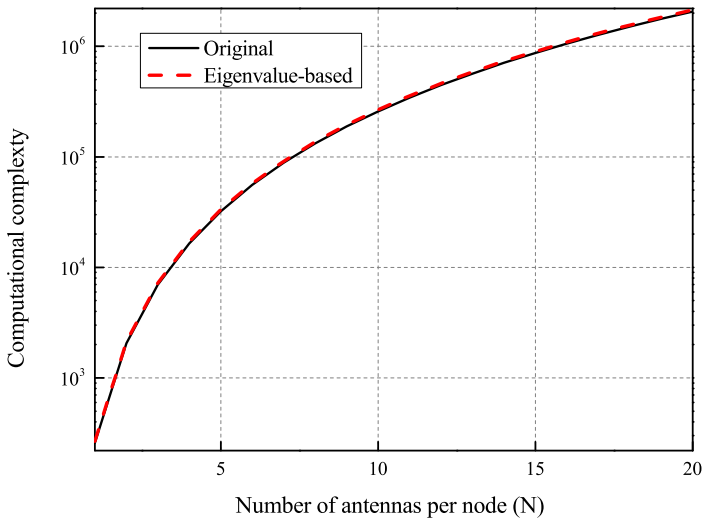

Figure 6.5. The computational complexity of the proposed scheme.

are given by a set of (α, β) such that $(1.5, 15)$, $(1, 10)$, $(0.75, 10)$, $(0, 0.05)$ and $(0, 0.001)$. Fig. 6.6 presents an insight into how imperfect CSI impacts on the achievable sum rates utilizing (2.7)–(2.9). When $\alpha = 0$ it can be seen that β has a significant impact where $\alpha = 0$ is the worst scenario because increasing SNR does not provide any increase in the achievable sum rate. At $\beta = 0.001$, it is feasible to apply the proposed scheme in the low SNR region (<12 dB). However, at $\beta = 0.05$, the DoF loss is too large for the whole range of SNR. For $\alpha = 0$, it should be noted that in the low SNR region the scheme provides poor performance; however, the dependence on SNR leads to a sum rate improvement when SNR increases. The larger α gets, the sharper the curve slope becomes.

In Fig. 6.7, we then exploit the eigenvalue-based method to calculate the achievable sum rates and compare them with the previous. A minor complication of the proposed algorithm allows us to achieve a noticeable increase in the sum rate (lines with symbols), i.e., we gain 5.67, 5.31, 5.1, 4.12, 4.18 and 5.8 bits/s/Hz for the perfect, $(1.5, 15)$, $(1, 10)$, $(0.75, 10)$, $(0, 0.05)$ and $(0, 0.001)$ CSI acquisition scenarios, respectively.

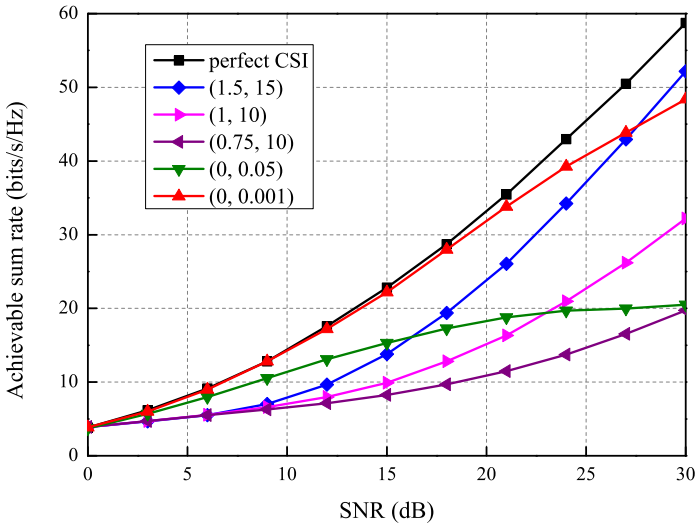

Figure 6.6. The overall sum rate under various CSI conditions.

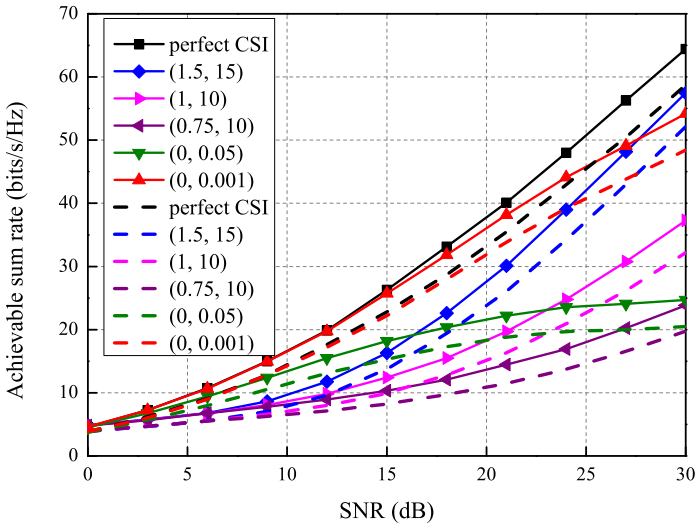

Figure 6.7. The comparison of sum rates achievable by the original and eigenvalue-based methods.

6.4 Chapter Summary

This Chapter proposed a closed-form IA scheme for the downlink three-user MIMO X-channel network without symbol extension. The proposed scheme is based on the idea of grouping the interfering signals at the receiver side such that the desired signal is allocated in the interference-free subspace. Then, the updated eigenvalue search based approach was proposed as the capacity enhancing technique. Moreover, it was shown that the proposed scheme obtains 58.75 and 64.42 bits/s/Hz by utilizing the original and eigenvalue-based methods, respectively. This difference is obtained by a minor sophistication of the proposed algorithm (Fig. 6.5). The effect of CSI mismatch on the achievable sum rate was also evaluated.

Chapter 7

Conclusions and Future Work

7.1 Conclusions

This thesis studied the fundamentals of Interference Alignment and the challenges facing this technique with a particular focus on the users in the most vulnerable area enduring a multi-source transmission scenario. Chapter 1 briefly described current trends in modern wireless systems and emphasized main obstacles on the road to fulfil the requirements to support the rapid mobile data traffic growth. Then, the literature review in Chapter 2 reiterated main features of MIMO technology and capacity attaining techniques. Moreover, the issue of interference was introduced and subsequently various techniques aiming to mitigate it in different layers were discussed. Finally, Chapter 2 presented the concept of Interference Alignment and consequently provided a variety of IA applications.

In Chapter 3, a compounded MIMO BC network scenario was determined, which can be briefly described as the scenario where a certain user desires to decode messages coming from several sources. Moreover, the user of interest was placed in the most vulnerable cell-edge area. For the considered case, a new method of interference mitigation was proposed that is able to provide up to $(L-1)$ DoF per user. The compounded MIMO BC generally undergoes two types of interference: IC interference and X-channel interference. It was shown that for a similar scenario, there were several two-step schemes that can cancel only the IC interference. Furthermore, the application of the proposed scheme allows one to treat the multi-cell MIMO network as a single-cell single-user MIMO case free from interference. The general interrelation between network parameters was also derived. The attainable performances were compared to one of the benchmarks

(ZFBF). Moreover, the system performances were also analysed for different CSI mismatch scenarios. Finally, the calculated computational complexity indicated the simplicity of this scheme compared to V-BLAST.

Chapter 4 also considered the compounded MIMO BC network. The study case consisting of three cells was examined, and the corresponding DoF region was analysed. An upper limit was defined by solving the dual problem for the linear maximization program. Moreover, the study case was expanded to the general network case. The minimum antenna configuration was obtained in order to maintain the maximum DoF. This Chapter also provided insights into the effect of various message set ups on the achievable DoF and the required number of antennas. It was shown that the proposed scheme with a certain antenna configuration achieves more DoF than the conventional ones.

Chapter 5 mainly focused on the effect of spatial correlation. Accordingly, the Kronecker model was considered for the sake of its simplicity. Based on the experimental measurements in [166], it was proved that the exponential and uniform models can be applied at the transmitter and receiver side, respectively. The compounded MIMO BC network was taken into account to analyse the antenna correlation. Therefore, different classes of users with various numbers of antennas were considered. Respectively, an updated version of the proposed scheme (presented in Chapter 3) was provided. Then, the computational complexity was calculated. Finally, the various system performances were analysed with respect to different antenna correlation modes and CSI acquisition scenarios.

Chapter 6 presented an alternative design of the IA-based interference mitigation scheme for achieving the maximum data rate. In particular, a special way of grouping of interfering signals was applied for efficiently allocating the interference at the receiver side. In addition, matrix reshuffling was used to design the interfering subspace. Furthermore, an update of the scheme was proposed that utilizes eigenvalue-based search for enhancing the achievable data throughput. Finally, computational complexity and the impact of the different CSI acquisitions on the data rate were evaluated.

7.2 Future Plan

Here we suggest some possible research extensions to the work in this thesis as follows.

- In Chapter 3, we proposed the IA-based scheme for the cell-edge users to mitigate the severe interference in the compounded MIMO BC scenario for Homogeneous networks under the assumption of no frequency reuse. Subsequently, the complexity of the scheme was shown to be low compared to the benchmark. However, it would be worthwhile to consider the Heterogeneous scenario with the macro/micro base station employment. Consequently, due to full overlapping of microcells with the macrocell, the number of users to be treated will dramatically increase. Consequently, the computational complexity of the proposed algorithm is likely to deteriorate. Therefore, additional work could be done by optimising the algorithm to reduce its complexity for the case of HetNets.

- In the emerging trends of green communications and Energy Harvesting (EH), IA techniques could be considered as potential means for energy harvesting. Some research on IA-based EH techniques has been carried out in, [170, 171], where the authors proposed user and antenna selection schemes to define active and idle users/antennas, i.e., among the total Q users only K ($K < Q$) users can obtain information data while the $(Q - K)$ users, instead of being idle, can obtain the same non-intended information symbols for harvesting (analogously, the same approach can be applied for the antenna selection scheme). Since Chapter 4 provided a comprehensive analysis on the achievable DoF for the compounded MIMO BC scenario with the appropriate algorithm for calculating the minimum required antenna configuration, it would be worthwhile to apply the concept of EH to the proposed scheme to synthesize both, the information and energy transfer modes in one design, when the user of interest simultaneously receives the desired signal and harvest the energy from the interference term; in other words, the user performs both modes (information transfer and energy harvesting) at a certain minimum required SINR.

- In Chapters 3, 4 and 5, we examined the users that experience the multi-source transmission from several BSs. Therefore, the proposed scheme is

also applicable for providing energy efficiency for network operators and users if a dynamic network planning can be taken into consideration, [172]. If so, all the involved BSs create a dynamic cluster to serve all the users efficiently. Since the provided algorithms proved in Chapter 5 that the case of LS-MIMO is applicable, the final network configuration can be regarded as distributed compounded LS-MIMO BC scenario. By combining all the benefits of the above-mentioned technologies, it is highly possible to obtain a novel technique suitable for next-generation wireless communication systems.

Bibliography

[1] "Cisco visual networking index: Global mobile data traffic forecast update 2014 – 2019," *White Paper*, February 3, 2015.

[2] V. Cadambe and S. Jafar, "Interference alignment and the degrees of freedom of the K-user interference channel," *IEEE Transactions on Information Theory*, vol. 54, no. 8, pp. 3425–3441, August 2008.

[3] A. Paulraj, R. Nabar, and D. Gore, *Introduction to space-time wireless communications*. Cambridge University Press, 2003.

[4] J. Hoydis, M. Kobayashi, and M. Debbah, "Green small-cell networks," *IEEE Vehicular Technology Magazine*, pp. 37–43, March 2011.

[5] H. Yanikomeroglu, *The building blocks of the 5th generation (5G) wireless networks for affordable and ubiquitous*. Tech. Rep., BCWS Seminar Series, Carleton University, 2011.

[6] L. Thiele, M. Kurras, M. Olbrich, and T. Haustein, "Boosting 4G networks with spatial interference management under feedback constraints: a non-cooperative downlink transmission scheme," *IEEE Vehicular Technology Magazine*, pp. 40–48, March 2013.

[7] G. Foschini, "Layered space-time architecture for wireless communication in a fading environment when using multi-element antennas," *Bell Labs Technical Journal*, vol. 1, no. 2, pp. 41–59, Autumn 1996.

[8] J. Winters, "On the capacity of radio communication systems with diversity in a Rayleigh fading environment," *IEEE Journal on Selected Areas in Communications*, vol. 5, no. 5, pp. 871–878, June 1987.

[9] E. Telatar, "Capacity of multi-antenna Gaussian channels," *European Transaction Telecommunications*, vol. 10, no. 6, pp. 585–595, November 1999.

[10] L. Liu, R. Chen, S. Geirhofer, K. Sayana, Z. Shi, and Y. Zhou, "Downlink MIMO in LTE-Advanced: SU-MIMO vs. MU-MIMO," *IEEE Communications Letters*, vol. 50, no. 2, pp. 140–147, February 2012.

[11] E. Biglieri, R. Calderbank, A. Constantinides, A. Goldsmith, A. Paulraj, and H. Poor, *MIMO Wireless Communications*. Cambridge, UK: Cambridge University Press, 2007.

[12] D. Tse and P. Viswanath, *Fundamentals of Wireless Communication*. Cambridge, UK: Cambridge University Press, 2005.

[13] L. Zheng and D. Tse, "Diversity and multiplexing: a fundamental trade-off in multiple antenna channels," *IEEE Transactions of Information Theory*, vol. 49, no. 5, pp. 1073–1096, May 2003.

[14] A. Goldsmith, S. Jafar, N. Jindal, and S. Vishwanath, "Capacity limits of MIMO channels," *IEEE Journal on Selected Areas in Communications*, vol. 21, no. 5, pp. 684–702, June 2003.

[15] V. Tarokh, N. Seshadri, and A. Calderbank, "Space-time codes for high data rate wireless communication: performance criterion and code construction," *IEEE Transactions on Information Theory*, vol. 44, no. 2, pp. 744–765, March 1998.

[16] V. Tarokh, H. Jafarkhani, and A. Calderbank, "Space-time block codes from orthogonal designs," *IEEE Transactions on Information Theory*, vol. 45, no. 5, pp. 1456–1467, July 1999.

[17] T. Gou and S. Jafar, "Degrees of freedom of the K-user $M \times N$ MIMO interference channel," *IEEE Transactions on Information Theory*, vol. 56, no. 12, pp. 6040–6057, December 2010.

[18] G. Caire and S. Shamai, "On the achievable throughput of a multi-antenna Gaussian broadcast channel," *IEEE Transactions on Information Theory*, vol. 49, no. 7, pp. 1691–1706, July 2003.

[19] P. Aquilina and T. Ratnarajah, "Performance analysis of IA techniques in the MIMO IBC with imperfect CSI," *IEEE Transactions on Communications*, vol. 63, no. 4, pp. 1259–1270, April 2015.

[20] J. Maurer, J. Jalden, D. Seethaler, and G. Matz, "Vector perturbation precoding revisited," *IEEE Transactions on Signal Processing*, vol. 59, no. 1, pp. 315–328, January 2011.

[21] J. Jose, A. Ashikhmin, T. Marzetta, and S. Vishwanath, "Pilot contamination and precoding in multi-cell TDD systems," *IEEE Transactions on Wireless Communications*, vol. 10, no. 8, pp. 2640–2651, August 2011.

[22] H. Ngo, E. Larsson, and T. Marzetta, "The multicell multiuser MIMO uplink with very large antenna arrays and a finite-dimensional channel," *IEEE Transactions on Communications*, vol. 61, no. 6, pp. 2350–2361, June 2013.

[23] F. Fernandes, A. Ashikhmin, and T. Marzetta, "Inter-cell interference in noncooperative TDD large scale antenna systems," *IEEE Journal on Selected Areas in Communications*, vol. 31, no. 2, pp. 192–201, February 2013.

[24] S. Kay, *Fundamentals of Statistical Signal Processing: Estimation Theory.* Prentice Hall, 1993.

[25] S. Razavi and T. Ratnarajah, "Performance analysis of interference alignment under CSI mismatch," *IEEE Transactions on Vehicular Technology*, vol. 63, no. 9, pp. 4740–4748, November 2014.

[26] S. Razavi and T. Ratnarajah, "Adaptively regularized phase alignment precoding for multiuser multiantenna downlink," *IEEE Transactions on Vehicular Technology*, vol. 64, no. 10, pp. 4863–4869, October 2015.

[27] S. Razavi and T. Ratnarajah, "Adaptive LS- and MMSE-based beamformer design for multiuser MIMO interference channels," *IEEE Transactions on Vehicular Technology*, vol. 65, no. 1, pp. 132–144, January 2016.

[28] R. Scheaffer and L. Young, *Introduction to Probability and its Applications.* 3rd edition, Brooks/Cole, Cengage Learning, 2010.

[29] K. Zheng, L. Zhao, W. Xiang, and L. Hanzo, "A survey of Large-Scale MIMO systems," *IEEE Communications Surveys and Tutorials*, vol. 17, no. 3, pp. 1738–1760, Third Quarter 2015.

[30] T. Zahir, K. Arshad, A. Nakata, and K. Moessner, "Interference management in femtocells," *IEEE Communications Surveys and Tutorials*, vol. 15, no. 1, pp. 293–311, First Quarter 2013.

[31] H. Kpojime and G. Safdar, "Interference mitigation in cognitive-radio-based femtocells," *IEEE Communications Surveys and Tutorials*, vol. 17, no. 3, pp. 1511–1534, Third Quarter 2015.

[32] J. Mietzner, R. Schober, L. Lampe, W. Gerstacker, and P. Hoeher, "Multiple-antenna techniques for wireless communications - a comprehensive literature survey," *IEEE Communications Surveys and Tutorials*, vol. 13, no. 2, pp. 87–105, Second Quarter 2009.

[33] J. Winters, J. Salz, and R. Gitlin, "The impact of antenna diversity on the capacity of wireless communication systems," *IEEE Transactions on Communications*, vol. 42, no. 234, pp. 1740–1751, February/March/April 1994.

[34] E. Larsson, F. Tufvesson, O. Edfors, and T. Marzetta, "Massive MIMO for next generation wireless systems," *IEEE Communications Magazine*, vol. 52, no. 2, pp. 186–195, February 2014.

[35] J. Proakis and M. Salehi, *Digital Communications*. McGraw-Hill, 5th ed., 2007.

[36] P. Li, R. de Lamare, and R. Fa, "Multiple feedback successive interference cancellation detection for multiuser MIMO systems," *IEEE Transactions on Wireless Communications*, vol. 10, no. 8, pp. 2434–2439, August 2011.

[37] O. Goussevskaia and R. Wattenhofer, "Scheduling wireless links with successive interference cancellation," in *IEEE 21st International Conference on Computer Communications and Networks (ICCCN)*, pp. 1–7, July-August 2012.

[38] A. Goldsmith, S. Jafar, N. Jindal, and S. Vishwanath, "Multiuser detection of DS-CDMA signals using partial parallel interference cancellation in satellite communications," *IEEE Journal on Selected Areas in Communications*, vol. 22, no. 3, pp. 584–593, April 2004.

[39] F. Han and K. Liu, "A multiuser TRDMA Uplink System with 2D parallel interference cancellation," *IEEE Transactions on Communications*, vol. 62, no. 3, pp. 1011–1022, March 2014.

[40] C. Ergun and K. Hacioglu, "Application of a genetic algorithm to multistage detection in CDMA systems," in *9th Mediterranean Electrotechnical Conference (Volume:2)*, pp. 846–850, May 1998.

[41] A. Gupta and A. Singer, "Multi-stage detection using constellation structure," in *40th Asilomar Conference on Signals, Systems and Computers*, pp. 585–589, October-November 2006.

[42] P. Wolniansky, G. Foschini, G. Golden, and R. Valenzuela, "V-BLAST: an architecture for realizing very high data rates over rich-scattering wireless channel," in *URSI International Symposium on Signals, Systems, and Electronics (Invited paper)*, pp. 295–300, October 1998.

[43] C. Windpassinger, *Detection and precoding for multiple input multiple output channels*. PhD thesis, University Erlangen-Nurnberg, 2004.

[44] F. Rusek, D. Persson, B. Lau, E. Larsson, T. Marzetta, O. Edfors, and F. Tufvesson, "Scaling up MIMO: opportunities and challenges with very large arrays," *IEEE Signal Processing Magazine*, vol. 30, no. 1, pp. 40–60, January 2013.

[45] M. Costa, "Writing on dirty paper," *IEEE Transactions on Information Theory*, vol. 29, no. 3, pp. 439–441, May 1983.

[46] H. Weingarten, Y. Steinberg, and S. Shamai, "The capacity region of the Gaussian multiple-input multiple-output broadcast channel," *IEEE Transactions on Information Theory*, vol. 52, no. 9, pp. 3936–3964, September 2006.

[47] C. Masouros, M. Sellathurai, and T. Ratnarajah, "Interference optimization for transmit power reduction in Tomlinson-Harashima precoded

MIMO downlinks," *IEEE Transactions on Signal Processing*, vol. 60, no. 5, pp. 2470–2481, May 2012.

[48] L. Sanguinetti and M. Morelli, "Non-linear pre-coding for multiple-antenna multiuser downlink transmissions with different QoS requirements," *IEEE Transactions on Wireless Communication*, vol. 6, no. 3, pp. 852–856, March 2007.

[49] C. Peel, B. Hochwald, and A. Swindlehurst, "A vector perturbation technique for near-capacity multianntenna multiuser communication - Part I: Channel inversion and regularization," *IEEE Transactions on Communications*, vol. 53, no. 1, pp. 195–202, January 2005.

[50] C. Masouros and E. Alsusa, "Dynamic linear precoding for the exploitation of known interference in MIMO broadcast systems," *IEEE Transactions on Wireless Communications*, vol. 8, no. 3, pp. 1396–1404, March 2009.

[51] V. Nguyen and J. Evans, "Multiuser transmit beamforming via regularized channel inversion: A large system analysis," in *Proceedings of IEEE GLOBECOM*, pp. 1–4, November-December 2008.

[52] U. Erez, S. Shamai, and R. Zamir, "Capacity and lattice strategies for cancelling known interference," *IEEE Transactions on Information Theory*, vol. 51, no. 11, pp. 3820–3833, November 2005.

[53] H. Gamal, G. Caire, and M. Damen, "Lattice coding and decoding achieve the optimal diversity-multiplexing tradeoff of MIMO channels," *IEEE Transactions on Information Theory*, vol. 50, no. 6, pp. 968–985, June 2004.

[54] C. Peel, B. Hochwald, and A. Swindlehurst, "A vector perturbation technique for near-capacity multianntenna multiuser communication - Part II: Perturbation," *IEEE Transactions on Communications*, vol. 53, no. 3, pp. 537–544, March 2005.

[55] A. Carleial, "A case where interference does not reduce capacity," *IEEE Transactions of Information Theory*, vol. 21, no. 5, pp. 569–570, September 1975.

[56] P. Minero, M. Franceschetti, and D. Tse, "Random access: An information-theoretic perspective," *IEEE Transactions on Information Theory*, vol. 58, no. 2, pp. 909–930, February 2012.

[57] F. Mugdim, *Interference Avoidance Concepts*. WINNER II project, 2007.

[58] E. Haro, S. Ruiz, D. Gonzalez, M. Garcia-Lozano, and J. Olmos, *Comparison of Different Distributed Scheduling Strategies for Static/Dynamic LTE Scenarios*. Technical University of Wien, 2009.

[59] Z. Xie and B. Walke, "Resource allocation and reuse for inter-cell interference mitigation in OFDMA based communication networks," in *5th Annual ICST Wireless Internet Conference (WICON)*, pp. 1–6, March 2010.

[60] R. Kwan and C. Leung, "A survey of scheduling and interference mitigation in LTE," *Electrical and Computer Engineering*, 2010.

[61] M. Rahman and H. Yanikomeroglu, "Enhancing cell-edge performance: a downlink dynamic interference avoidance scheme with inter-cell coordination," *IEEE Transactions on Wireless Communications*, vol. 9, no. 4, pp. 1414–1425, April 2010.

[62] L. Chen and D. Yuan, "Soft frequency reuse in large networks with irregular cell pattern: How much gain to expect?," in *IEEE 20th International Personal, Indoor and Mobile Radio Communications Symposium*, pp. 1467–1471, September 2009.

[63] A. Triki and L. Nuaymi, "Intercell interference coordination algorithms in OFDMA wireless systems," in *IEEE 73rd Vehicular Technology Conference (VTC Spring)*, pp. 1–6, May 2011.

[64] 3GPP R1-050629, "Inter-cell interference mitigation," in *Huawei, 2005.*, July 2012.

[65] T. Quek, Z. Lei, and S. Sun, "Adaptive interference coordination in multi-cell OFDMA systems," in *IEEE 20th International Symposium on Personal, Indoor and Mobile Radio Communications*, pp. 2380–2384, September 2009.

[66] A. Gjendemsjo, D. Gesbert, G. Oien, and S. Kiani, "Optimal power allocation and scheduling for two-cell capacity maximization," in *4th International Modeling and Optimization in Mobile, Ad Hoc and Wireless Networks Symposium*, pp. 1–6, April 2006.

[67] S. Das, H. Viswanathan, and G. Rittenhouse, "Dynamic load balancing through coordinated scheduling in packet data systems," in *IEEE 22nd Annual Joint Conference of the IEEE Computer and Communications, vol. 1*, pp. 786–796, March-April 2003.

[68] T. Bonald, S. Borst, and A. Proutiere, "Inter-cell scheduling in wireless data networks," in *11th European Wireless Conference*, pp. 1–7, April 2005.

[69] M. Rahman and H. Yanikomeroglu, "Multicell downlink OFDM subchannel allocations using dynamic intercell coordination," in *IEEE Global Telecommunications Conference (GLOBECOM)*, pp. 5220–5225, November 2007.

[70] G. Li and H. Liu, "Downlink radio resource allocation for multi-cell OFDMA system," *IEEE Transactions on Wireless Communications*, vol. 5, no. 12, pp. 3451–3459, December 2006.

[71] A. Stolyar and H. Viswanathan, "Self-organizing dynamic fractional frequency reuse for best-effort traffic through distributed inter-cell coordination," in *IEEE INFOCOM*, pp. 1287–1295, April 2009.

[72] S. Cicalo, V. Tralli, and A. Perez-Neira, "Centralized vs distributed resource allocation in multi-cell OFDMA systems," in *IEEE 73rd Vehicular Technology Conference*, pp. 1–6, May 2011.

[73] A. Ghasemi, A. Motahari, and A. Khandani, "Interference alignment for the K-user MIMO interference channel," in *Proceedings of IEEE International Symposium on Information Theory*, pp. 360–364, 2010.

[74] T. Gou and S. Jafar, "Capacity of a class of symmetric SIMO Gaussian interference channels within o(1)," *IEEE Transactions on Information Theory*, vol. 57, no. 4, pp. 1932–1958, April 2011.

[75] M. Maddah-Ali, A. Motahari, and A. Khandani, "Communication over

MIMO X channels: interference alignment, decomposition and performance analysis," *IEEE Transactions on Information Theory*, vol. 54, no. 8, pp. 3457–3470, August 2008.

[76] V. Cadambe and S. Jafar, "Interference alignment and the degrees of freedom of wireless X networks," *IEEE Transactions on Information Theory*, vol. 55, no. 9, pp. 3893–3908, September 2009.

[77] C. Suh, M. Ho, and D. Tse, "Downlink interference alignment," *IEEE Transactions on Communications*, vol. 59, no. 9, pp. 2616–2626, September 2011.

[78] C. Suh and D. Tse, "Interference alignment for cellular networks," in *Proceedings of Annual Allerton Conference on Communication, Control, and Computing*, pp. 1037–1044, September 2008.

[79] W. Shin, N. Lee, J. Lim, and K. Jang, "On the design of interference alignment scheme for two-cell MIMO interfering broadcast channels," *IEEE Transactions on Wireless Communications*, vol. 10, no. 2, pp. 437–442, February 2011.

[80] G. Bresler, A. Parekh, and D. Tse, "The approximate capacity of the many-to-one and one-to-many Gaussian interference channels," *IEEE Transactions on Information Theory*, vol. 56, no. 9, pp. 4566–4592, September 2010.

[81] A. Avestimehr, S. Diggavi, and D. Tse, "Wireless network information flow: A deterministic approach," *IEEE Transactions on Information Theory*, vol. 57, no. 4, pp. 1872–1905, April 2011.

[82] V. Cadambe, S. Jafar, and S. Shamai, "Interference alignment on the deterministic channel and application to Gaussian networks," *IEEE Transactions on Information Theory*, vol. 55, no. 1, pp. 269–274, January 2009.

[83] R. Etkin and E. Ordenlich, "The degrees-of-freedom of the K-user Gaussian interference channel is discontinuous at rational channel coefficients," *IEEE Transactions on Information Theory*, vol. 55, no. 11, pp. 4932–4946, November 2009.

[84] V. Cadambe, S. Jafar, H. Maleki, K. Ramchandran, and C. Suh, "Asymptotic interference alignment for optimal repair of MDS codes in distributed storage," *IEEE Transactions on Information Theory*, vol. 59, no. 5, pp. 2974–2987, May 2013.

[85] V. Cadambe, S. Jafar, and C. Wang, "Interference alignment with asymmetric complex signaling settling the Host-Madsen-Nosratinia conjecture," *IEEE Transactions on Information Theory*, vol. 56, no. 9, pp. 4552–4565, September 2010.

[86] L. Yang and W. Zhang, "Interference alignment with asymmetric complex signaling on MIMO X channels," *IEEE Transactions on Communications*, vol. 62, no. 10, pp. 3560–3570, October 2014.

[87] S. Perlaza, N. Fawaz, S. Lasaulce, and M. Debbah, "From spectrum pooling to space pooling: Opportunistic interference alignment in MIMO cognitive networks," *IEEE Transactions on Signal Processing*, vol. 58, no. 7, pp. 3728–3741, July 2010.

[88] G. Liu, M. Sheng, X. Wang, W. Jiao, Y. Li, and J. Li, "Opportunistic interference alignment and cancellation for the uplink of cellular networks," *IEEE Communication Letters*, vol. 19, no. 4, pp. 645–648, April 2015.

[89] B. Nazer, M. Gastpar, S. Jafar, and S. Vishwanath, "Ergodic interference alignment," in *ISIT*, pp. 1769–1773, July 2009.

[90] V. Cadambe and S. Jafar, "Parallel Gaussian interference channels are not always separable," *IEEE Transactions on Information Theory*, vol. 55, no. 9, pp. 3983–3990, September 2009.

[91] B. Nazer, M. Gastpar, S. Jafar, and S. Vishwanath, "Interference alignment at finite SNR: General message sets," in *Proceedings of Annual Allerton Conference on Communication, Control, and Computing*, pp. 843–848, 2009.

[92] V. Cadambe and S. Jafar, "Degrees of freedom of wireless networks with relays, feedback, cooperation and full duplex operation," *IEEE Transactions on Information Theory*, vol. 55, no. 5, pp. 2334–2344, May 2009.

[93] R. Tannious and A. Nosratinia, "The interference channel with MIMO relay: Degrees of freedom," in *Proceedings of IEEE International Symposium on Information Theory*, pp. 1908–1912, 2008.

[94] T. Gou, S. Jafar, and S.-Y. Chung, "Aligned interference neutralization and the degrees of freedom of the $2 \times 2 \times 2$ interference channel," *IEEE Transactions on Information Theory*, vol. 58, no. 7, pp. 4381–4395, July 2012.

[95] S. Jafar, "Blind interference alignment," *IEEE Journal of selected topics in Signal Processing*, vol. 6, no. 3, pp. 216–227, June 2012.

[96] T. Gou, C. Wang, and S. Jafar, "Aiming perfectly in the dark - blind interference alignment through staggered antenna switching," *IEEE Transactions on Signal Processing*, vol. 59, no. 6, pp. 2734–2744, June 2011.

[97] A. Lapidoth, S. Shamai, and M. Wigger, "On the capacity of fading MIMO broadcast channels with imperfect transmitter side-information," in *Proceedings of Annual Allerton Conference on Communication, Control, and Computing*, pp. 28–30, 2005.

[98] H. Maleki, S. Jafar, and S. Shamai, "Retrospective interference alignment," in *Proceedings of IEEE International Symposium on Information Theory*, pp. 2756–2760, 2011.

[99] C. Vaze and M. Varanasi, "The degrees of freedom region of the two-user MIMO broadcast channel with delayed CSIT," in *Proceedings of IEEE International Symposium on Information Theory*, pp. 199–203, 2011.

[100] H. Weingarten, S. Shamai, and G. Kramer, "On the compound MIMO broadcast channel," in *Proceedings of Annual Information Theory and Applications Workshop*, 2007.

[101] T. Gou, S. Jafar, and C. Wang, "On the degrees of freedom of finite state compound wireless networks," *IEEE Transactions on Information Theory*, vol. 57, no. 6, pp. 3286–3308, June 2011.

[102] Y. Birk and T. Kol, "Informed-source coding-on-demand (ISCOD) over

broadcast channels," in *Proceedings of the Seventeenth Annual Joint Conference of the IEEE Computer and Communications Societies*, pp. 1257–1264, 1998.

[103] Y. Birk and T. Kol, "Coding on demand by an informed source (ISCOD) for efficient broadcast of different supplemental data to caching clients," *IEEE Transactions on Information Theory*, vol. 52, no. 6, pp. 2825–2830, June 2006.

[104] C. Yetis, T. Gou, S. Jafar, and A. Kayran, "On feasibility of interference alignment in MIMO interference networks," *IEEE Transactions on Information Theory*, vol. 58, no. 9, pp. 4771–4782, September 2010.

[105] M. Razaviyayn, G. Lyubeznik, and Z. Luo, "On the degrees of freedom achievable through interference alignment in a MIMO interference channel," *IEEE Transactions on Signal Processing*, vol. 60, no. 2, pp. 812–821, February 2012.

[106] S. Jafar, S. Chung, and S. Choi, "On the beamforming design for efficient interference alignment," *IEEE Communications Letter*, vol. 13, no. 11, pp. 847–949, November 2009.

[107] K. Gomadam, V. Cadambe, and S. Jafar, "A distributed numerical approach to interference alignment and applications to wireless interference networks," *IEEE Transactions on Information Theory*, vol. 57, no. 6, pp. 3309–3322, June 2011.

[108] S. Peters and R. Heath, "Cooperative algorithms for MIMO interference channels," *IEEE Transactions on Vehicular Technology*, vol. 60, no. 1, pp. 206–218, January 2011.

[109] H. Yu and Y. Sung, "Least squares approach to joint beam design for interference alignment in multiuser multi-input multi-output interference channels," *IEEE Transactions on Signal Processing*, vol. 58, no. 9, pp. 4960–4966, September 2010.

[110] D. Papailiopoulos and A. Dimakis, "Interference alignment as a rank constrained rank minimization," *IEEE Transactions on Signal Processing*, vol. 60, no. 8, pp. 4278–4288, August 2012.

[111] H. Du, T. Ratnarajah, M. Sellathurai, and C. Papadias, "Reweighted nuclear norm approach for interference alignment," *IEEE Transactions on Communications*, vol. 61, no. 9, pp. 3754–3765, September 2013.

[112] S. Peters and R. Heath Jr., "Interference alignment via alternating minimization," in *IEEE International Conference on Acoustics, Speech and Signal Processing*, pp. 2445–2448, April 2009.

[113] J. Tang and S. Lambotharan, "Interference alignment techniques for MIMO multi-cell interfering broadcast channels," *IEEE Transactions on Communications*, vol. 61, no. 1, pp. 164–175, January 2013.

[114] B. Rynne and M. Youngson, *Linear Functional Analysis*. 2nd edition, Springer, 2008.

[115] X. Qu and C. Kang, "A closed-form solution to implement interference alignment and cancellation for a Gaussian interference Multiple Access Channel," *IEEE Transactions on Wireless Communication*, vol. 13, no. 2, pp. 710–723, February 2014.

[116] G. Bresler, D. Cartwright, and D. Tse, "Feasibility of interference alignment for the MIMO interference channel," *IEEE Transactions on Information Theory*, vol. 60, no. 9, pp. 5573–5586, September 2014.

[117] S. Jafar and M. Fakhereddin, "Degrees of freedom for the MIMO interference channel," *IEEE Transactions on Information Theory*, vol. 53, no. 7, pp. 2637–2642, July 2007.

[118] P. Mohapatra, K. Nissar, and C. Murthy, "Interference alignment algorithms for the K-user constant MIMO interference channel," *IEEE Transactions on Signal Processing*, vol. 59, no. 11, pp. 5499–5508, November 2011.

[119] H. Shen, B. Li, M. Tao, and Y. Luo, "The new interference alignment scheme for the MIMO interference channel," in *Proceedings of the Wireless Communications and Networking Conference*, April 2010.

[120] B. Li, Y. Luo, and H. Shen, "A new precoding scheme using interference alignment on modulation signal for multi-user MIMO downlink," in *IEEE*

International Conference on Wireless Communications and Signal Processing 2009, pp. 1–5, November 2009.

[121] M. Maddah-Ali, A. Motahari, and A. Khandani, "Signaling over MIMO multibase systems - combination of multi-access and broadcast schemes," in *Proceeding of IEEE International Symposium on Information Theory*, pp. 2104–2108, July 2006.

[122] Z. Xiang, M. Tao, J. Mo, and X. Wang, "Degrees of freedom for MIMO two-ray X relay channel," *IEEE Transactions on Signal Processing*, vol. 61, no. 7, pp. 1711–1720, April 2013.

[123] S. Jafar and S. Shamai, "Degrees of freedom region for the MIMO X channel," *IEEE Transactions on Information Theory*, vol. 54, no. 1, pp. 151–170, January 2008.

[124] H. Sun, C. Geng, T. Gou, and S. Jafar, "Degrees of freedom of MIMO X networks: Spatial scale invariance, one-sided decomposability and linear feasibility," *CoRR*, vol. abs/1207.6137, 2012.

[125] W. Ho, T. Quek, S. Sumei, and R. Heath, "Decentralized precoding for multicell MIMO downlink," *IEEE Transactions on Wireless Communications*, vol. 10, no. 6, pp. 1798–1809, June 2011.

[126] K. Gomadam, V. Cadambe, and S. Jafar, "Approaching the capacity of wireless networks through distributed interference alignment," in *IEEE Global Telecommunications Conference 2008*, pp. 1–6, November 2008.

[127] N. Jindal, S. Vishwanath, and A. Goldsmith, "On the duality of Gaussian multiple-access and broadcast channels," *IEEE Transactions on Information Theory*, vol. 50, no. 5, pp. 768–783, May 2004.

[128] J. Kim, S. Park, H. Sung, and I. Lee, "Sum rate analysis of two-cell MIMO broadcast channels: spatial multiplexing gain," in *Proceedings of IEEE International Conference on Communications*, pp. 1–5, May 2010.

[129] Q. Spencer, A. Swindlehurst, and M. Haardt, "Zero-forcing methods for downlink spatial multiplexing in multiuser MIMO channels," *IEEE Transactions on Signal Processing*, vol. 52, no. 2, pp. 461–471, January 2004.

[130] P. Komulainen, A. Tölli, and M. Juntti, "Effective CSI signaling and decentralized beam coordination in TDD multi-cell MIMO systems," *IEEE Transactions on Signal Processing*, vol. 61, no. 9, pp. 2204–2218, May 2013.

[131] J. Alcaraz and M. van der Schaar, "Coalitional games with intervention: Application to spectrum leasing in cognitive radio," *IEEE Transactions on Wireless Communications*, vol. 13, no. 11, pp. 6166–6179, November 2014.

[132] D. Zhao, "Throughput fairness in infrastructure-based IEEE 802.11 mesh networks," *IEEE Transactions on Vehicular Technology*, vol. 56, no. 5, pp. 3210–3219, September 2007.

[133] V. Annapureddy, A. El-Gamal, and V. Veeravalli, "Degrees of freedom of interference channels with comp transmission and reception," *IEEE Transactions on Information Theory*, vol. 58, no. 9, pp. 5740–5760, September 2012.

[134] U. Jang, H. Son, J. Park, and S. Lee, "CoMP-CSB for ICI nulling with user selection," *IEEE Transactions on Wireless Communications*, vol. 10, no. 9, pp. 2982–2993, September 2011.

[135] G. Nigam, P. Minero, and M. Haenggi, "Coordinated multipoint joint transmission in heterogeneous networks," *IEEE Transactions on Communications*, vol. 62, no. 11, pp. 4134–4146, November 2014.

[136] Q. Zhang and C. Yang, "Transmission mode selection for downlink coordinated multipoint systems," *IEEE Transactions on Vehicular Technology*, vol. 62, no. 1, pp. 465–471, January 2013.

[137] S. Han, C. Yang, G. Wang, D. Zhu, and M. Lei, "Coordinated multipoint transmission strategies for TDD systems with non-ideal channel reciprocity," *IEEE Transactions on Communications*, vol. 61, no. 10, pp. 4256–4270, October 2013.

[138] M. Holmes, A. Gray, and C. Isbell, *Fast SVD for large scale matrices*. College of Computing, Georgia Institute of Technology, Atlanta, GA.

[139] G. Nauryzbayev and E. Alsusa, "Interference alignment cancellation in Compounded MIMO Broadcast Channels with general message sets,"

[140] S. Song, M. Hasna, and K. Letaief, "Prior Zero Forcing for Cognitive Relaying," *IEEE Transactions on Wireless Communication*, vol. 12, no. 2, pp. 938–947, February 2013.

[141] R. Louie, L. Yonghui, and B. Vucetic, "Zero Forcing in general Two-Hop Relay Networks," *IEEE Transactions on Vehicular Technology*, vol. 59, no. 1, pp. 191–202, January 2010.

[142] H. Kim, H. Yu, and Y. Lee, "Limited feedback for Multicell Zero-Forcing Coordinated Beamforming in Time-Varying Channels," *IEEE Transactions on Vehicular Technology*, vol. 64, no. 6, pp. 2349–2360, June 2015.

[143] H. Huh, A. Tulino, and G. Caire, "Network MIMO With Linear Zero-Forcing Beamforming: Large System Analysis, Impact of Channel Estimation, and Reduced-Complexity Scheduling," *IEEE Transactions on Information Theory*, vol. 58, no. 5, pp. 2911–2934, May 2012.

[144] W. Li and M. Latva-aho, "An efficient Channel Block Diagonalization Method for Generalized Zero Forcing Assisted MIMO Broadcasting Systems," *IEEE Transactions on Wireless Communication*, vol. 10, no. 3, pp. 739–744, March 2011.

[145] C. Wang, K. Ren, and J. Wang, "Secure optimization computation outsourcing in cloud computing: A Case Study of Linear Programming," *IEEE Transactions on Computers*, vol. 65, no. 1, pp. 216–229, January 2016.

[146] D. Luenberger and Y. Ye, *Linear and Nonlinear Programming*. 3rd edition, Springer, 2008.

[147] G. Nauryzbayev and E. Alsusa, "Enhanced multiplexing gain using interference alignment cancellation in multi-cell MIMO networks," *IEEE Transactions on Information Theory*, vol. 62, no. 1, pp. 357–369, January 2016.

[148] J. Kotecha and A. Sayeed, "Transmit signal design for optimal estimation of correlated MIMO channels," *IEEE Transactions on Signal Processing*, vol. 52, no. 2, pp. 546–557, February 2004.

[149] V. Raghavan, J. Kotecha, and A. Sayeed, "Why does the Kronecker model result in misleading capacity estimates?," *IEEE Transactions on Information Theory*, vol. 56, no. 10, pp. 4843–4864, October 2010.

[150] J. Choi and D. Love, "Bounds on eigenvalues of a spatial correlation matrix," *IEEE Communications Letter*, vol. 18, no. 8, pp. 1391–1394, August 2014.

[151] C. Oestges, "Validity of the Kronecker model for MIMO correlated channels," in *Proceedings of IEEE VTC*, pp. 2818–2822, May 2006.

[152] S. Loyka, "Channel capacity of MIMO architecture using the exponential correlation matrix," *IEEE Communications Letter*, vol. 5, no. 9, pp. 369–371, September 2001.

[153] K. Yu, M. Bengtsson, B. Ottersten, D. McNamara, P. Karlsson, and M. Beach, "Second order statistics of NLOS indoor MIMO channels based on 5.2 GHz measurements," in *IEEE Global Telecommunications Conference (GLOBECOM)*, pp. 156–160, November 2001.

[154] R. Stridh, K. Yu, B. Ottersten, and P. Karlsson, "MIMO channel capacity and modeling issues on a measured indoor radio channel at 5.8 GHz," *IEEE Transactions on Wireless Communications*, vol. 4, no. 3, pp. 895–903, May 2005.

[155] H. Ozcelik, M. Herdin, W. Weichselberger, J. Wallace, and E. Bonek, "Deficiencies of Kronecker MIMO radio channel model," *IEEE Electronics Letter*, vol. 39, no. 16, pp. 1209–1210, August 2003.

[156] S. Wyne, A. Molisch, P. Almers, G. Eriksson, J. Karedal, and F. Tufvesson, "Outdoor-to-indoor office MIMO measurements and analysis at 5.2 GHz," *IEEE Transactions on Vehicular Technology*, vol. 57, no. 3, pp. 1374–1386, May 2008.

[157] H. Tong and S. Zekavat, "On the suitable environments of the kronecker product form in MIMO channel modeling," in *IEEE Wireless Communications and Networking Conference (WCNC')*, pp. 780–784, March-April 2008.

[158] R. Ertel, P. Cardieri, K. Sowerby, T. Rappaport, and J. Reed, "Overview of spatial channel models for antenna array communication systems," *IEEE Personal Communications*, vol. 5, no. 1, pp. 10–22, February 1998.

[159] D. Shiu, G. Foschini, M. Gans, and J. Kahn, "Fading correlation and its effect on the capacity of multielement antenna systems," *IEEE Transactions on Communications*, vol. 48, no. 3, pp. 502–513, March 2000.

[160] J. Kermoal, L. Schumacher, K. Pedersen, P. Mogensen, and F. Frederiksen, "A stochastic MIMO radio channel model with experimental validation," *IEEE Journal on Selected Areas in Communications*, vol. 20, no. 6, pp. 1211–1226, June 2002.

[161] D. Chizhik, F. Rashid-Farrokhi, J. Ling, and A. Lozano, "Effect of antenna separation on the capacity of BLAST in correlated channels," *IEEE Communication Letters*, vol. 4, no. 11, pp. 337–339, November 2000.

[162] A. Abouda, H. El-Sallabi, L. Vuokko, and S. Haggman, "Performance of stochastic Kronecker MIMO radio channel model in urban microcells," in *IEEE 17th International Symposium on Personal, Indoor and Mobile Radio Communications (PIMRC'2006)*, pp. 1–5, September 2006.

[163] D. Gesbert, H. Bolcskei, D. Gore, and A. Paulraj, "Outdoor MIMO wireless channels: Models and performance prediction," *IEEE Transactions on Communications*, vol. 50, no. 12, pp. 1926–1934, December 2002.

[164] C. Masouros, M. Sellathurai, and T. Ratnarajah, "Large-scale MIMO transmitters in fixed physical spaces: The effect of transmit correlation and mutual coupling," *IEEE Transactions on Communications*, vol. 61, no. 7, pp. 2794–2804, July 2013.

[165] D. Chizhik, J. Ling, P. Wolniansky, R. Valenzuela, N. Costa, and K. Huber, "Multiple-Input Multiple-Output measurements and modeling in Manhattan," *IEEE Journal on Selected Areas in Communications*, vol. 21, no. 3, pp. 321–331, April 2003.

[166] S. Salous, *Radio Propagation Measurement and Channel Modelling*. Hoboken, NJ: Wiley, ch. 3.12.2, pp. 122-123, 2013.

[167] Y. Jiang, X. Zheng, and J. Li, "Asymptotic performance analysis of V-BLAST," in *IEEE*, vol. 6, pp. 3882–3886, December 2005.

[168] "User Equipment (UE) radio transmission and reception," *3rd Generation Partnership Project; Technical Specification Group Radio Access Network;*

Evolved Universal Terrestrial Radio Access (E-UTRA), TS 36.101 V13.0.0, 2015.

[169] M. Heath, *Scientific Computing: An Introductory Survey*. 3rd edition, New York: McGraw-Hill, 2002.

[170] N. Zhao, F. Yu, and V. Leung, "Opportunistic communications in interference alignment networks with wireless power transfer," *IEEE Wireless Communications Magazine*, vol. 22, no. 1, pp. 88–95, February 2015.

[171] N. Zhao, F. Yu, and V. Leung, "Wireless energy harvesting in interference alignment networks," *IEEE Communications Magazine*, vol. 53, no. 6, pp. 72–88, June 2015.

[172] M. Ismail, M. Kashef, E. Serpedin, and K. Qaraqe, "On balancing energy efficiency for network operators and mobile users in dynamic planning," *IEEE Communications Magazine*, vol. 53, no. 11, pp. 162–169, November 2015.